Ditopic ligand effects on stabilization of copper sulfide nanoclusters: control of solution-phase equilibria and redox chemistry in discrete [$Cu_{12}S_6$] clusters with labile Cu–S bonds

Michael J. Trenerry and Gwendolyn A. Bailey

Department of Chemistry, University of Minnesota – Twin Cities
207 Pleasant St SE, Minneapolis, MN 55455, USA

Supporting Information

EXPERIMENTAL DETAILS

General considerations

Unless otherwise specified, all synthetic procedures and electrochemical measurements were performed in an MBraun glovebox under an N_2 atmosphere. Organic solvents were dried over alumina columns within a solvent purification system (Pure Process Technology) and degassed by sparging with Ar. Solvents, once dried and degassed, were stored in the glovebox over 3 Å molecular sieves. NMR solvents (THF-d_8, C_6D_6, CD_2Cl_2) were purchased from Cambridge Isotopes, degassed via at least 3 consecutive freeze/pump/thaw cycles, and dried over freshly activated 3 Å molecular sieves. Crystalline samples of **1•PPh$_2$Et** and **1•dppt** were synthesized according to literature procedure.[1,2] Phase purity was confirmed by comparison of the powder X-ray diffraction (PXRD) patterns with simulated and experimental values.[1,2]

Cu(OAc), S(SiMe$_3$)$_2$, and the phosphine ligands ethyldiphenylphosphine, 1,5-bis(diphenylphosphino)pentane, and 1,8-bis(diphenylphosphino)octane were purchased from commercial sources: [Cu(OAc) (Strem), S(SiMe$_3$)$_2$ (TCI), 1,8-bis(diphenylphosphino)octane (Sigma Aldrich), 1,5-bis(diphenylphosphino)pentane (Sigma Aldrich), ethyldiphenylphosphine (Sigma Aldrich)]and used as received. All NMR spectra were recorded on a Bruker Avance III HD 400 MHz spectrometer. ^{1}H, ^{13}C{^{1}H} NMR spectra are referenced to residual solvent peaks.[3] ^{31}P{^{1}H} NMR spectra were referenced to an external standard of 85% phosphoric acid. Multiplicities are abbreviated as follows: s = singlet, d = doublet, t = triplet, m = multiplet, br = broad. PXRD patterns were collected on a Rigaku Smartlab SE diffractometer.

Synthetic Protocols

Synthesis of **1•dppo**. **1•dppo** was prepared according to a modified version of the previously reported literature protocol,[1] using THF instead of toluene solvent for improved solubility of reagents. Additionally, the crystalline product was isolated from excess dppo ligand through vapor diffusion with pentane. In the glovebox, a 20 mL vial was charged with solid Cu(OAc) (126.8 mg, 1.03 mmol), dppo (328.1 mg, 0.68 mmol, 0.7 equiv), and THF (12 mL). The resulting light tan suspension was filtered through a celite plug into a separate vial, yielding a clear, colorless solution. After chilling the solution to –40° C, S(SiMe$_3$)$_2$ (110 µL, 0.52 mmol, 0.5 equiv) was added dropwise with vigorous stirring, resulting in a color change to yellow-orange and then deep red within one minute. The solution was stirred at –40 °C for 30 min and then was evenly distributed between three vials. These vials were left uncapped and were placed inside a jar containing pentane antesolvent. The jar was then sealed and placed inside a freezer (–25 °C) to crystallize. After 24 h, filtration through a coarse porosity frit followed by washing with pentane and drying in vacuo yielded bright pink-red crystals of **1•dppo** (145 mg, 53.7% yield). ^{1}H NMR (THF-d_8, 400 MHz, 25 °C): δ 8.43 (br s, 16H), 7.31 (t, 8H), 7.15 (t, 16H), 7.02 (br s, 16H), 6.93 (t, 8H), 6.85 (t, 16H), 2.68 (dd, 8H), 1.47 (br s, 16H), 0.99 (br dm, 16), 0.70 (br dm, 16), 0.11 (br s, 8). ^{31}P{^{1}H} NMR (THF-d_8, 162 MHz, 25 °C): δ -23.0 (br s). ^{1}H DOSY NMR (THF-d_8, 400 MHz, 25 °C) D = 5.1 ×10^{-10} m^2/s; r_H = 9.4 Å.

The collected powder X-ray diffraction (PXRD) pattern of **1•dppo** closely matched the simulated and experimental pattern of the literature report.[1]

Synthesis of **1•dppt.** Crystalline samples of **1•dppt** were synthesized according to the literature procedure.[1]

^{1}H NMR (THF-d_8, 400 MHz, 25 °C): δ 7.39 (br s), 7.26 (br s), 2.02 (br s), 1.61 (br s), 1.40 (br s). ^{31}P{^{1}H} NMR (THF-d_8, 162 MHz, 25 °C): δ -16.2 (br s). ^{1}H DOSY NMR (THF-d_8, 400 MHz, 25 °C) D = 6.8 ×10^{-10} m^2/s; r_H = 7.0 Å.

The collected powder X-ray diffraction (PXRD) pattern of **1•dppt** closely matched the reported simulated and experimental patterns.[1]

Synthesis of **1•PPh_2Et.** Crystalline samples of **1• PPh_2Et** were synthesized according to the literature procedure.[2]

^{1}H NMR (THF-d_8, 400 MHz, 25 °C): δ 7.46 (br s), 7.20 (br s), 2.03 (q), 0.98 (p). $^{31}P\{^1H\}$ NMR (THF-d_8, 162 MHz, 25 °C): δ -11.9 (br s). ^{1}H DOSY NMR (THF-d_8, 400 MHz, 25 °C) D = 11.0 ×10^{-10} m^2/s; r_H = 4.3 Å.

The collected powder X-ray diffraction (PXRD) pattern of **1•PPh_2Et** closely matched the reported simulated and experimental patterns.[2]

Synthesis of $[Cp^*_2Fe][PF_6]$. $[Cp^*_2Fe][PF_6]$ was synthesized according to an adapted literature procedure for the synthesis of the corresponding ferrocenium salt, $[Cp_2Fe][PF_6]$.[4] The procedure was performed on the bench using standard benchtop solvents, including HPLC-grade deionized water which was used throughout. On the bench, a 20 mL vial was charged with solid yellow Cp^*_2Fe (660.0 mg, 2.02 mmol) and a stir bar. To this vial was added concentrated sulfuric acid (2.5 mL) with magnetic stirring, resulting in the formation of a deep green mixture. This mixture was stirred for 45 min at RT and then added to a 100 mL round bottom flask containing a solution of ^{t}BuOH (1.254 g) in deionized water (43 mL). The combined mixture was stirred for 30 min and then filtered through a medium porosity frit to obtain a translucent green filtrate. The filtrate was chilled to 0 °C (ice/water bath) and was then added to a 250 mL round bottom flask containing a solution of KPF_6 (1.048 g, 5.69 mmol, 2.81 equiv) in pre-chilled deionized water (60 mL; 0 °C). The resulting mixture was stirred for 1 h at 0 °C during which time a fluffy green precipitate formed. The precipitate was filtered through a fine-porosity frit, washed with chilled water (2 x 30 mL) and chilled diethyl ether (3 x 20 mL) and then dried in vacuo yielding $[Cp^*_2Fe][PF_6]$ as a dark green solid (0.7410 g, 78.6% yield). ^{1}H NMR (CD_3CN, 400 MHz, 25 °C): silent. MS (ESI^+): *m/z* calcd for $[Cp^*_2Fe]^+$ 326.3, found 326.3.

Independent synthesis of **$dppoS_2$**. In an N_2-filled glovebox, a 20 mL vial was charged with dppo (105.3 mg, 0.22 mmol) and toluene (8 mL). Elemental sulfur (160.4 mg, 0.63 mmol, 11.5 equivalents) was gradually added over the course of 5 minutes, after which the reaction mixture was allowed to stir at room temperature for 16 hours. The reaction mixture was then filtered to remove residual sulfur and solvent was removed in vacuo yielding $dppoS_2$ as a white solid. (74.9 mg, 62.7% yield). ^{1}H NMR (THF-d_8, 400 MHz, 25 °C): δ 7.91 (m 8H), 7.43 (m , 12H), 2.45 (m, 4H), 1.56 (m, 4H), 1.35 (m, 4H), 1.23 (m, 4H). $^{31}P\{^1H\}$ NMR (THF-d_8, 162 MHz, 25 °C): δ 41.6 (s).

MALDI-MS Characterization of Cluster Compounds

Matrix and analyte solutions for matrix-assisted laser desorption/ionization mass spectrometry (MALDI-MS) were prepared in a nitrogen-filled glovebox at concentrations of ca. 200 and 0.35 mM, respectively. Cocrystallized samples were prepared by successively spotting ca. 5-10 μL aliquots of matrix and analyte solutions on the MALDI target plate and allowing it to dry, yielding cocrystallized matrix and analyte. Data collection was performed in both positive and negative ion modes using a Bruker Autoflex Max MALDI/TOF-MS instrument with recorded masses calibrated to a known mixture of peptide calibrants. Positive ion mode mass spectra for **1•dppo** and **1•dppt** (Figures S1-S5) depict prominent signals for monocationic species containing intact or dimerized $[Cu_{12}S_6]$ clusters from which one or more phosphine ligands have dissociated. No such signals were observed in the mass spectra collected for samples of **1•PPh_2Et** prepared in the same manner, consistent with cluster degradation. By contrast, negative ion mode mass spectra for **1•dppo** and **1•dppt** (Figures S6-S9) depict prominent signals for the monoanionic cluster

core $[Cu_{12}S_6]^-$ as well as the monoanionic aggregates $[Cu_{24}S_{12}]^-$, $[Cu_{36}S_{18}]^-$, and $[Cu_{48}S_{24}]^-$ bearing no supporting phosphine ligands. Interestingly, the negative ion mode mass spectrum of **1•dppt** additionally shows prominent signals corresponding to the monoanionic, ligand-free clusters $[Cu_{20}S_{10}]^-$ and $[Cu_{38}S_{19}]^-$.

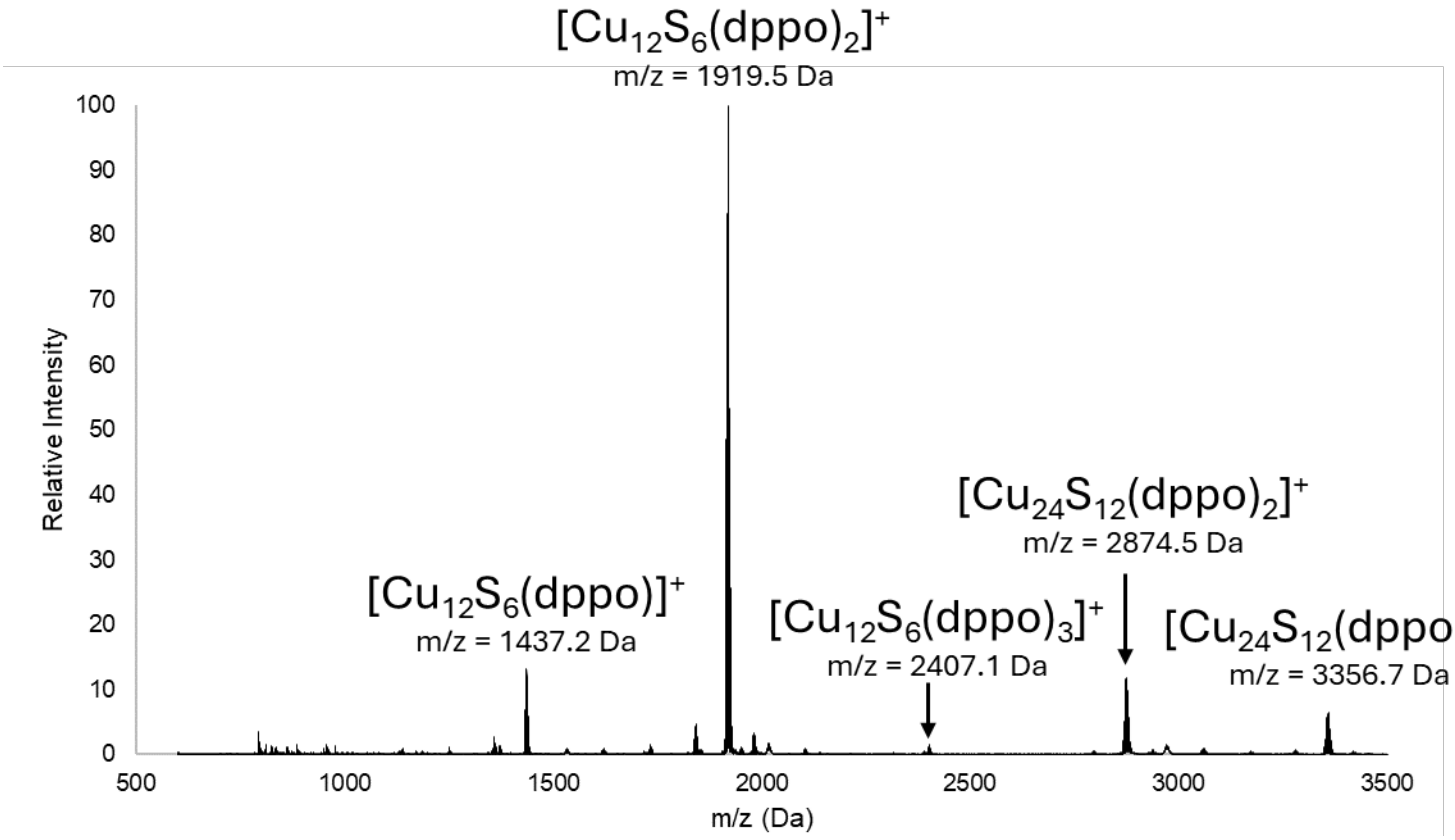

Figure S1: Positive ion mode mass spectrum of **1•dppo**, collected by MALDI-MS using an anthracene matrix.

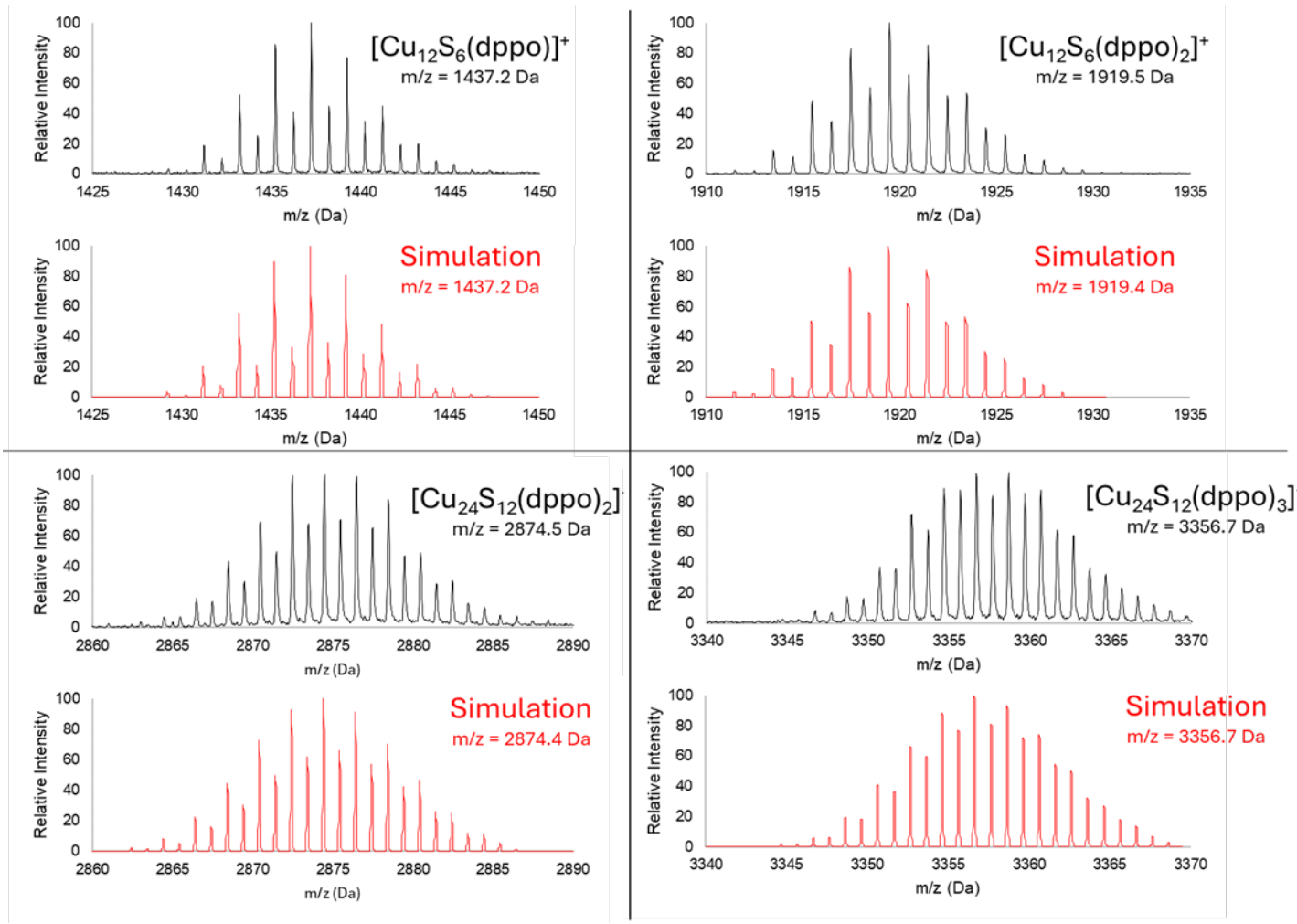

Figure S2: Positive ion mode mass spectra of **1•dppo**, collected by MALDI-MS using an anthracene matrix, and simulated mass spectral data for prominent signals.

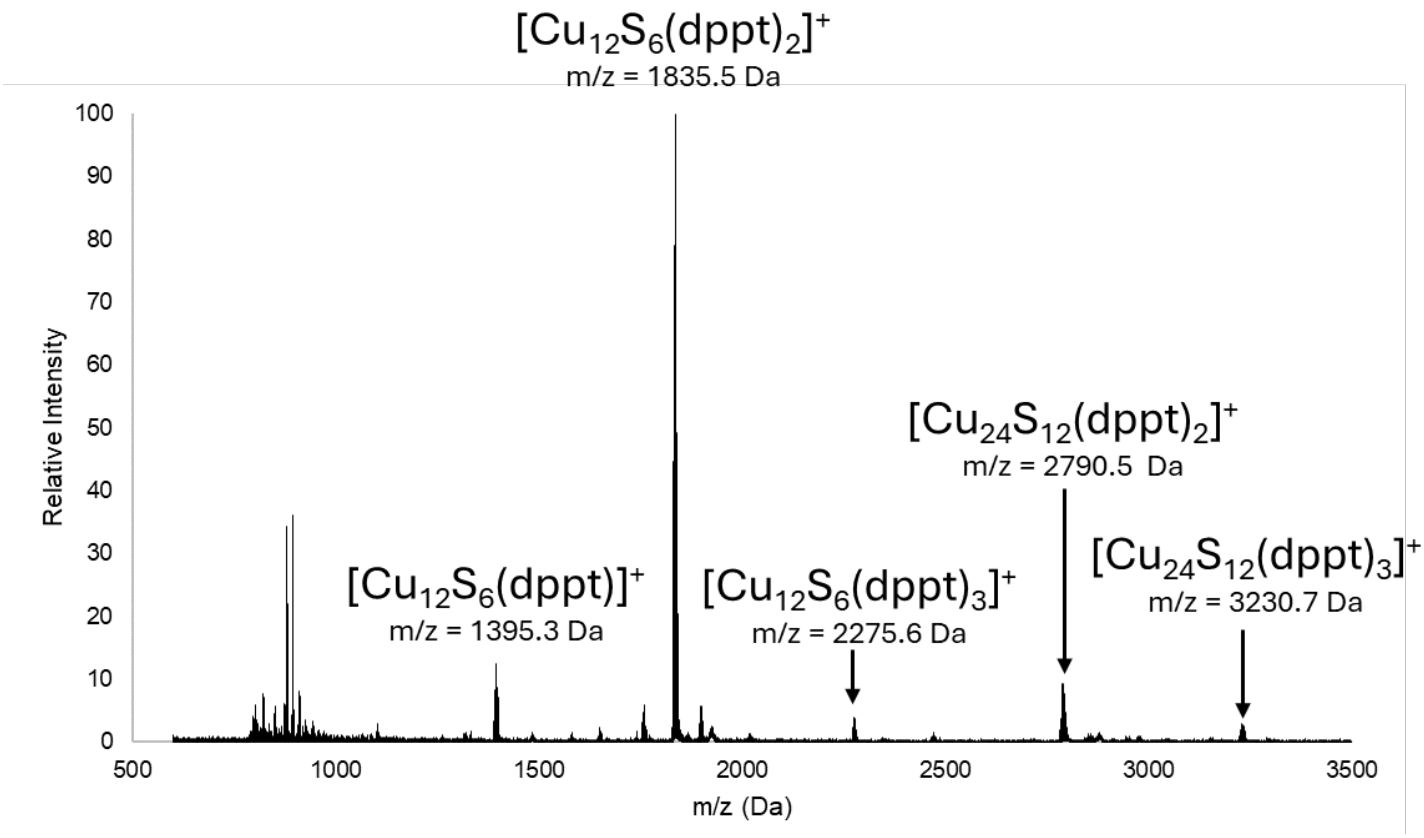

Figure S3: Positive ion mode mass spectrum of **1•dppt**, collected by MALDI-MS using an anthracene matrix.

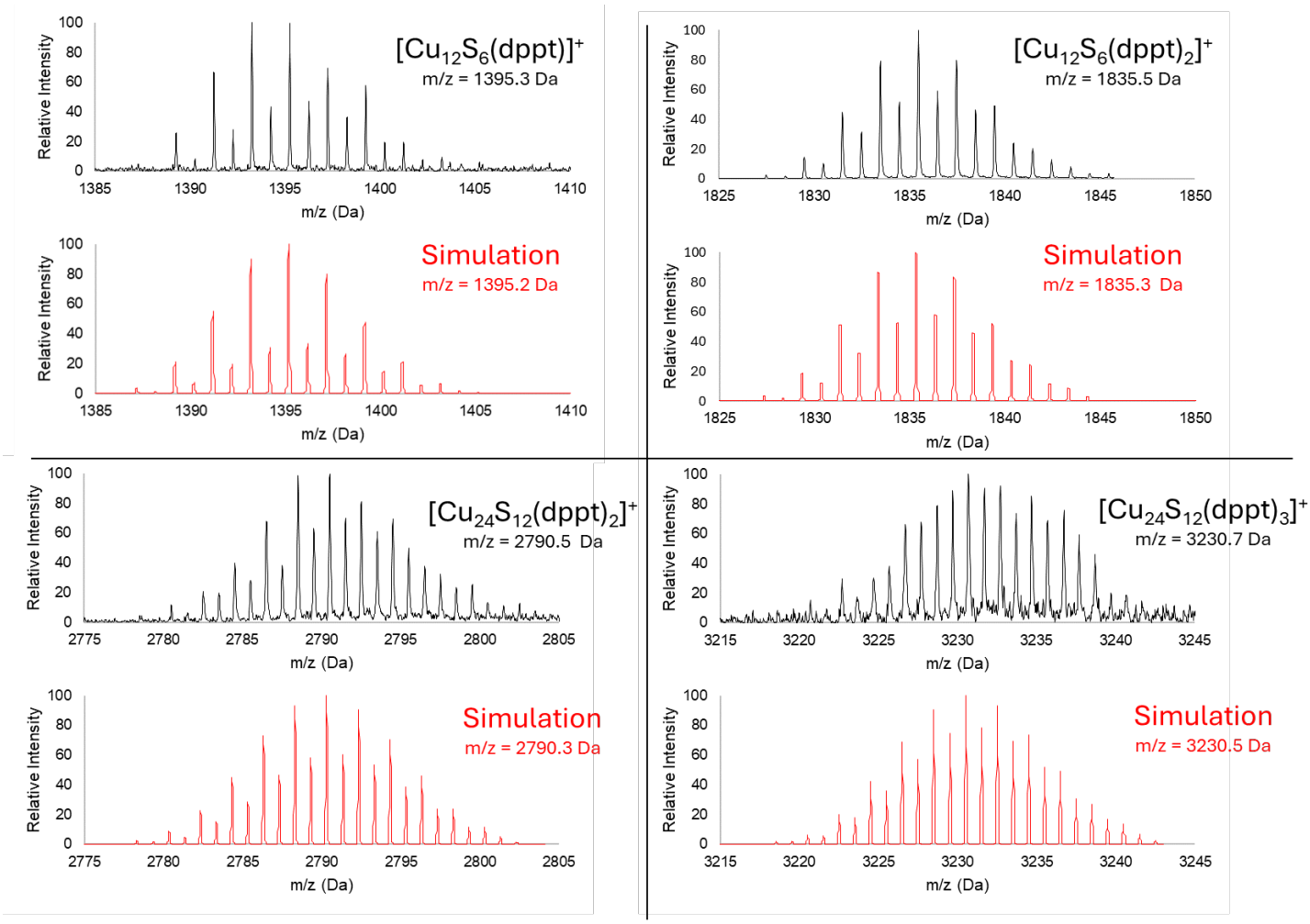

Figure S4: Positive ion mode mass spectra of **1•dppt**, collected by MALDI-MS using an anthracene matrix, and simulated mass spectral data for prominent signals.

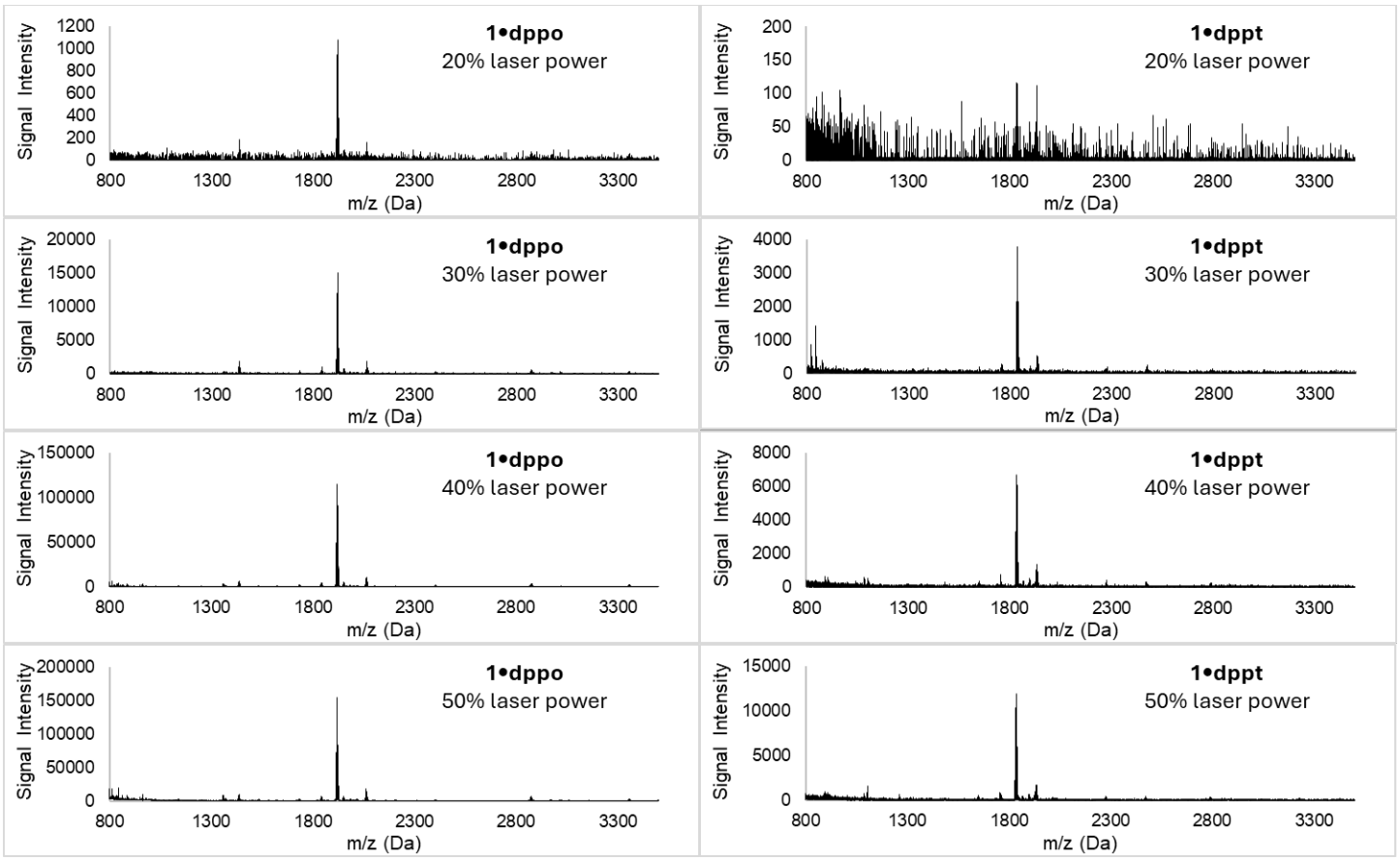

Figure S5: Positive ion mode mass spectra of **1•dppo** (left) and **1•dppt** (right), collected by MALDI-MS using an anthracene matrix at laser power levels ranging from 20% to 50%.

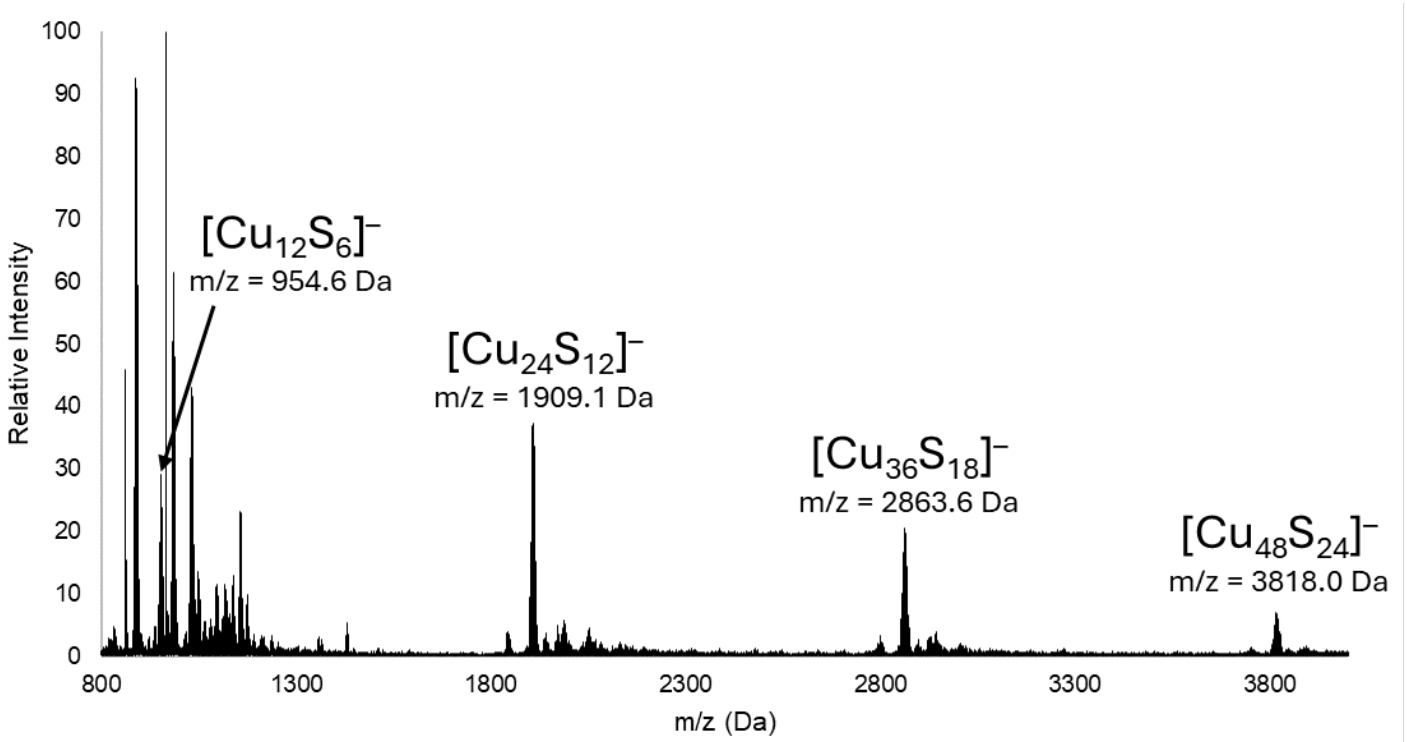

Figure S6: Negative ion mode mass spectrum of **1•dppo**, collected by MALDI-MS using an anthracene matrix.

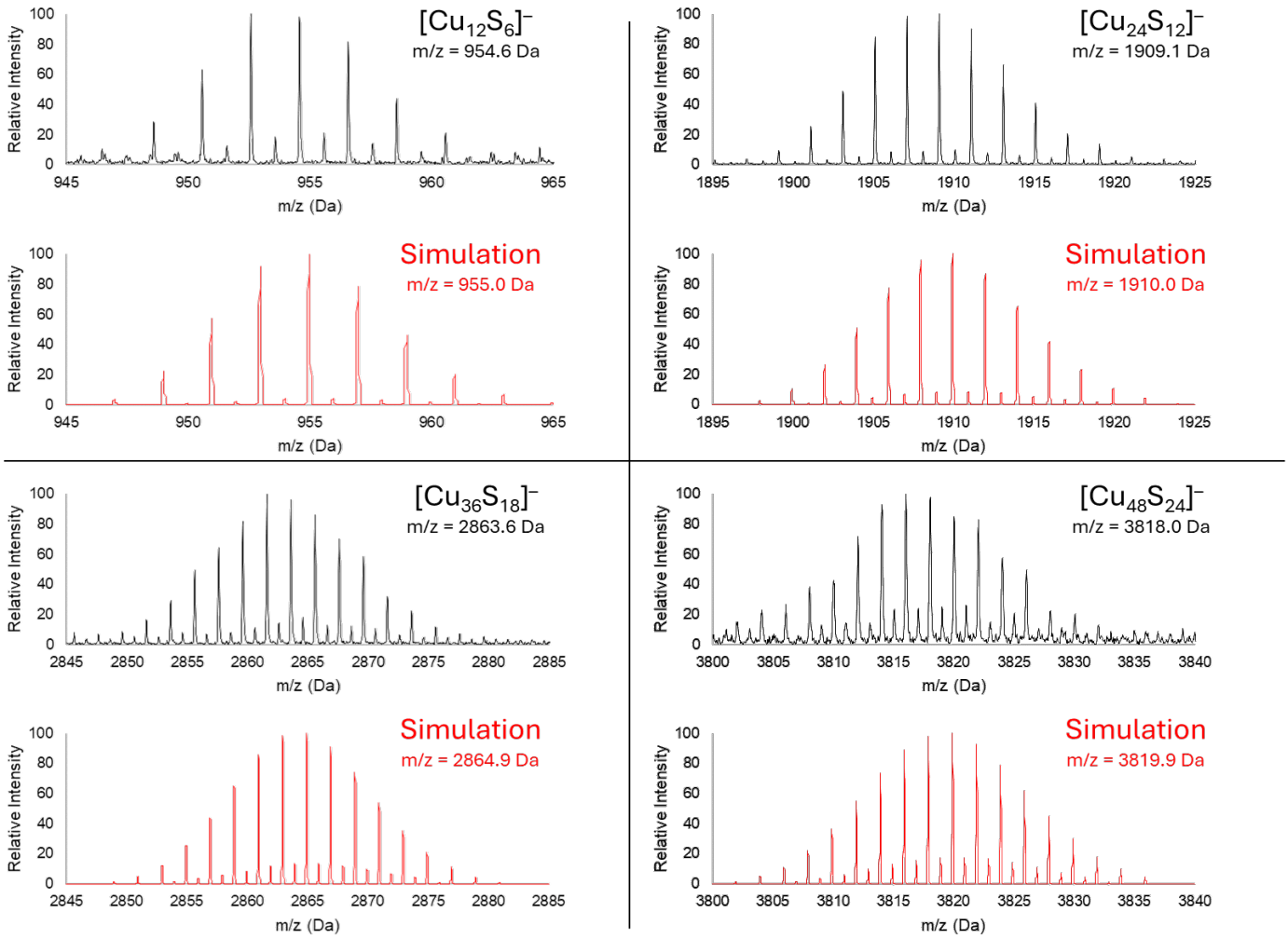

Figure S7: Negative ion mode mass spectra of **1•dppo**, collected by MALDI-MS using an anthracene matrix, and simulated mass spectral data for prominent signals.

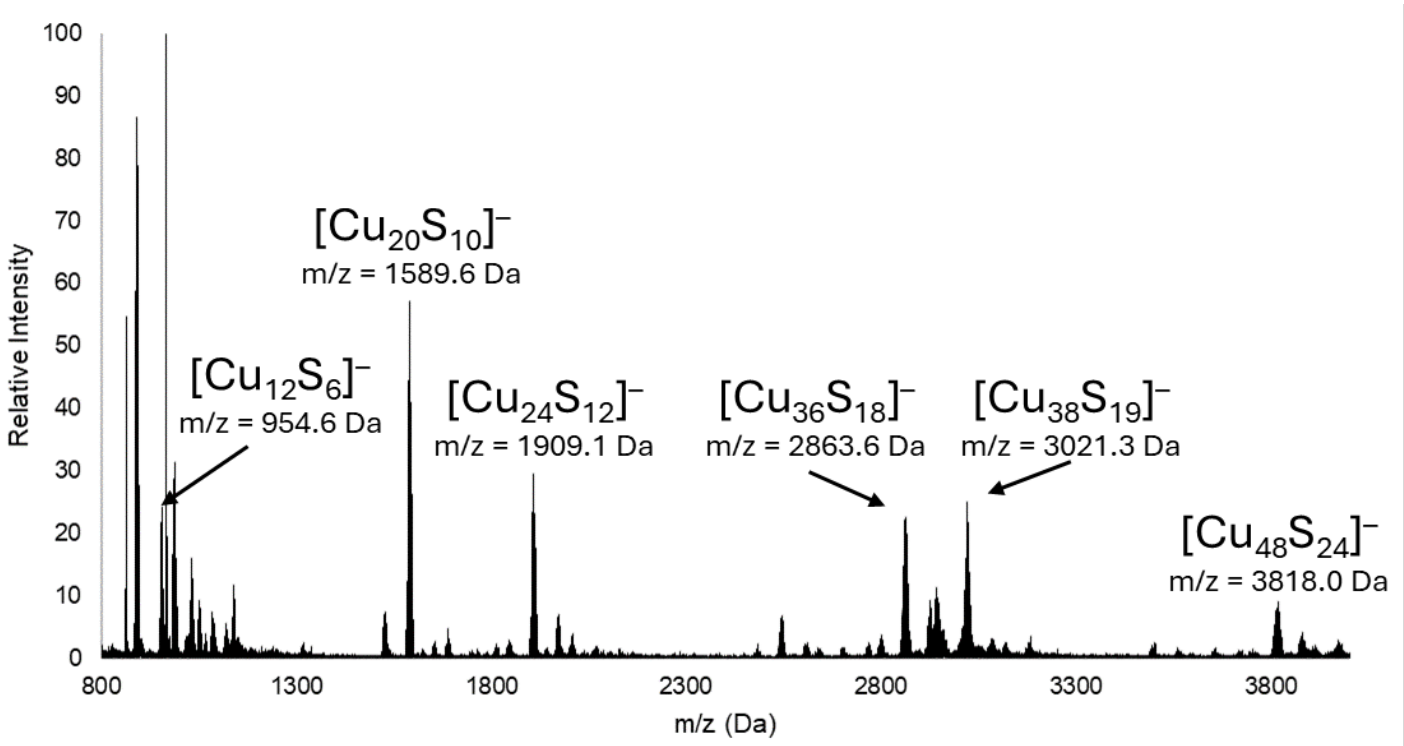

Figure S8: Negative ion mode mass spectrum of **1•dppt**, collected by MALDI-MS using an anthracene matrix.

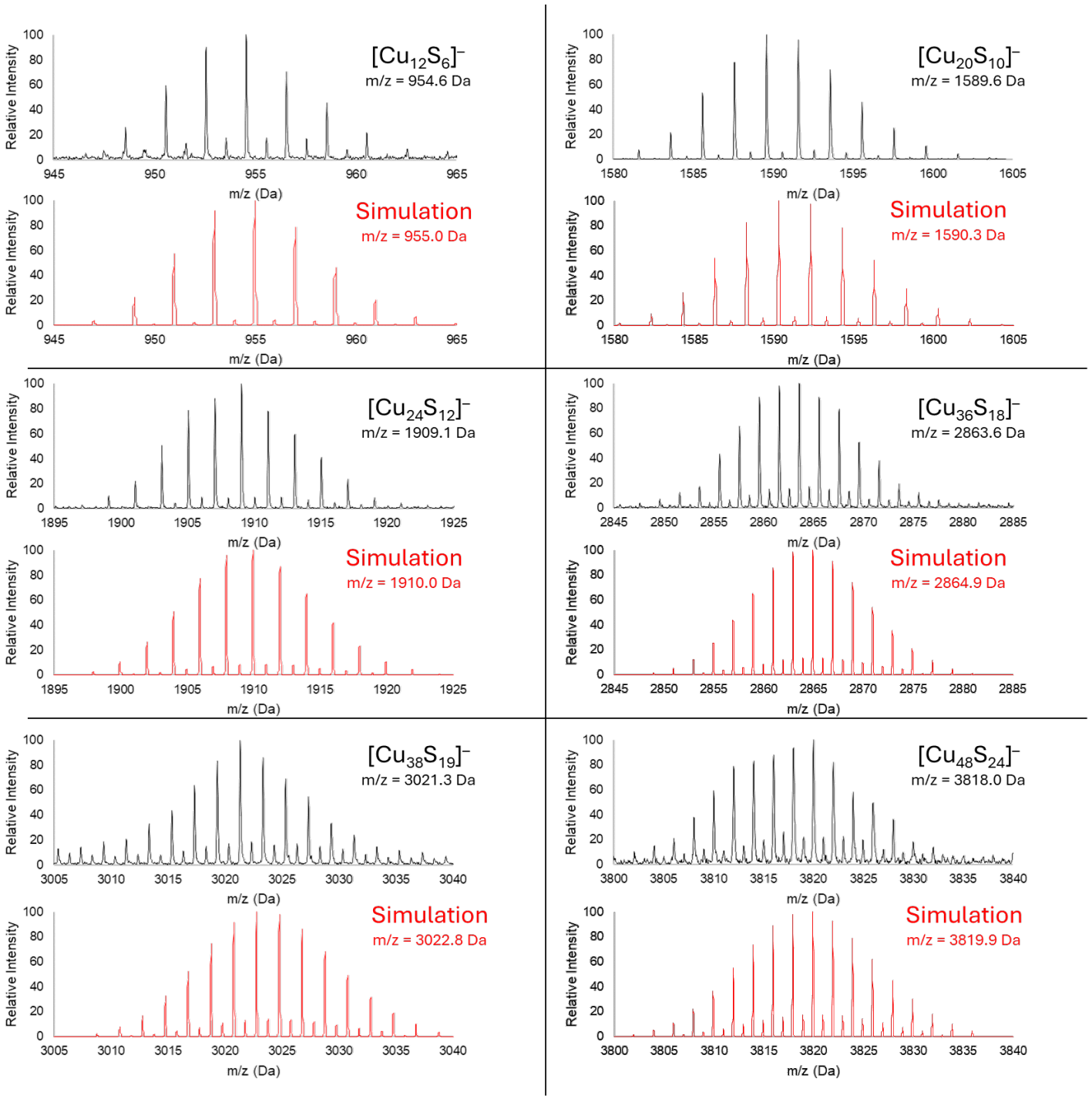

Figure S9: Negative ion mode mass spectra of **1•dppt**, collected by MALDI-MS using an anthracene matrix, and simulated mass spectral data for prominent signals.

Interpretation of ^{1}H DOSY NMR

The hydrodynamic radii r_H of solvated species were calculated from measured diffusion coefficients D according to the Stokes-Einstein equation (equation S1), where k_B is the Boltzmann constant (1.38×10^{-23} J K^{-1}), T is temperature (measured at 298.15 K), and η is the viscosity of solvent (for tetrahydrofuran, η = 0.46 cP at 298.15 K.[5] As part of this analysis, dissolved analyte molecules are assumed to be roughly spherical.

Eq. S1
$$D = \frac{k_B\, T}{6\pi\, \eta\, r_H}$$

The expected molecular radii of intact nanocluster species are estimated from reported single-crystal X-ray diffraction data, where r_{XRD} is calculated according to equation S2 based on the method described by Macchioni and coworkers.[6]

Eq. S2
$$r_{XRD} = \sqrt[3]{\frac{3\, V}{4\pi\, Z}}$$

The volume of the crystallographic unit cell V is divided by the number of nanocluster molecules Z contained therein, which are treated as space-filling spherical objects. Due to the implicit simplifying assumption of perfect packing efficiency within the crystallographic unit cell, r_{XRD} is effectively an upper-bound for the hydrodynamic radius r_H of an intact nanocluster.

Calculated values of r_{XRD} for the nanocluster species considered by this manuscript are presented in Table S1. These values are calculated for unit cell volumes V as reported, and after subtracting the molecular volume of solvent molecules[7] within the unit cell.

Table S1: Calculated values of r_{XRD} for clusters **1**.

Cluster	Z	Solvent in reported unit cell	V (Å^3)	r_{XRD} (Å)
1•PPh$_2$Et[8]	1	None	2852	8.80
1•dppt[1]	4	2 (C_7H_8)	13137 (12933) [a]	9.22 (9.17) [b]
1•dppo[1]	2	3.5 (C_7H_8)	7322 (6966) [a]	9.56 (9.40) [b]

[a] Values in parentheses show the unit cell volume with the total molecular volume of solvent molecules subtracted. [b] Values in parentheses show estimated r_{XRD} using unit cell volumes excluding the molecular volumes of solvent molecules.

Extended Solution Stability Studies

The extended solution stability of **1•dppo** was tested in tetrahydrofuran (THF)-d$_8$, toluene-d$_8$, benzene-d$_6$ (C_6D_6), and dichloromethane-d$_2$ (CD_2Cl_2) over 21 days. Solutions were prepared inside a rigorously air- and water-free N_2-filled glovebox by dissolving **1•dppo** in the deuterated solvent of choice together with and 1,3,5-trimethoxybenzene (TMB) internal standard ([**1•dppo**]: ca. 0.6–1.2 mM, according to solubility; ca. 1:2 molar ratio vs. TMB). Samples were kept stirring within the glovebox for the duration of this experiment and sampled (~0.4 mL aliquots) for NMR analysis at various timepoints: immediately after sample preparation, and 1/2/4/21 days after sample preparation.

The raw ^{1}H and ^{31}P{^{1}H} NMR spectra are presented in Figures S10-S13 while relative concentrations over time are plotted in Figure S14. In THF-d$_8$ and C_6D_6, little change is observed the ^{1}H and ^{31}P{^{1}H} NMR spectra of **1•dppo**, and concentrations of intact cluster remain constant (as determined by the integration of the diagnostic downfield cisoid *o*-Ph C*H* at 8.45 ppm vs. internal TMB standard; Figures S10-S11). In contrast, the integration of ^{1}H NMR signals for **1•dppo** in toluene-d$_8$ decrease from 0.6–0.3

mM over the course of 1-2 days, and then remain constant (Figure S12). However, no new signals are observed and the color of the solution remains the characteristic bright pink color of **1•dppo**. This may indicate the gradual precipitation of **1•dppo,** as this cluster is observed to be much less soluble in toluene than in benzene and THF, and partially remains as undissolved pink solid when attempting to create solutions of ca. 1 mM **1•dppo** in toluene. Based on this information, we conclude that **1•dppo** is the most stable and solution-processible in THF and benzene, is stable though markedly less soluble in toluene.

By contrast, the ^{1}H and $^{31}P\{^{1}H\}$ NMR spectra of **1•dppo** in CD_2Cl_2 show the most drastic changes over time, with consistent decreases in ^{1}H signal integrations for intact **1•dppo** along with the growth of new signals corresponding to phosphine-bound cluster degradation products and phosphine sulfide ($RPh_2P{=}S$; δ_P -12 and +43 ppm, respectively; Figure S13), thus indicating that the mechanism of cluster degradation in dichloromethane involves S-atom extrusion from the $[Cu_{12}S_6]$ core. While the specific mechanism of **1•dppo** degradation is currently unclear, S-atom extrusion may potentially arise from the spontaneous abstraction of chloride from dichloromethane solvent and its binding to copper sites in place of sulfide.

A similar pathway has been shown to play a key role in the formation of multinuclear Cu^{I} clusters from tetrakis(acetonitrile) copper(i) hexafluorophosphate ($[Cu(CH_3CN)_4][PF_6]$) and a combination of bis(diphenylphosphino)methane and dialkyldithiophosphate ligands, as reported by Liu and coworkers.[9] Notably, syntheses performed in dichloromethane and chloroform yielded chloride-bridged tricopper and hexacopper clusters via the abstraction of chloride from solvent, whereas synthesis performed in tetrahydrofuran yielded a tricopper cluster with a different core configuration and no bridging chloride.[9]

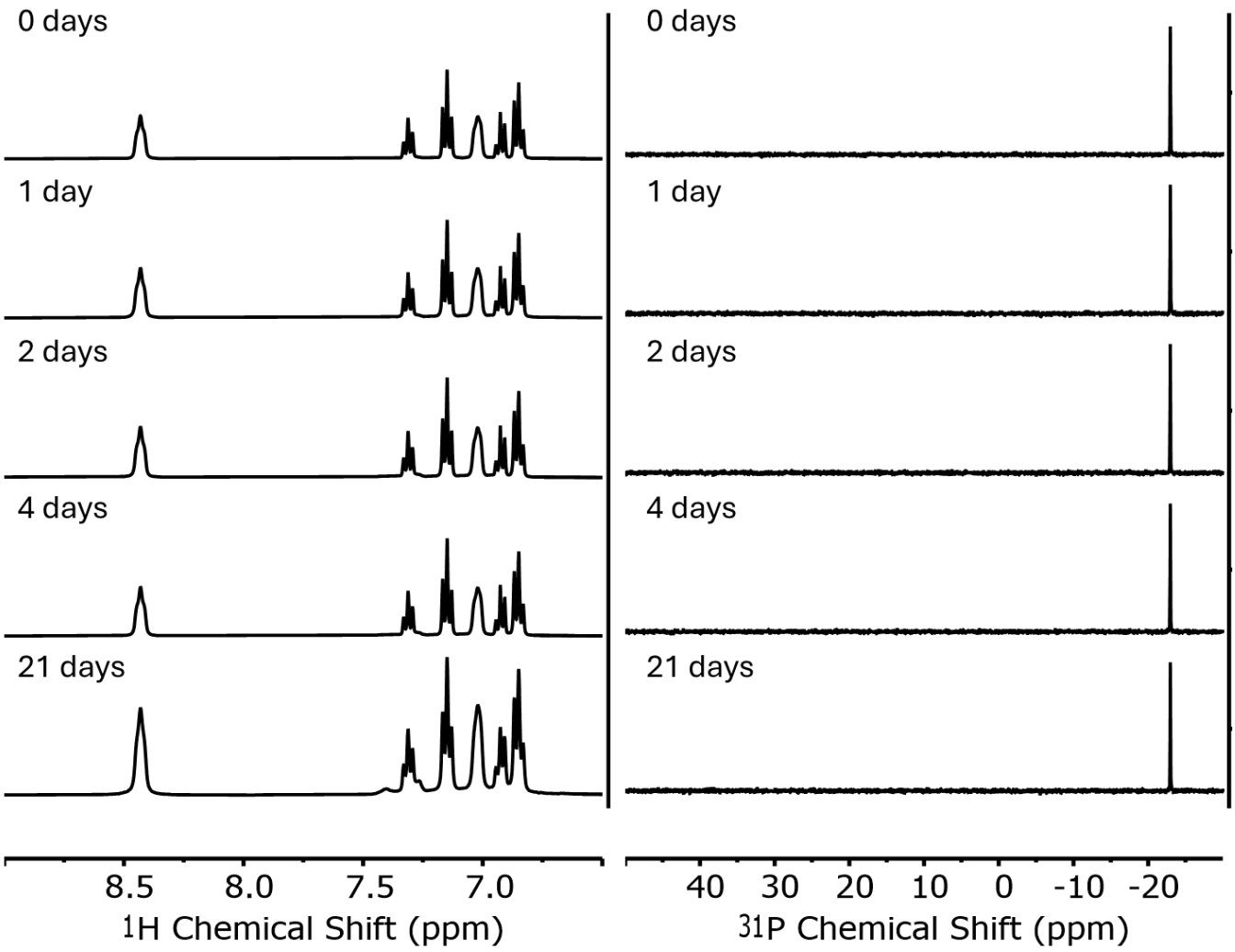

Figure S10: ^{1}H NMR spectra (left, 400 MHz, THF-d_8) and ^{31}P{^{1}H} NMR spectra (right, 162 MHz, THF-d_8) of **1•dppo** in THF-d_8 over the course of 21 days.

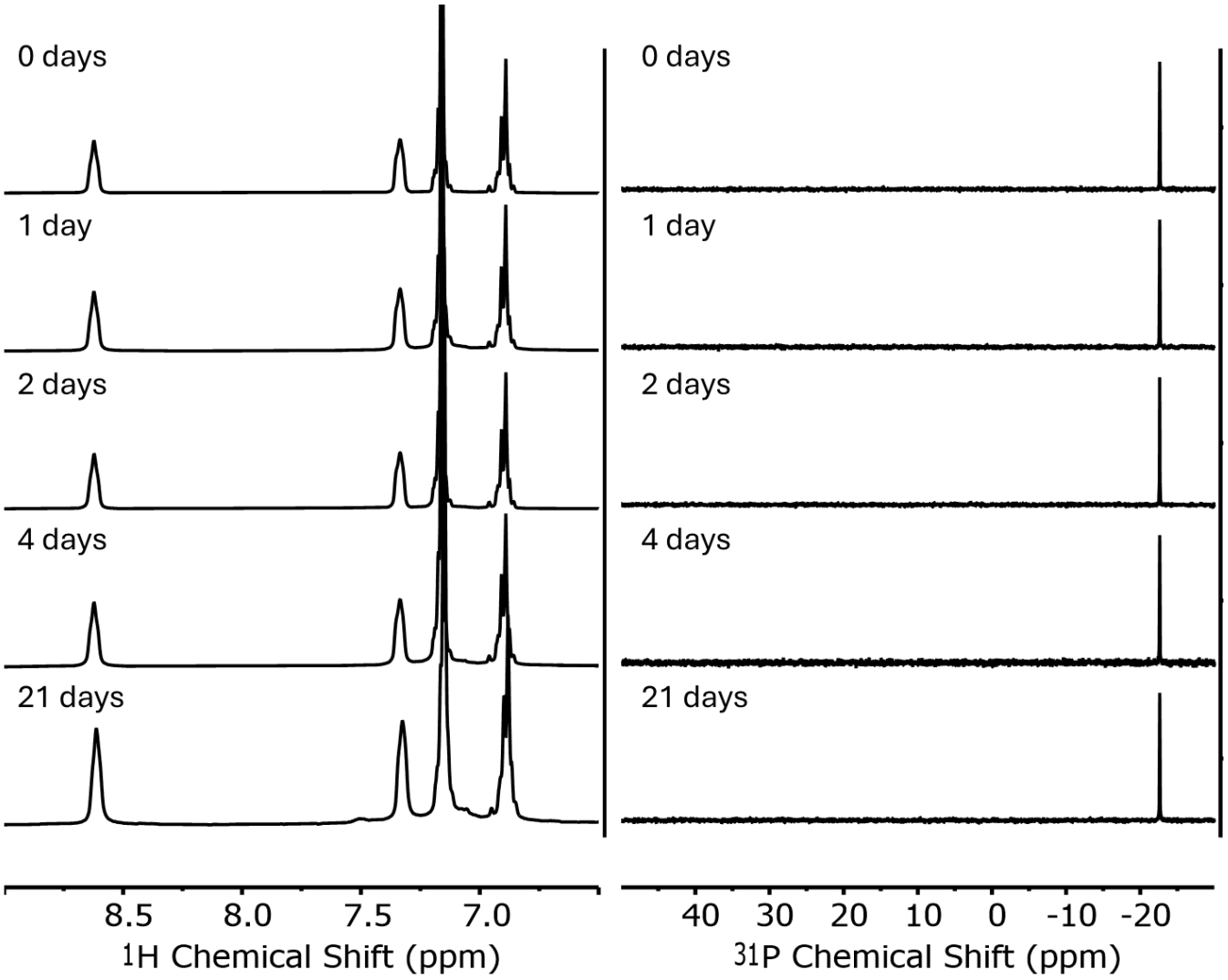

Figure S11: ^{1}H NMR spectra (left, 400 MHz, C_6D_6) and $^{31}P\{^{1}H\}$ NMR spectra (right, 162 MHz, C_6D_6) of **1•dppo** in C_6D_6 over the course of 21 days.

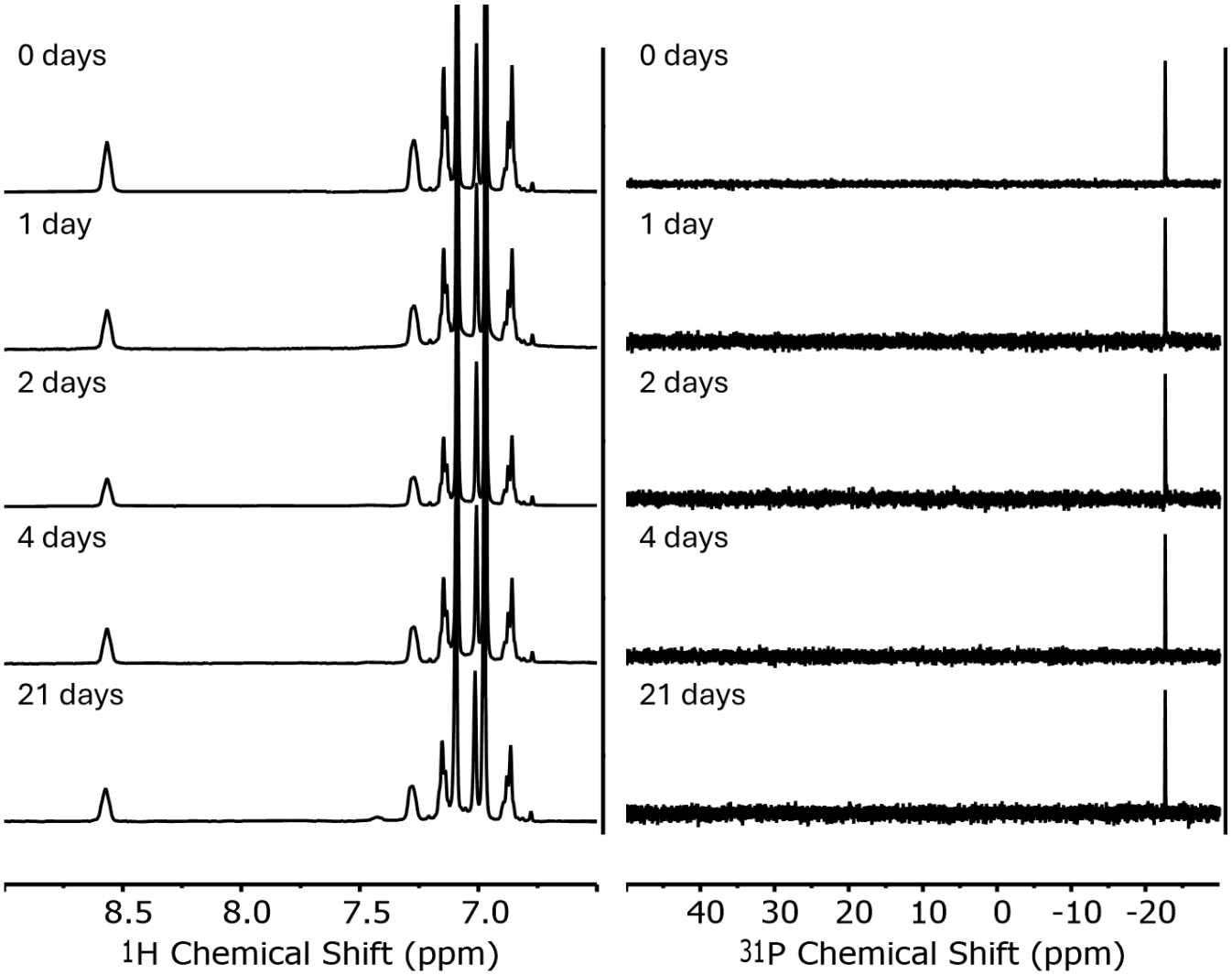

Figure S12: ^{1}H NMR spectra (left, 400 MHz, toluene-d_8) and ^{31}P{^{1}H} NMR spectra (right, 162 MHz, toluene-d_8) of **1•dppo** in toluene-d_8 over the course of 21 days.

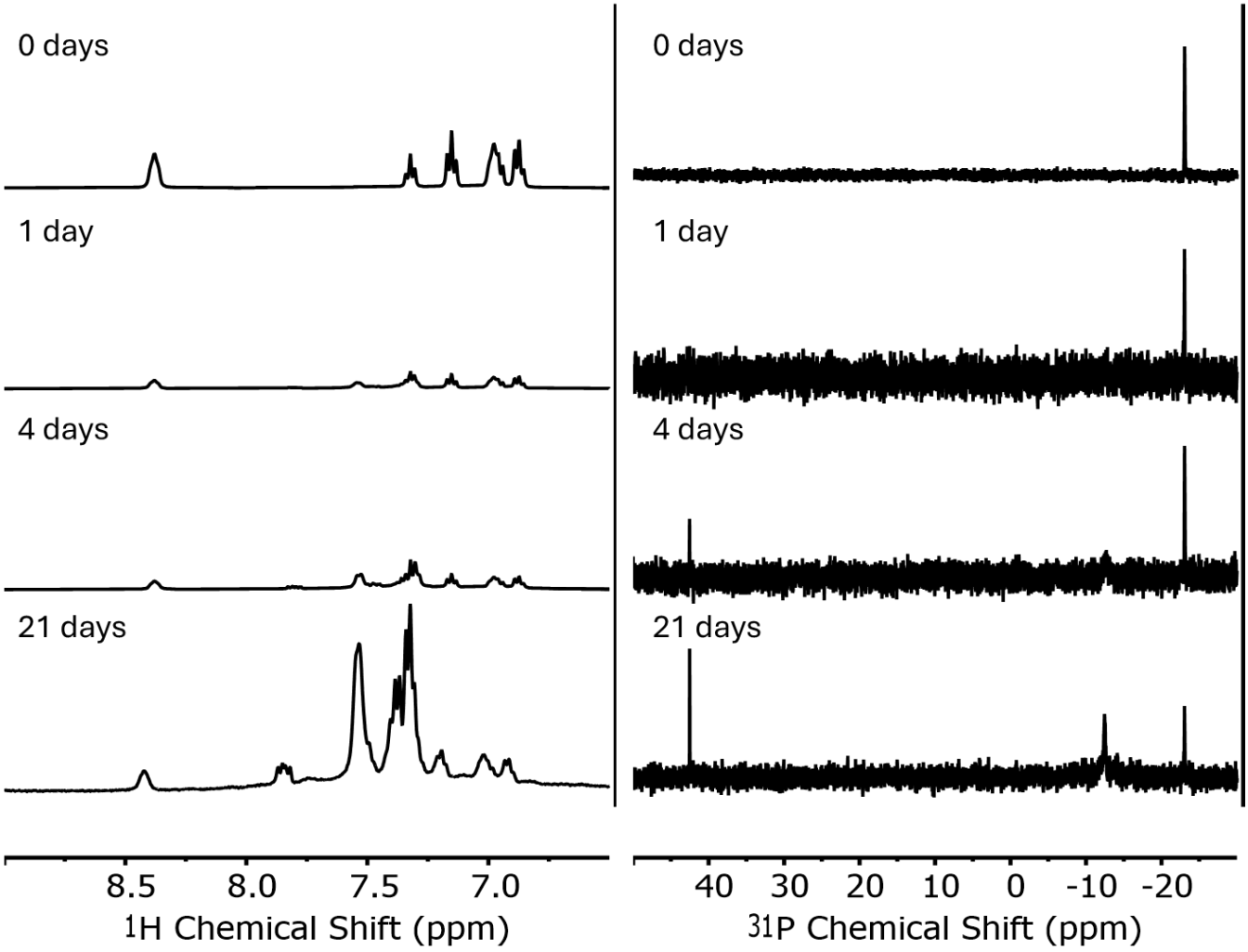

Figure S13: ^{1}H NMR spectra (left, 400 MHz, CD_2Cl_2) and $^{31}P\{^{1}H\}$ NMR spectra (right, 162 MHz, CD_2Cl_2) of **1•dppo** in CD_2Cl_2 over the course of 21 days.

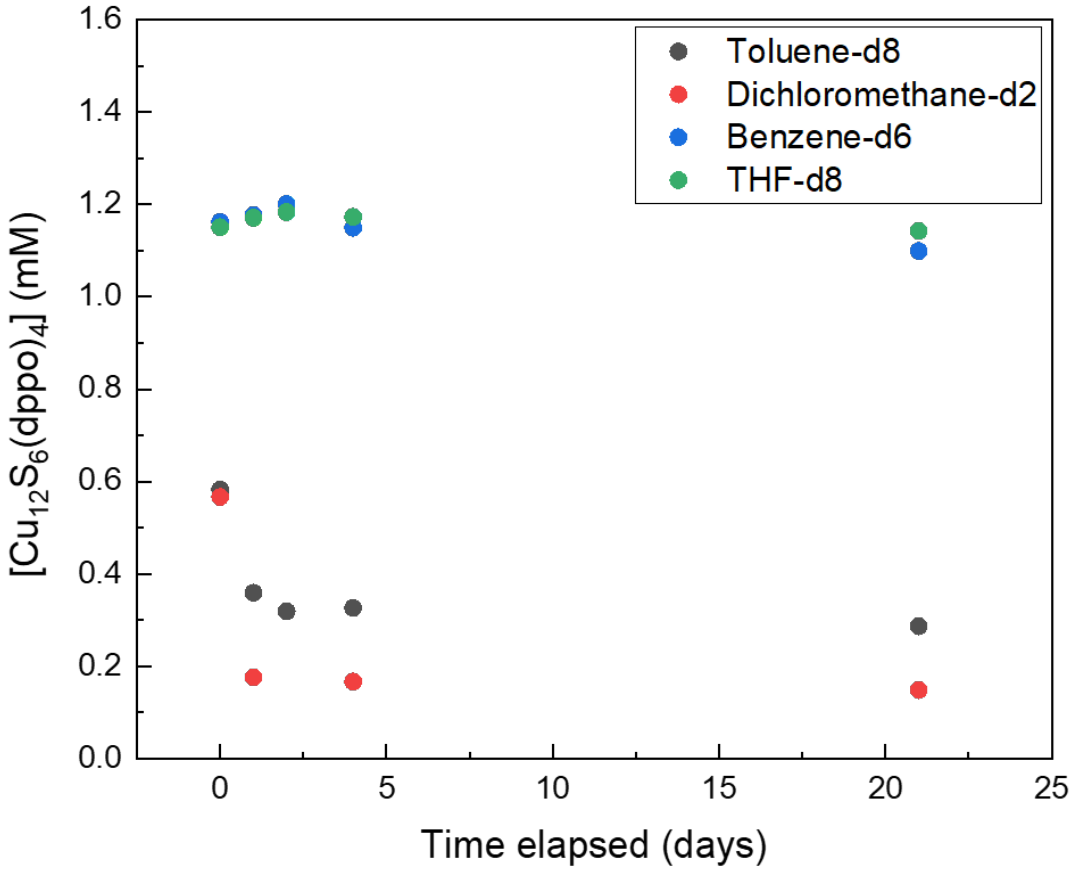

Figure S14: Concentration of **1•dppo** over time in solutions of toluene-d_8, dichloromethane-d_2, benzene-d_6, and THF-d_8. For each solvent, solutions of **1•dppo** are stirred in an air-free and water-free environment inside a nitrogen-filled glovebox. Concentration of **1•dppo** is determined by ^{1}H NMR versus a 1,3,5-trimethoxybenzene internal quantitaive standard.

Electrochemical Characterization

Electrochemical experiments were performed in an N_2-filled glovebox using a WaveNowXV Potentiostat. Data processing was performed using the Aftermath software package (Pine Research). Measurements were taken using a three-electrode setup consisting of a 3 mm diameter glassy carbon disk working electrode (CH Instruments), a platinum wire counter electrode (CH Instruments), and a low-profile non-aqueous silver wire reference electrode and capillary (Pine Research). The glassy carbon disk working electrode was polished with an alumina and water slurry (0.05 μm particle size, BASi Research Products), rinsed with methanol, and dried prior to use. The silver wire reference electrode was lightly polished using 600 grit sandpaper, rinsed with methanol, and dried before insertion into a capillary containing a solution of 100 mM Bu_4NPF_6 electrolyte and 10 mM $AgNO_3$ in acetonitrile. All working electrode potentials were measured versus the $Ag/AgNO_3$ redox couple and calibrated to the $Fc^{0/+}$ redox couple using an internal ferrocene reference. Analyte solutions were prepared from dry, degassed solvent containing 100 mM $[Bu_4N][PF_6]$ as the supporting electrolyte. $[Bu_4N][PF_6]$ electrolyte was purified by thermal recrystallization from ethyl acetate prior to use.

Analysis of the [**1•dppo**]$^{0/+}$ redox couple

The Randles–Ševčík equation, shown below, was used to determine the number of electrons (n) involved in a well-behaved redox couple according to equation S3:

Eq. S3
$$i_p = 0.4463\, nFAC \left(\frac{nF\nu D}{RT}\right)^{1/2}$$

In this equation, i_p is peak current measured at a given scan rate v. The surface area of the working electrode is denoted by A (0.07 cm^2); C is the concentration of analyte (1.00 mM); D is the diffusion coefficient of the analyte in solution at temperature T (298.15 K); F is Faraday's constant (96485 C mol^{-1}); and R is the ideal gas constant (8.3145 J mol^{-1} K^{-1}). The diffusion coefficient of **1•dppo** was determined by ^1H DOSY NMR measurements taken under identical conditions (THF-d_8 at 25 °C: $D = 5.1 \times 10^{-6}$ cm^2/s) and used to solve for the number of electrons involved in the redox couple measured at –0.50 V vs $Fc^{0/+}$ (Table S2). Based on these results, we conclude that the wave measured at –0.50 V vs $Fc^{0/+}$ corresponds to a one-electron redox couple, and thus assign this feature as the [**1•dppo**]$^{0/+}$ redox couple. Minor systematic decreases in i_{pa} arise from distortion of the baseline at faster scan rates.

Table S2: Randles–Ševčík analysis of [**1•dppo**]$^{0/+}$

Scan rate (mV/s)	Anodic peak current (i_{pa}, μA)	Estimated number of electrons (n)
10	3.95	0.95
20	5.26	0.91
50	7.64	0.86
100	11.1	0.87
250	15.7	0.81
500	21.0	0.79

A scan rate dependence study was conducted to assess the (electro)chemical reversibility of the [**1•dppo**]$^{0/+}$ redox couple. Within a scan window of –0.15 to –0.85 V, the ratio of the anodic and cathodic peak currents i_{pa}/i_{pc} is measured to be 1.12, indicating quasireversibility. The peak-to-peak separation, ΔE_p, increases from 84 mV at a scan rate of 10 mV/s to 224 mV at 500 mV/s consistent with the low conductivity of the THF solvent medium.

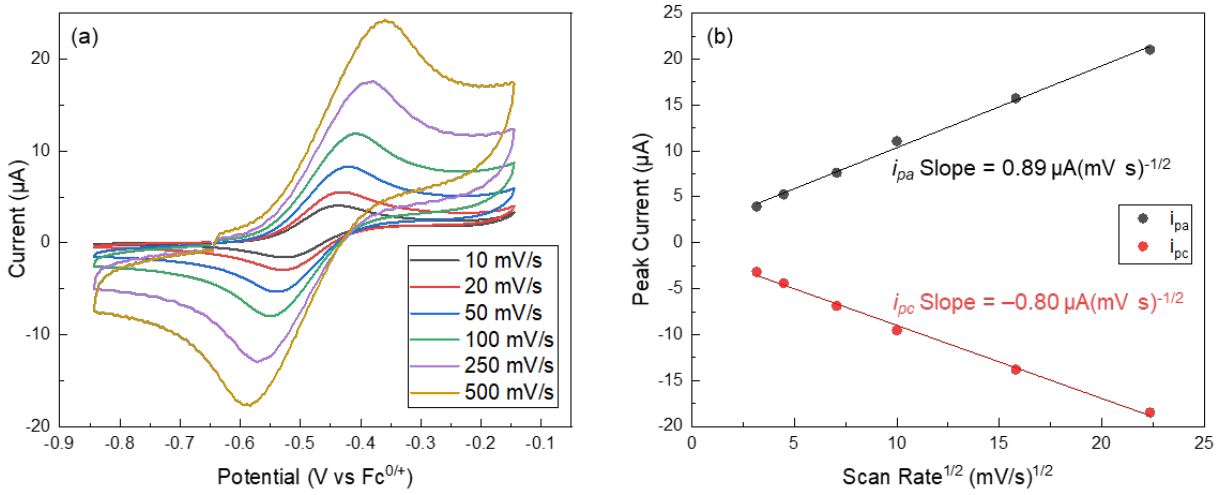

Figure S15: Cyclic voltammograms of **1•dppo** (1 mM **1•dppo**; 100 mM $[Bu_4N][PF_6]$ in THF) collected at scan rates of 10-500 mV/s (a) and anodic (i_{pa}) and cathodic (i_{pc}) peak currents, plotted versus the square root of scan rate (b).

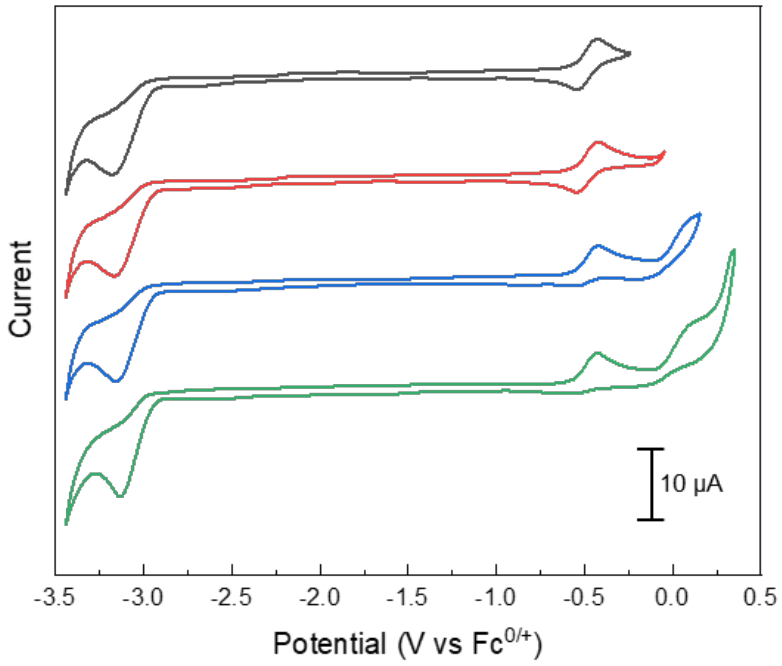

Figure S16: Cyclic voltammograms collected for **1•dppo** (1 mM **1•dppo** and 100 mM $[Bu_4N][PF_6]$ in THF; 20 mV/s) with varied scan windows showing that the quasireversibility of the $[\mathbf{1•dppo}]^{0/+}$ redox couple is lost when scanning is performed beyond the onset of irreversible oxidation events.

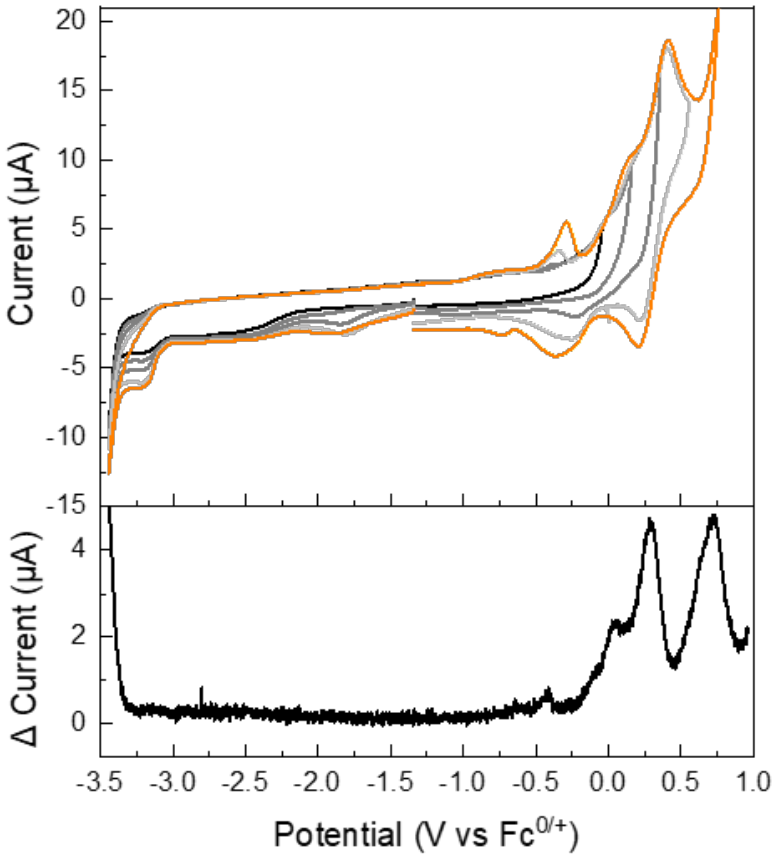

Figure S17. (Top) Cyclic voltammetry and (Bottom) differential pulse voltammetry measurements of **1•dppt** (<1 mM **1•dppt** and 100 mM $[Bu_4N][PF_6]$ in THF; 100 mV/s) collected over a range of anodic vertex potentials. Voltammograms collected over the narrowest and widest scan windows are highlighted in black and orange traces, respectively.

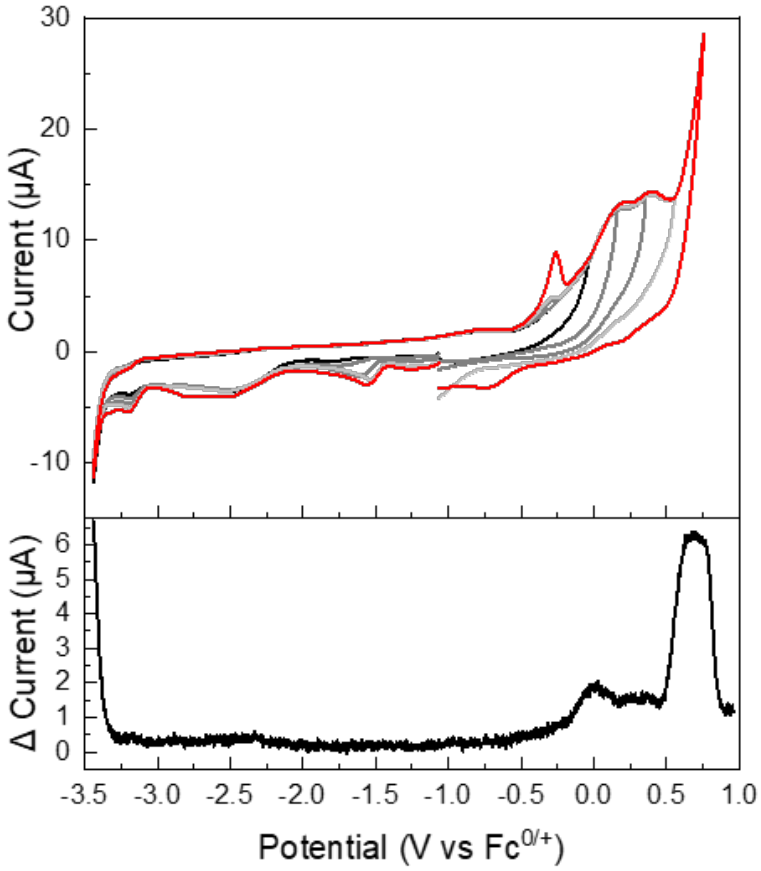

Figure S18. (Top) Cyclic voltammetry and (Bottom) differential pulse voltammetry measurements of **1•PPh$_2$Et** (1 mM **1• PPh$_2$Et** and 100 mM [Bu$_4$N][PF$_6$] in THF; 100 mV/s) collected over a range of anodic vertex potentials. Voltammograms collected over the narrowest and widest scan windows are highlighted in black and red traces, respectively.

Oxidative Reactivity Studies

Redox titrations of **1•dppo** with [Cp*$_2$Fe][PF$_6$]. Redox titrations were performed using stock solutions of **1•dppo** (2.5 mM) and 1,3,5-trimethoxybenzene (TMB; 2.5 mM) in THF-d$_8$ and a stock solution of [Cp*$_2$Fe][PF$_6$] in CD$_3$CN (62.5 mM). Seven separate vials were charged with 0.25 mL each of the **1•dppo** and TMB stock solution and then chilled to 0 °C in the glovebox cold well. To each vial was added [Cp*$_2$Fe][PF$_6$] stock solution (0/10/20/30/40/50/60 μL; 0.0/0.5/1.0/1.5/2.0/ 2.5/3.0 equivalents of [Cp*$_2$Fe]$^+$). The contents were stirred for 30 min at 0 °C followed by 30 min at RT. Reaction solutions, ranging from red to orange in color depending on the number of [Cp*$_2$Fe][PF$_6$] equivalents added, were transferred to NMR tubes for analysis. Concentrations of **1•dppo** and phosphine sulfide products were determined by quantitative ^{1}H NMR relative to TMB. Concentrations of **1•dppo** were determined via the summed integrations of the signals for the cisoid Ph *o*-C*H* (8.47 ppm) and transoid Ph *o*-C*H* (7.06 ppm), while the phosphine sulfide products were quantitated by the integration of the Ph *o*-C*H* (7.94 ppm). Because this latter signal may correspond to either the monosulfide or the disulfide products dppoS and dppoS$_2$, we track the concentrations shown in Figure 5 of the main text according to phosphorus atom equivalents (in **1•dppo**, dppoS, and dppoS$_2$, there are four diagnostic Ph *o*-C*H* per phosphorus atom).

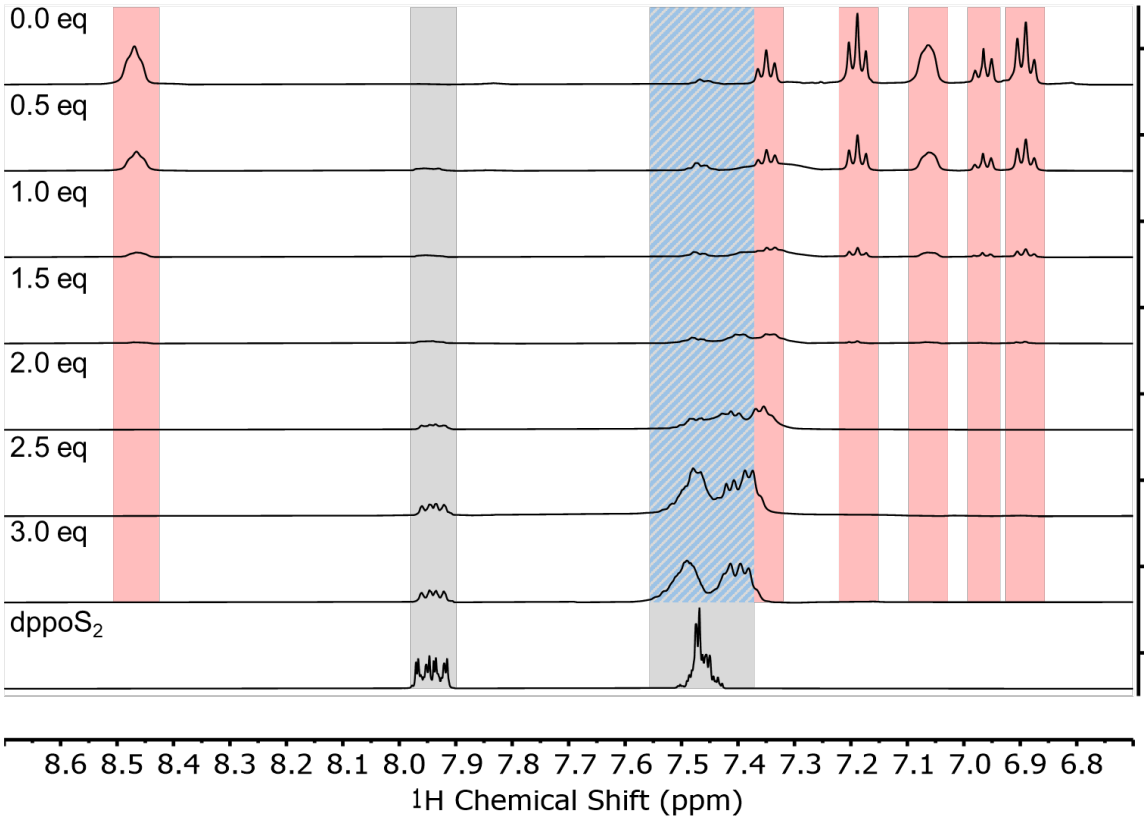

Figure S19: Redox titrations of **1•dppo** and [Cp*$_2$Fe][PF$_6$]: ^{1}H NMR analysis conducted in THF-d$_8$/CD$_3$CN (400 MHz) for reactions in which 0.0/0.5/1.0/1.5/2.0/2.5/3.0 equiv [Cp*$_2$Fe][PF$_6$] together with independently synthesized dppoS$_2$ (THF-d$_8$, 400 MHz; bottom). Color scheme: **1•dppo**, red; phosphine sulfide Ph *o*-C*H*, grey. Other signals corresponding to residual dppo of cluster decomposition products overlap with meta and para phenyl protons of phosphine sulfide products. These signals are highlighted in a grey and blue striped pattern.

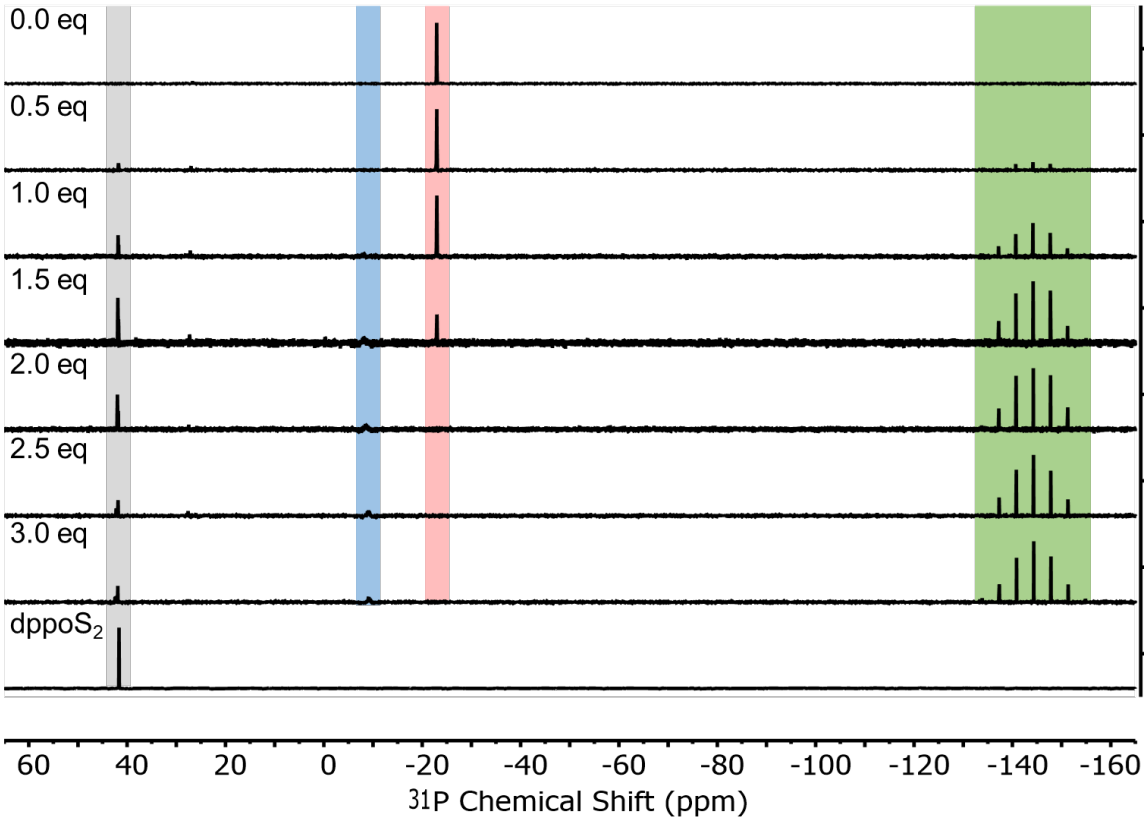

Figure S20: $^{31}P\{^{1}H\}$ NMR spectra for **1•dppo** reacted with 0.0/0.5/1.0/1.5/2.0/2.5/3.0 equivalents of $[Cp^*_2Fe][PF_6]$ (THF-d_8/CD_3CN, 162 MHz) and independently synthesized $dppoS_2$ (THF-d_8, 400 MHz). Color scheme: **1•dppo**, red; phosphine sulfide Ph *o*-C*H*, grey. Other signals corresponding to residual dppo of cluster decomposition products overlap with meta and para phenyl protons of phosphine sulfide products. These signals are highlighted in a grey and blue striped pattern. Signals corresponding to the $[PF_6]^-$ counterion are highlighted in green.

Reactivity of **1•dppo** with air.

A THF-d_8 solution of **1•dppo** and TMB (internal standard for quantitative NMR; ca. 1:1 concentration versus **1•dppo**) was prepared in an NMR tube. After collecting initial ^{1}H and $^{31}P\{^{1}H\}$ NMR spectra, the sample was briefly exposed to air (ca. 1 min), shaken vigorously, and then recapped. ^{1}H and $^{31}P\{^{1}H\}$ NMR spectra were then collected again 1 week later. After this period, the amount of **1•dppo** present in solution was 30% of its original concentration based on integration of the diagnostic ^{1}H NMR signal for the cisoid Ph *o*-C*H* proton.

^{1}H NMR (THF-d_8, 400 MHz; t = 0): δ 8.43(**1•dppo**, cisoid Ph o-C*H*; 30%). $^{31}P\{^{1}H\}$ NMR (THF-d_8, 400 MHz; t = 0): δ -23.0 (**1•dppo**, $[Cu_{12}S_6]$-**P**).

The major oxidation products observed by ^{1}H and $^{31}P\{^{1}H\}$ NMR were assigned as the corresponding dppo phosphine oxides and phosphine sulfides (dppoO/$dppoO_2$ and dppoS/$dppoS_2$) by comparison of the diagnostic ^{1}H NMR signals (for the Ph *o*-C*H* protons) and $^{31}P\{^{1}H\}$ NMR signals to authentic samples of $dppoO_2$ and $dppoS_2$. These results demonstrate that **1•dppo** is air-sensitive in solution and slowly degrades via intramolecular P=S bond formation or direct oxygenation of the supporting dppo ligands.

NMR characterization for 1,8-bis(diphenylphosphino)octane dioxide is reported for deuterated chloroform. ^{1}H NMR ($CDCl_3$, 400 MHz): δ 7.75-7.66 (Ph o-C*H*), ^{31}P{^{1}H} NMR ($CDCl_3$, 400 MHz): δ 33.2.[10] These values closely match our observations in THF-d_8 for what we assign as 1,8-bis(diphenylphosphino)octane dioxide: ^{1}H NMR (THF-d_8, 400 MHz): δ 7.80 (Ph o-C*H*; 51%). ^{31}P{^{1}H} NMR (THF-d_8, 400 MHz): δ 27.4.

We performed the independent synthesis and characterization of 1,8-bis(diphenylphosphino)octane disulfide as outlined in the synthesis section above: ^{1}H NMR (THF-d_8, 400 MHz): δ 7.91 (Ph o-C*H*; 19%). ^{31}P{^{1}H} NMR (THF-d_8, 400 MHz): δ 41.6.

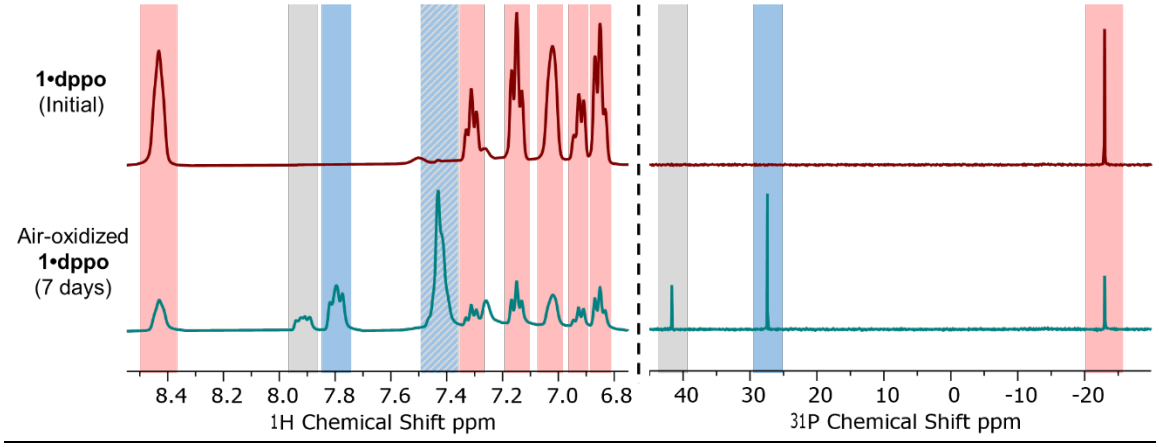

Figure S21: Stacked ^{1}H and ^{31}P{^{1}H} NMR spectra (left and right, respectively, 400 MHz, THF-d_8)of **1•dppo** prepared under a nitrogen atmosphere (top) and the same sample after exposure to air for one week (bottom). Color scheme: **1•dppo**, red; phosphine sulfide Ph *o*-C*H*, grey. Other signals corresponding to residual dppo of cluster decomposition products overlap with meta and para phenyl protons of phosphine sulfide products. These signals are highlighted in a grey and blue striped pattern.

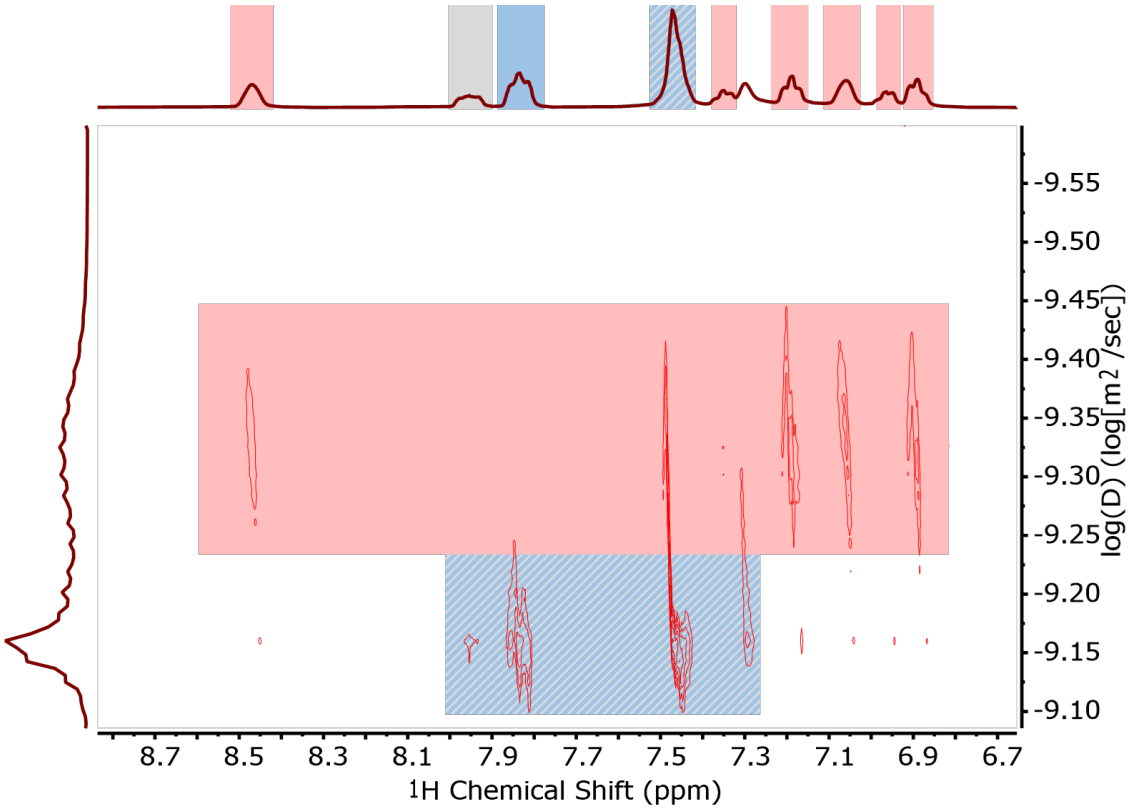

Figure S22: ^{1}H DOSY spectrum of **1•dppo** (400 MHz, THF-d_8) after exposure to air for one week. Color scheme: **1•dppo**, red; phosphine sulfide Ph *o*-C*H*, grey. Other signals corresponding to residual dppo of cluster decomposition products overlap with meta and para phenyl protons of phosphine sulfide products. These signals are highlighted in a grey and blue striped pattern.

Powder X-ray Diffraction (PXRD) Analysis

Powder X-ray diffraction (PXRD) measurements were performed at RT using a Rigaku Smartlab SE diffractometer. Optics alignment was performed prior to each measurement, and the signal intensities presented in Figure S23 are scaled according to the peak intensity detected along the ω-axis. Samples for PXRD were prepared by grinding the dried crystalline material to a fine powder using a glass mortar and pestle.

Oxidative reactivity studies of **1•dppo**. To assess the air-sensitivity of **1•dppo**, samples of **1•dppo** were exposed to air in the solid state and then subjected to PXRD analysis. For comparison, a chemically oxidized sample of **1•dppo** was subjected to a similar analysis as follows.

1) *Air oxidation in the solid state:* **1•dppo** was freshly prepared as described above and a sample was subjected to PXRD analysis (Figure S23, red trace). The same sample was then left exposed to air under ambient conditions for 14 days, after which time the PXRD pattern was measured again (Figure S23, black trace). The air-oxidized sample showed brown discoloration from the original red color of fresh **1•dppo** but exhibited a very similar PXRD pattern to the original cluster, with a slightly higher baseline.

2) *Chemical oxidation:* These studies followed a similar protocol to the redox titrations described above. A 250 mL bottle was charged with solid **1•dppo** (153.5 mg, 0.05 mmol) and 2-methyltetrahydrofuran (45 mL) and the resulting red solution was chilled to 0 °C. Separately, a 20 mL vial was charged with solid

[Cp^*_2Fe][PF_6] (56.2 mg, 0.12 mmol, 2.4 equiv) and acetonitrile (2 mL). This stock solution of [Cp^*_2Fe][PF_6] was added to the chilled **1•dppo** solution and allowed to stir at 0 °C for 2 hours before warming to RT and stirring for an additional hour. During this time, the solution changed from red to orange in color. Solvent was removed in vacuo and the resulting brown solid was triturated with diethyl ether to dissolve Cp^*_2Fe formed from the reaction. The diethyl ether suspension was filtered through a coarse porosity glass frit, and dried in vacuo to afford a brown powder (159.2 mg) that was analyzed by PXRD (Figure S23, gray trace). The PXRD pattern of the chemically-oxidized sample appeared amorphous with a wide, low-intensity signal at ~20° that roughly aligns with the distorted baseline of the partially oxidized air-exposed sample of **1•dppo** (black trace, Figure S23)

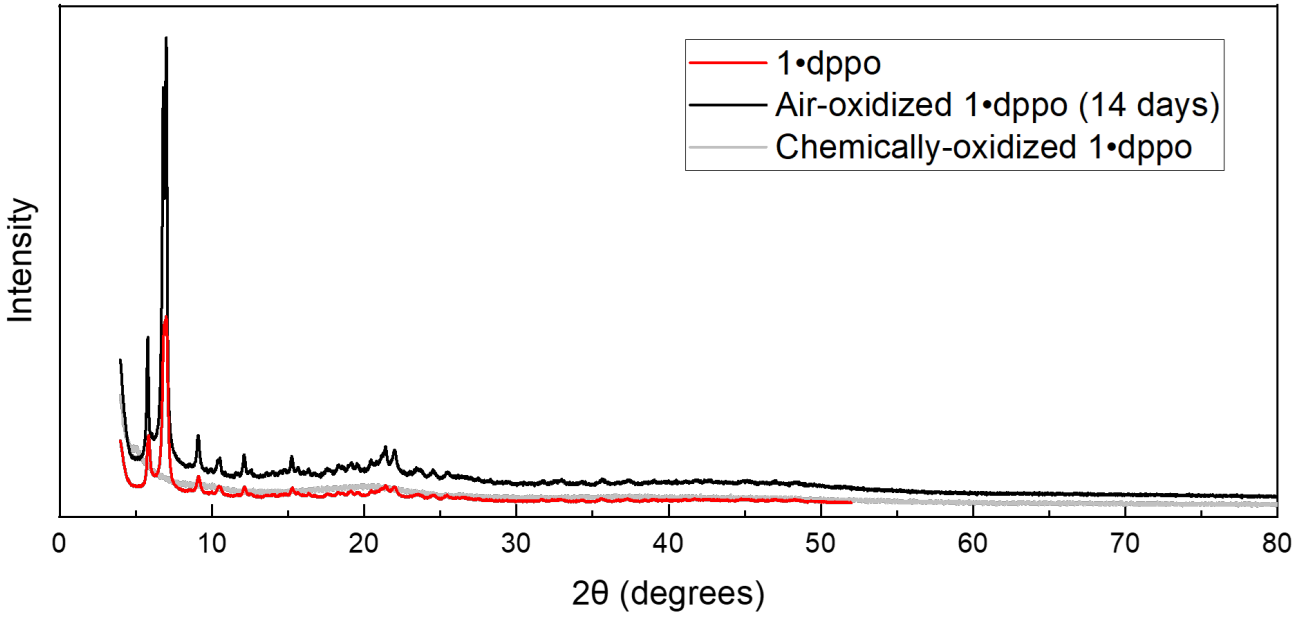

Figure S23: Powder X-ray diffraction patterns collected for **1•dppo** (red trace), the same sample of **1•dppo** after exposure to air for 14 days (black trace), and a sample of **1•dppo** treated with [Cp^*_2Fe][PF_6] (grey trace).

Analysis of crystallographic metrics for clusters 1

Based on reported crystallographic data for clusters **1**,[1,8] there exist three types of Cu–S bonds within the [$Cu_{12}S_6$] nanocluster core: those that comprise the Cu_4S pyramid substructures present at opposite ends of the cluster (colored blue in Figure S24), those that comprise the Cu_4S_4 equator substructure at center of the cluster (colored green in Figure S24), and those that span across the cluster to connect the Cu_4S and Cu_4S_4 substructures (colored red in Figure S24). Among these three types of Cu–S bonds, those spanning across the cluster display consistently longer bond lengths (Table S3), suggesting that they are relatively weaker. Among clusters **1•PPh_2Et, 1•dppt,** and **1•dppo**, only **1•dppo** possesses ditopic ligands that support these Cu–S bonds by binding at opposite ends of the cluster core. This is consistent with the unique solution stability observed for **1•dppo**.

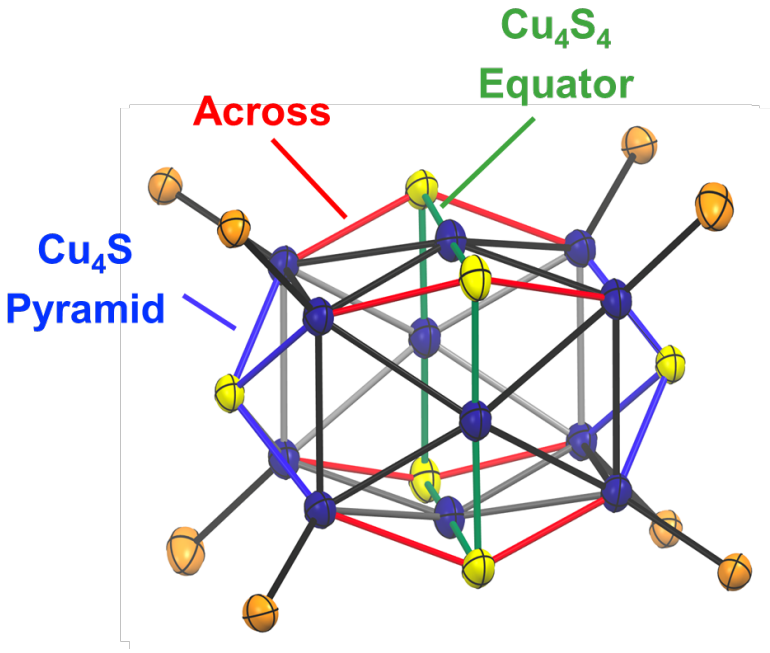

Figure S24: Classification of Cu–S bonds in $Cu_{12}S_6$ clusters **1**.

Table S3: Crystallographic Cu–S bond distances (Å) reported for clusters **1**

1•PPh_2Et[8]			**1•dppt**[1]			**1•dppo**[1]		
Cu_4S Pyramid	Cu_4S_4 Equator	Across	Cu_4S Pyramid	Cu_4S_4 Equator	Across	Cu_4S Pyramid	Cu_4S_4 Equator	Across
2.264	2.175	2.399	2.261	2.155	2.378	2.261	2.170	2.372
2.271	2.136	2.387	2.268	2.168	2.378	2.270	2.174	2.367
2.252	2.183	2.377	2.261	2.159	2.368	2.266	2.175	2.357
2.267	2.152	2.373	2.268	2.169	2.368	2.271	2.180	2.364
2.264	2.175	2.387	2.261	2.155	2.378	2.60	2.176	2.364
2.271	2.136	2.399	2.268	2.168	2.378	2.266	2.179	2.371
2.252	2.183	2.373	2.261	2.159	2.368	2.268	2.174	2.368
2.267	2.152	2.377	2.268	2.169	2.368	2.252	2.174	2.368
Avg. 2.264	**Avg. 2.162**	**Avg. 2.384**	**Avg. 2.265**	**Avg. 2.163**	**Avg. 2.373**	**Avg. 2.264**	**Avg. 2.175**	**Avg. 2.366**
St. Dev. 0.006	**St. Dev. 0.003**	**St. Dev. 0.004**	**St. Dev. 0.004**	**St. Dev. 0.006**	**St. Dev. 0.005**	**St. Dev. 0.007**	**St. Dev. 0.019**	**St. Dev. 0.010**

From the same crystallographic data sets, we note that one set of the phenyl rings in coordinated phosphine ligands are closely packed in a propeller-shaped configuration about the Cu_4S pyramid substructures of the cluster **1•dppo** (Figure 2c in the main text).[1,8] This places half of the Ph *o*-C*H* (the position of which in reported crystallographic data is calculated using a riding model) in close proximity to the apical Cu_4S sulfides (CH---S: 2.78 ± 0.2 Å, ∠142–164°; Table S4). By comparison, tabulated data compiled from the Cambridge Crystallographic Data Center (CCDC)[11] reveals most CH---SM (M = group 11 transition metal) contacts to lie in the range of 2.84-3.40 Å with CH---S angles between 117–135° or 144–180°, and thus the values observed for **1•dppo** Ph *o*-CH are among the shortest of CH---SM contacts observed for group 11 metals to date. In addition, these values lie well below the sum of the van der Waals radii (3.00 Å) for H and S and are consistent with substantial attractive CH---S interactions being present.

Relatively short Ph o-CH---S distances are also observed for **1•dppt** and **1•PPh_2Et**, suggesting that attractive interactions may exist in these clusters as well (avg. 2.92 ± 0.21 & 2.87 ± 0.12 Å, respectively; Table S4). However, even with the dppt and PPh_2Et ligands remaining bound in place, the clusters **1•dppt** and **1•PPh_2Et** still contain unsupported Cu–S bonds along at least two axes of the $[Cu_{12}S_6]$ core. We conclude that while attractive CH---S interactions may contribute to the rigid, locked configuration of ligands about **1•dppo**, the primary cause of stability remains the long octyl linker which allows the ligands to favourably span across all 3 axes of the core.

Table S4: Crystallographic Ph *o*-CH---S distances and angles reported for clusters **1**

1•PPh_2Et[8]		**1•dppt**[1]		**1•dppo**[1]	
d(CH---S) (Å)	∠(C-H-S) (°)	d(CH---S) (Å)	∠(C-H-S) (°)	d(CH---S) (Å)	∠(C-H-S) (°)
2.892	158.1	3.051	133.8	2.841	141.9
2.814	163.1	2.890	160.3	2.681	162.1
2.945	161.4	2.795	133.5	2.818	153.5
2.842	165.6	2.924	152.9	2.790	155.4
2.892	158.1	3.051	133.8	2.778	158.7
2.814	163.1	2.890	160.3	2.702	164.0
2.945	161.4	2.795	133.5	2.985	148.9
2.842	165.6	2.924	152.9	2.694	158.9
Avg. 2.873	**Avg. 162.0**	**Avg. 2.915**	**Avg. 145.1**	**Avg. 2.786**	**Avg. 155.4**
Std. Dev. 0.115	**Std. Dev. 6.3**	**Std. Dev. 0.212**	**Std. Dev. 27.3**	**Std. Dev. 0.100**	**Std. Dev. 7.3**

NMR SPECTRA

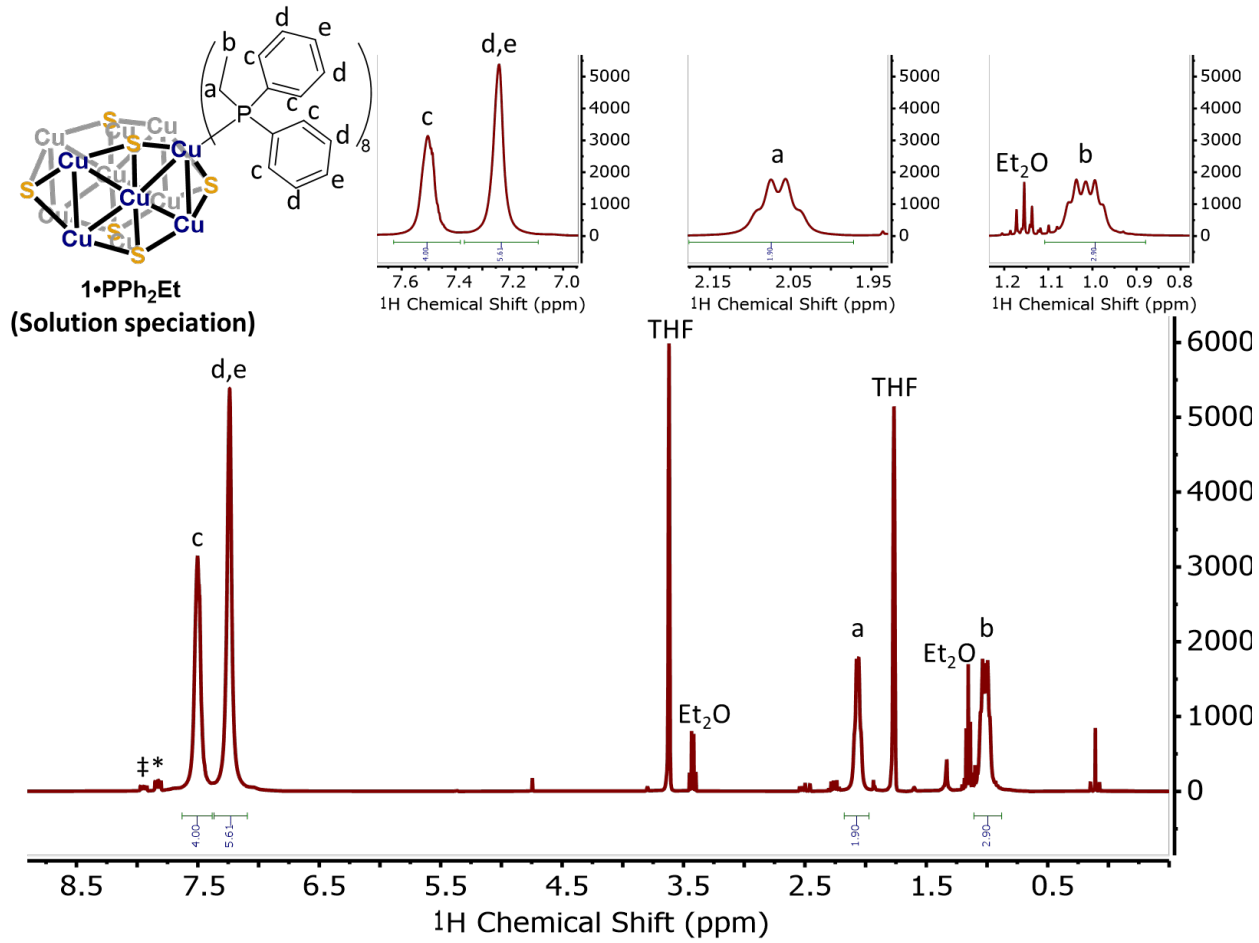

Figure S25: ^{1}H NMR spectrum of **1•PPh$_2$Et** (400 MHz, THF-d$_8$) showing solution speciation. Trace phosphine oxides and phosphine sulfides are marked by * and ‡, respectively.

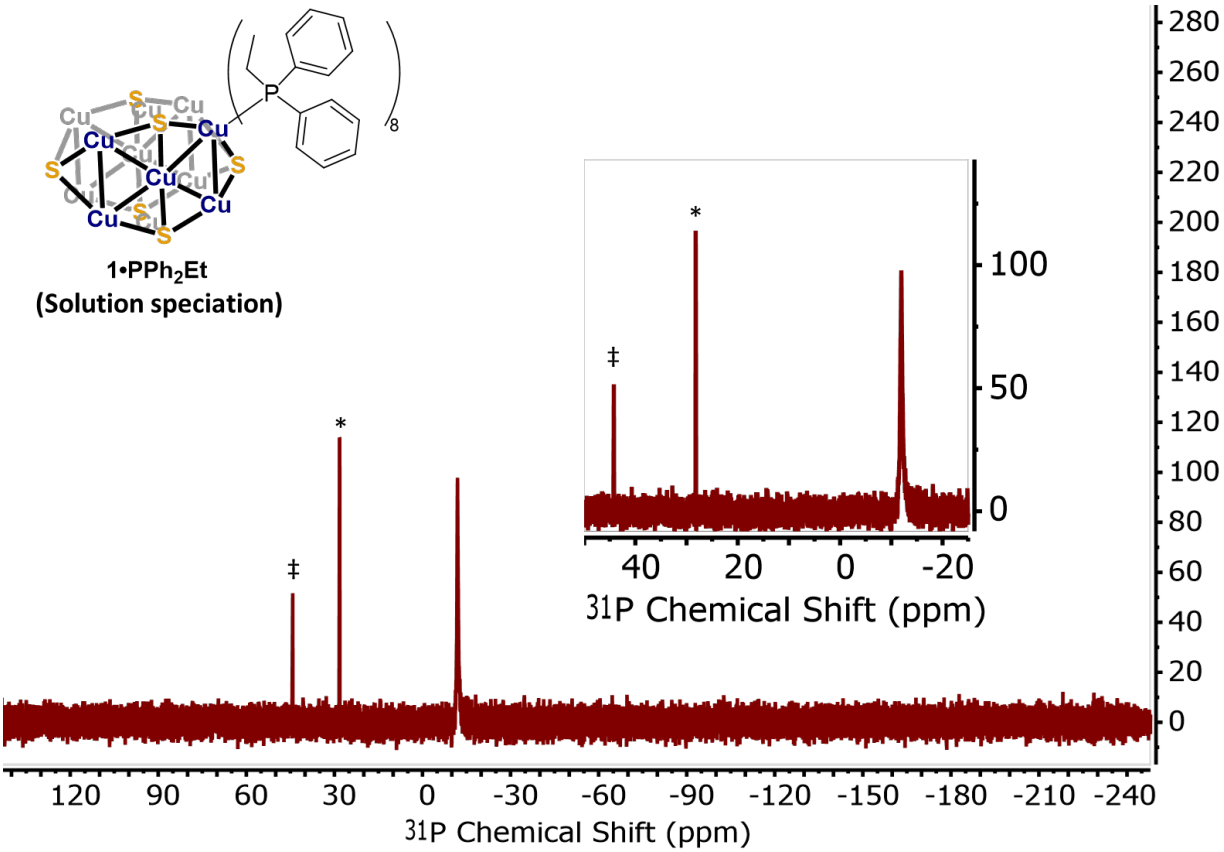

Figure S26: $^{31}P\{^{1}H\}$ NMR spectrum of **1•PPh$_2$Et** (162 MHz, THF-d$_8$) showing evidence of solution speciation. The ^{31}P NMR shift of **1•PPh$_2$Et** matches that of free ligand PPh$_2$Et but shows a broadened signal. Trace phosphine oxides and phosphine sulfides are marked by * and ‡, respectively.

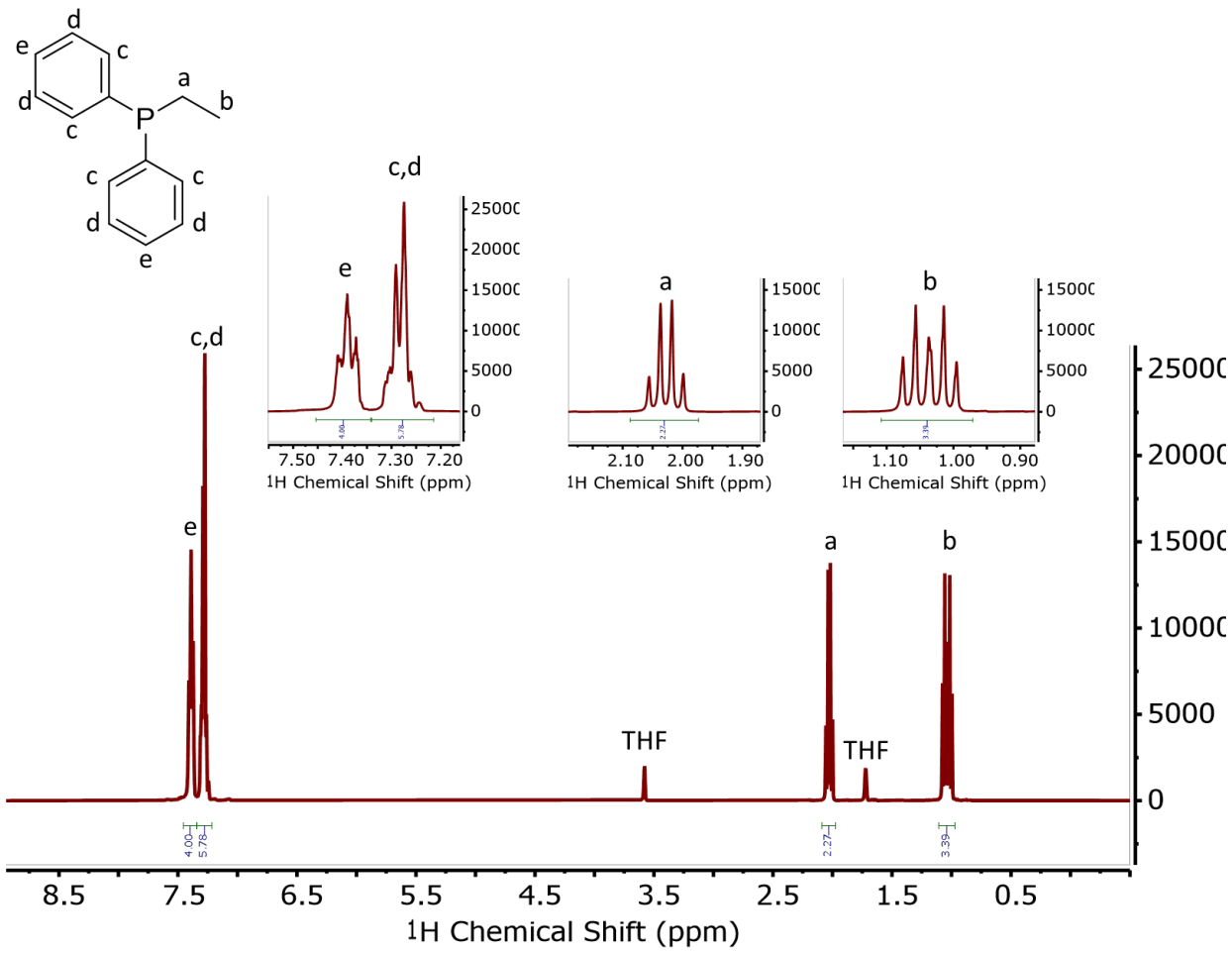

Figure S27: ^{1}H NMR spectrum of the free ligand PPh_2Et (400 MHz, THF-d_8).

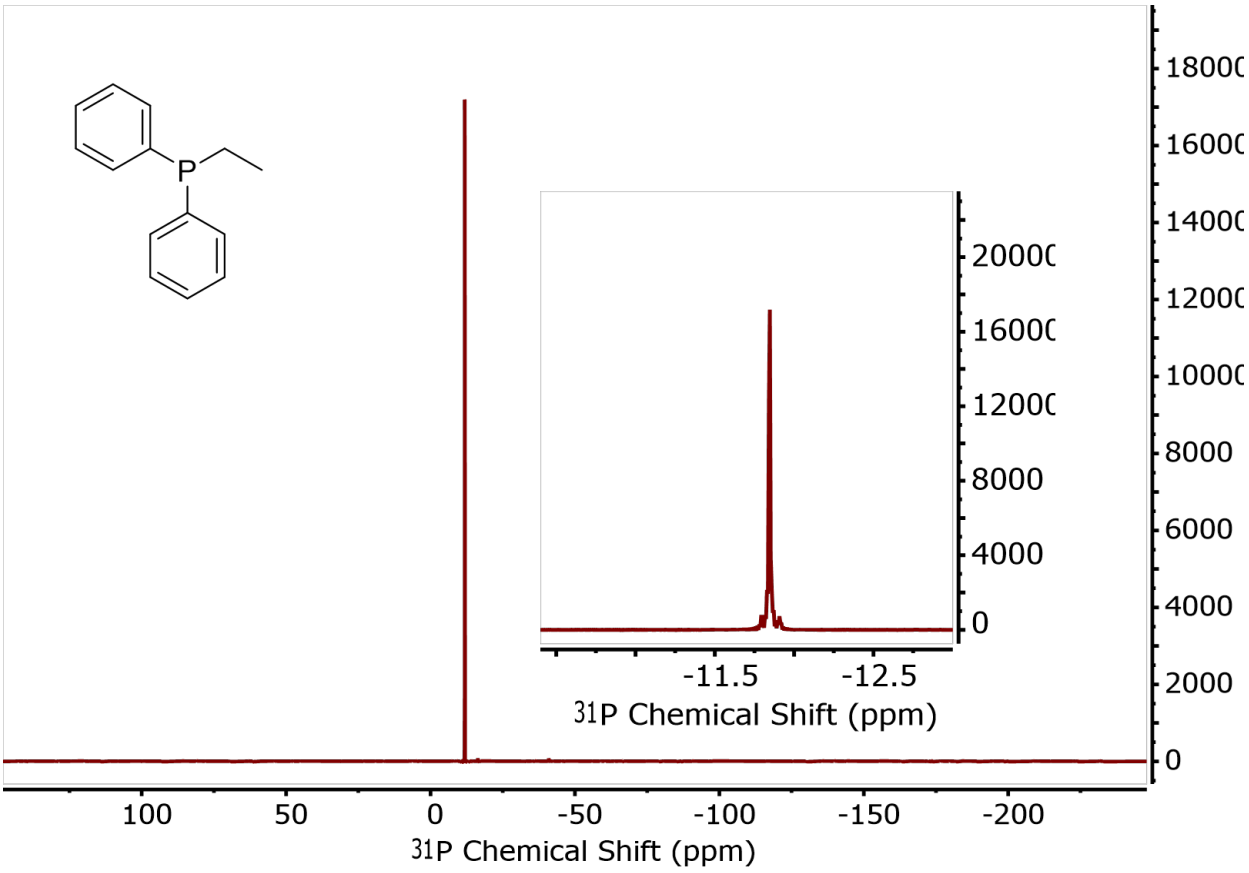

Figure S28: $^{31}P\{^{1}H\}$ NMR spectrum of the free ligand PPh_2Et (162 MHz, THF-d_8).

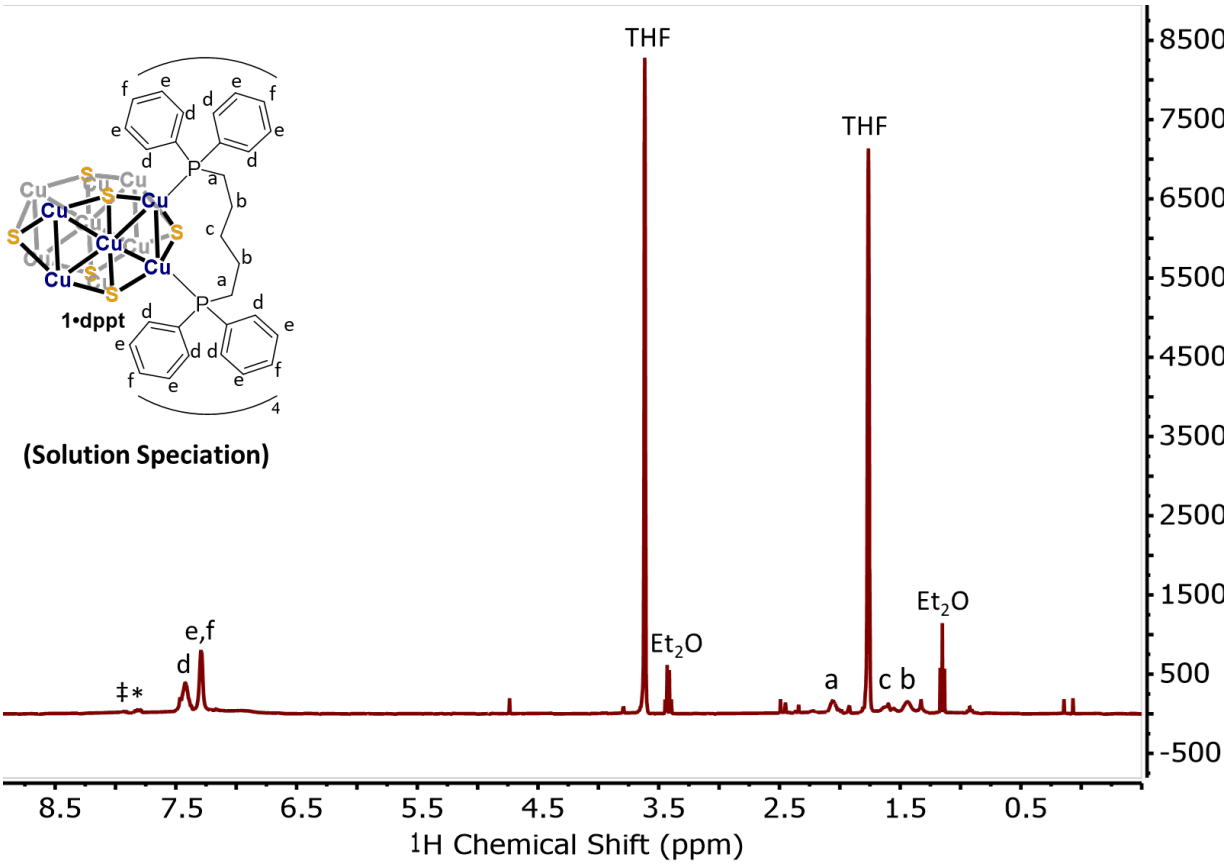

Figure S29: ^{1}H NMR spectrum of **1•dppt** (400 MHz, THF-d_8) showing evidence of solution speciation. Trace phosphine oxides and phosphine sulfides are marked by * and ‡, respectively.

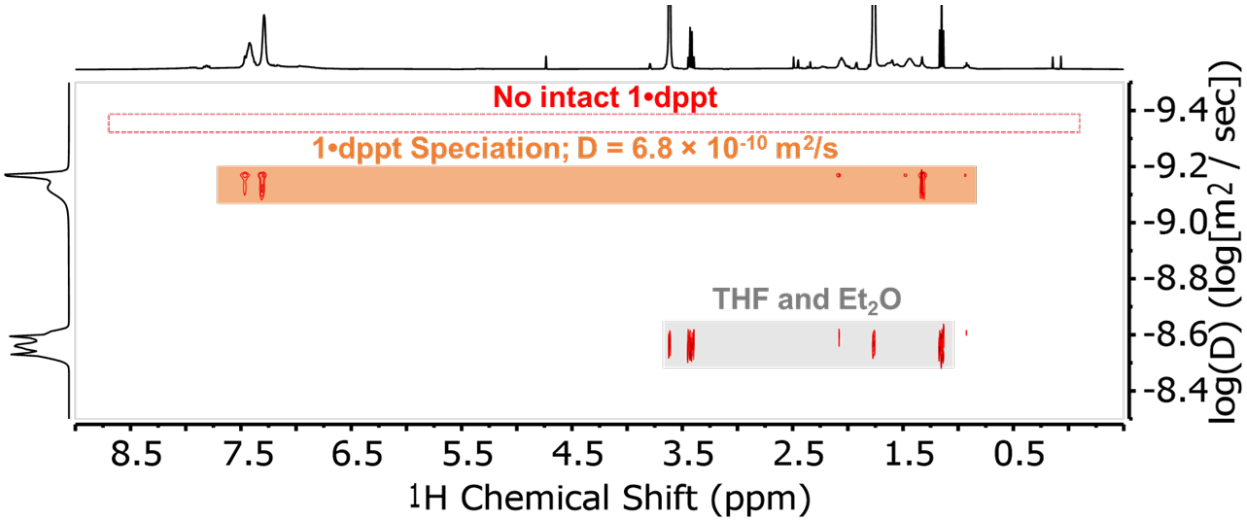

Figure S30: ^{1}H DOSY NMR spectrum of **1•dppt** (400 MHz, THF-d_8) showing evidence of solution speciation. The measured diffusion coefficient D = 6.8 × 10^{-10} m^2/s corresponds to a hydrodynamic radius of r_H = 7.0 Å, whereas crystallographic characterization of **1•dppt**[1] predicts a radius of 9.2 Å for the intact cluster.

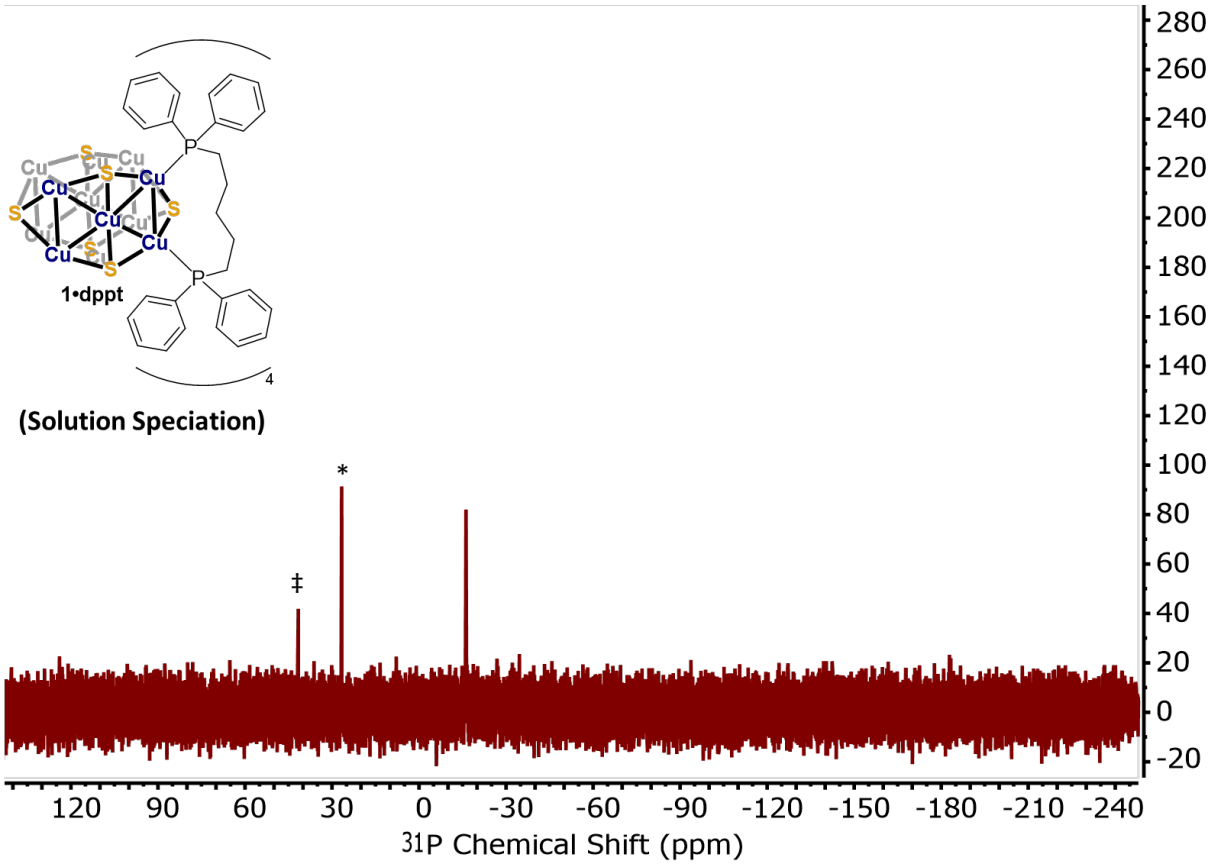

Figure S31: $^{31}P\{^{1}H\}$ NMR spectrum of **1•dppt** (162 MHz, THF-d_8) showing evidence of solution speciation. Trace phosphine oxides and phosphine sulfides are marked by * and ‡, respectively.

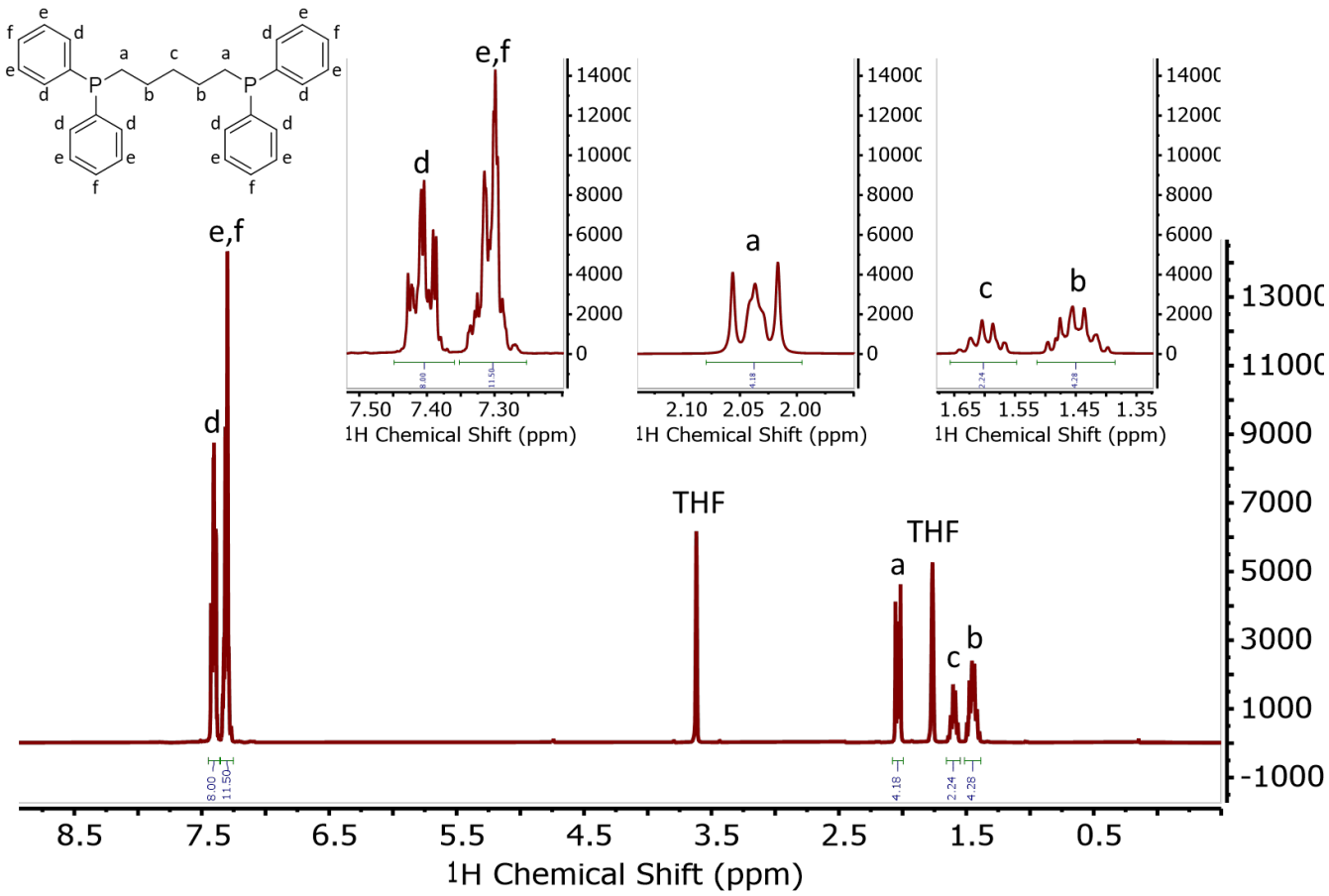

Figure S32: ^{1}H NMR spectrum of the free ligand dppt (400 MHz, THF-d_8).

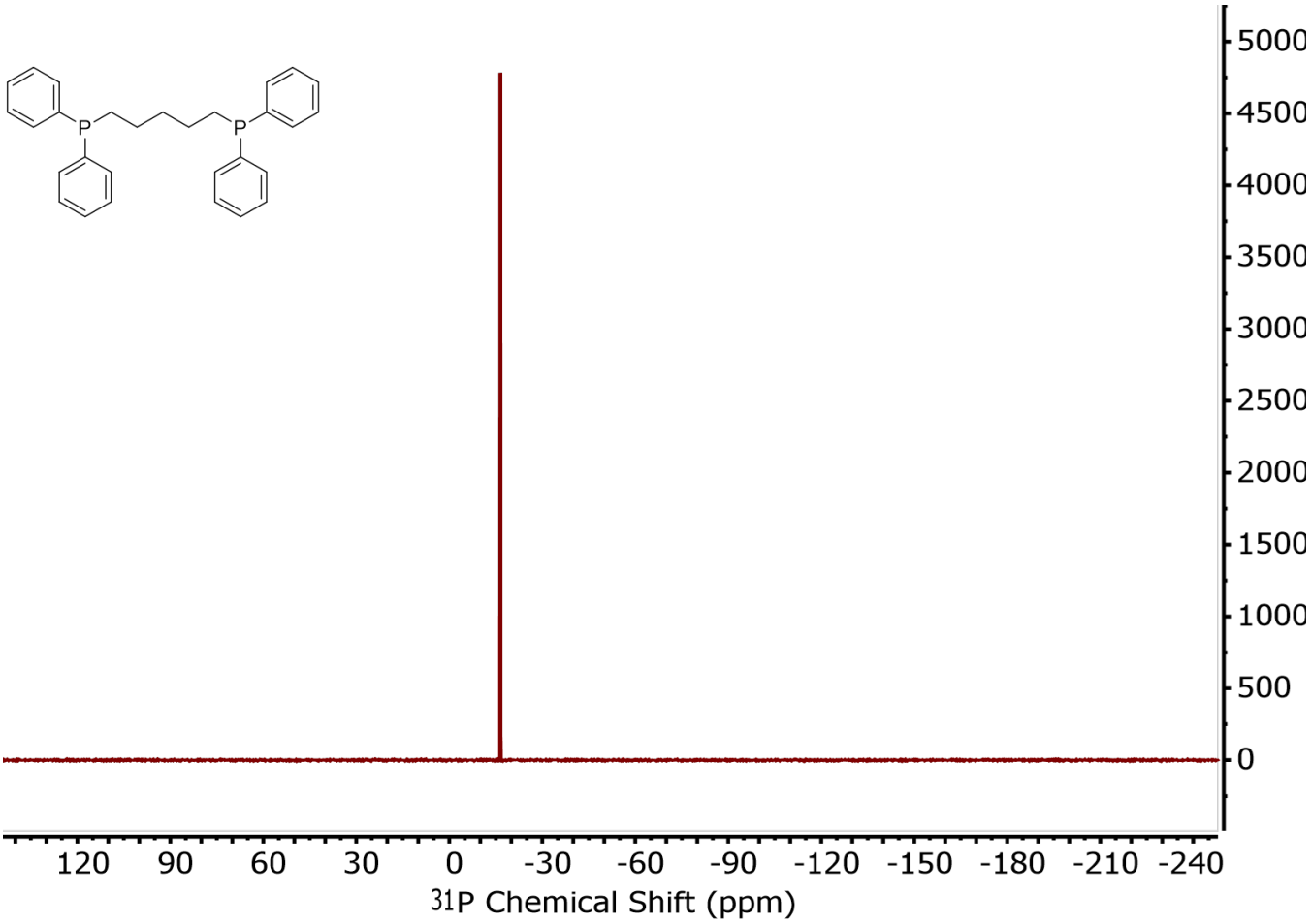

Figure S33: $^{31}P\{^{1}H\}$ NMR spectrum of the free ligand dppt (162 MHz, THF-d_8).

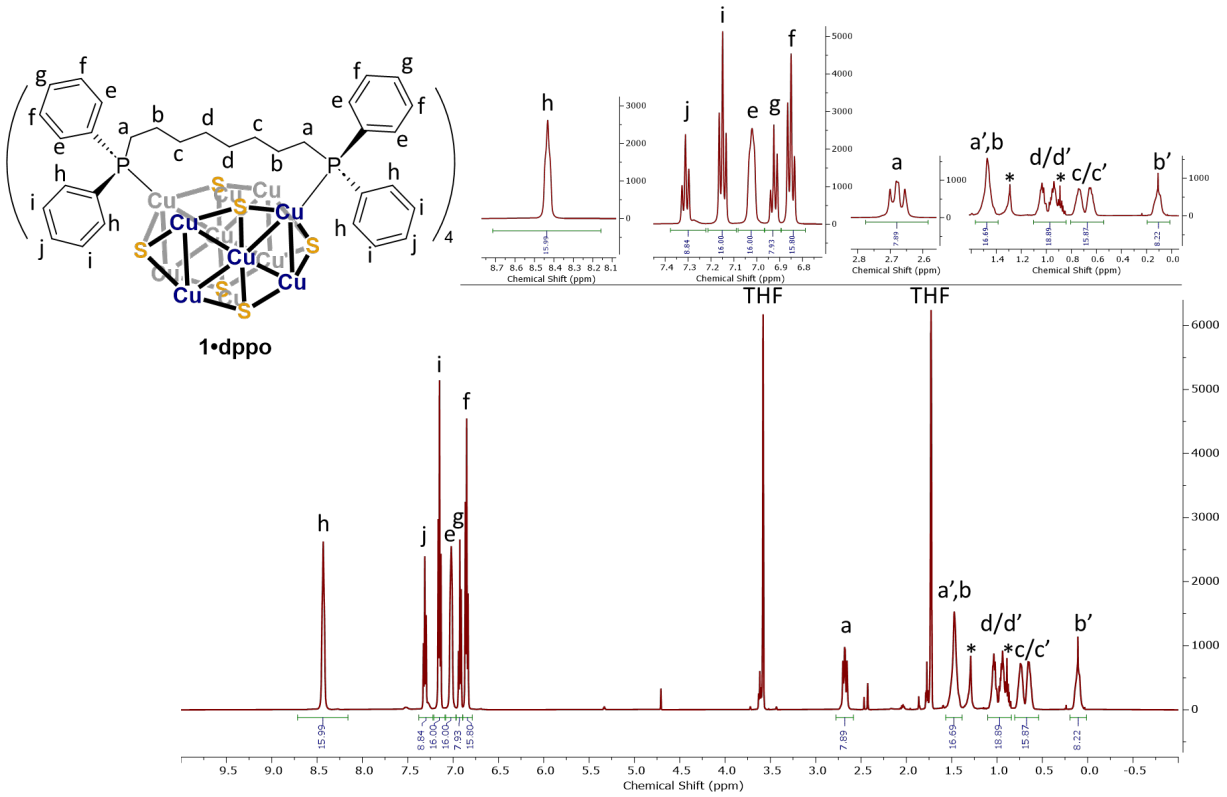

Figure S34: ^{1}H NMR spectrum of **1•dppo** (400 MHz, THF-d_8).

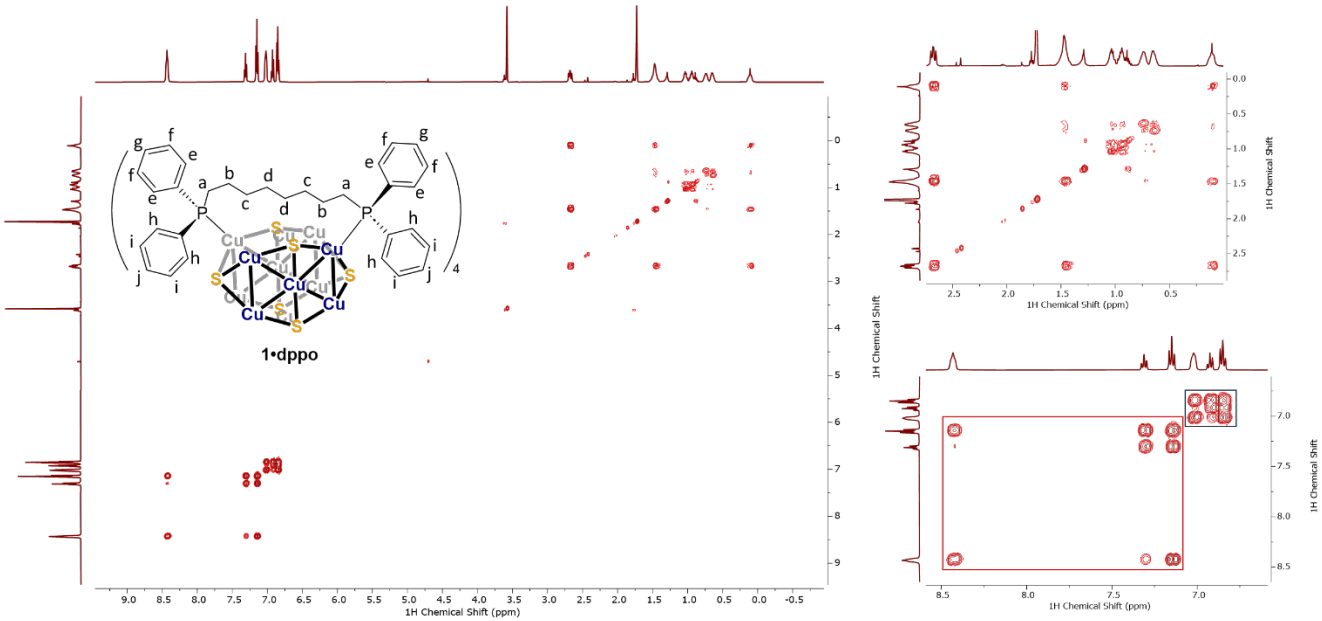

Figure S35: ^{1}H ^{1}H COSY NMR spectrum of **1•dppo** (400 MHz, THF-d_8).

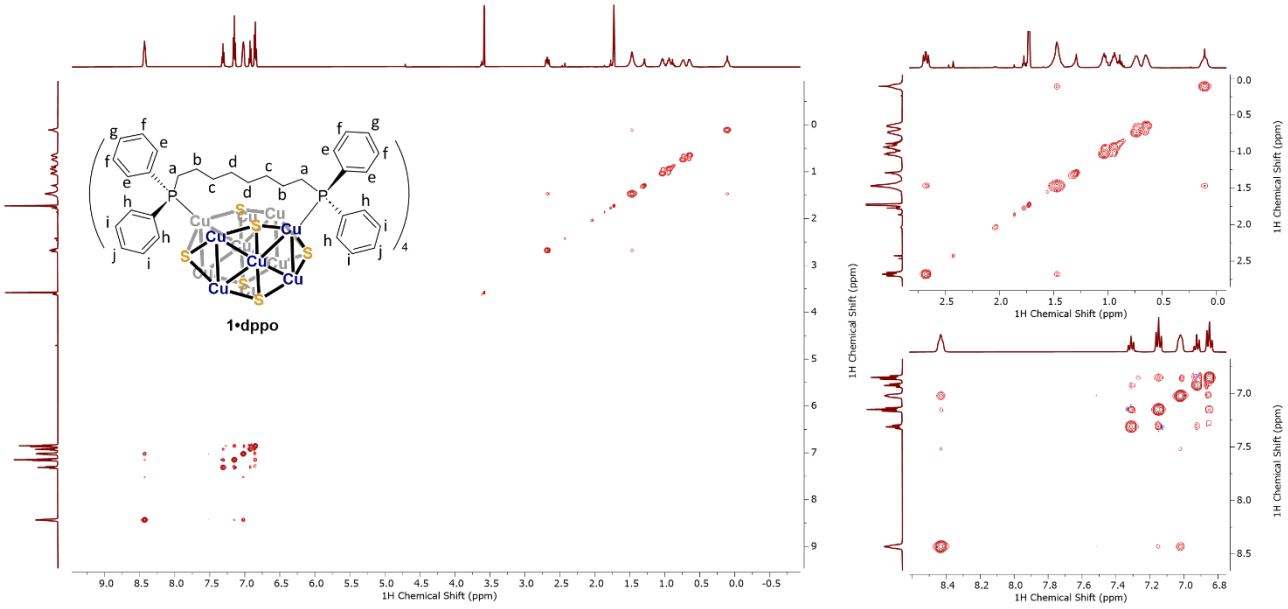

Figure S36: ^{1}H ^{1}H NOESY NMR spectrum of **1•dppo** (400 MHz, THF-d_8).

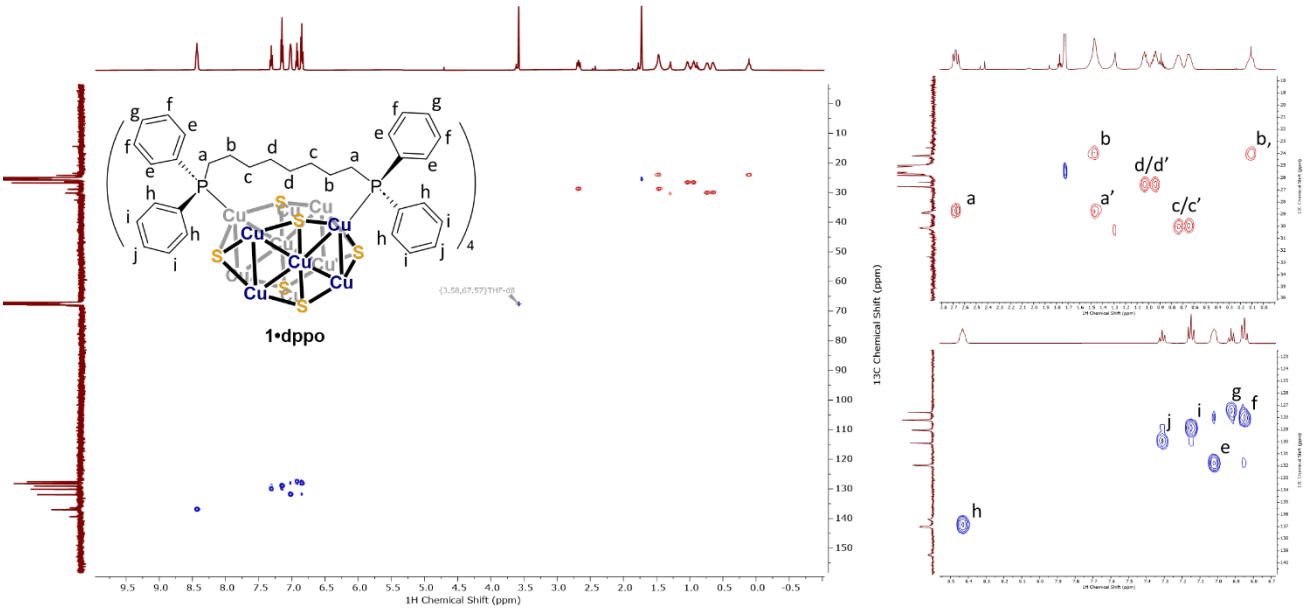

Figure S37: ^{1}H ^{13}C HSQC NMR spectrum of **1•dppo**. (400 MHz, THF-d_8).

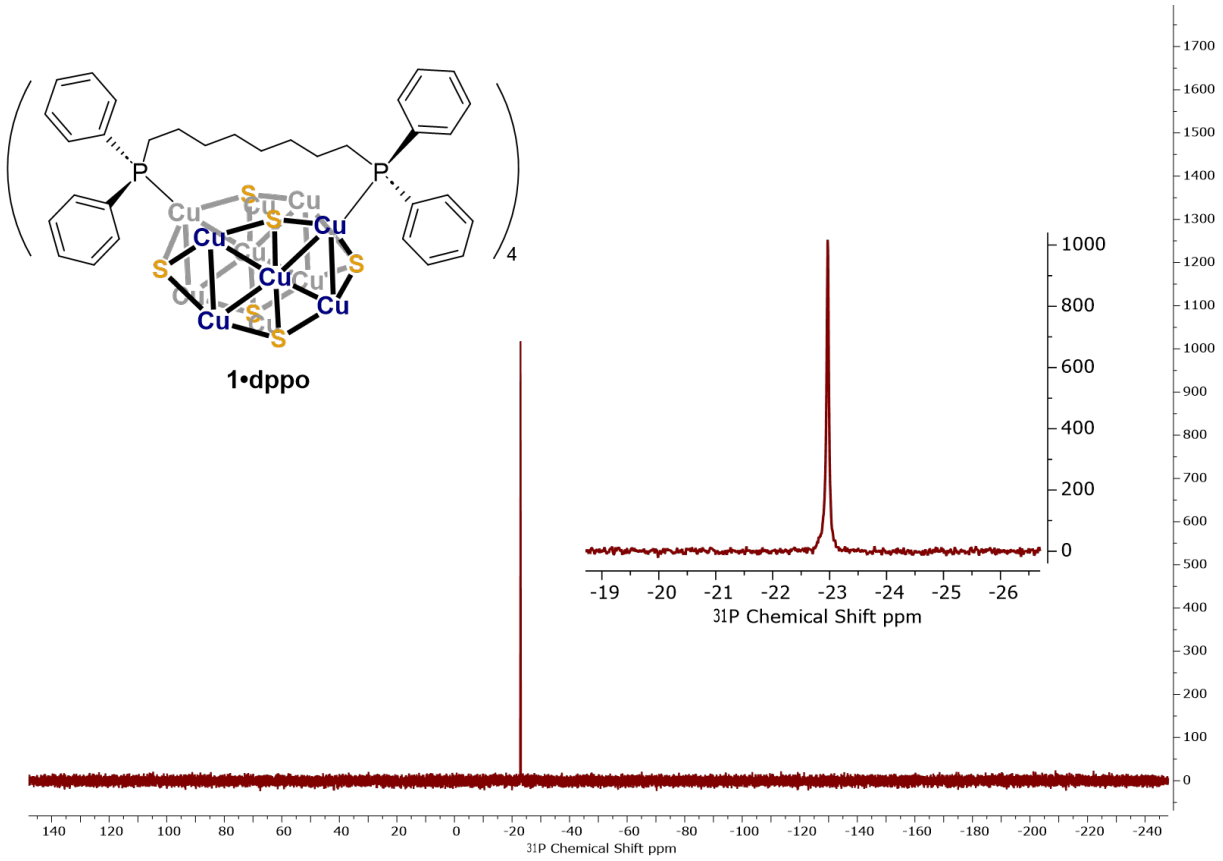

Figure S38: $^{31}P\{^{1}H\}$ NMR spectrum of **1•dppo** (162 MHz, THF-d_8).

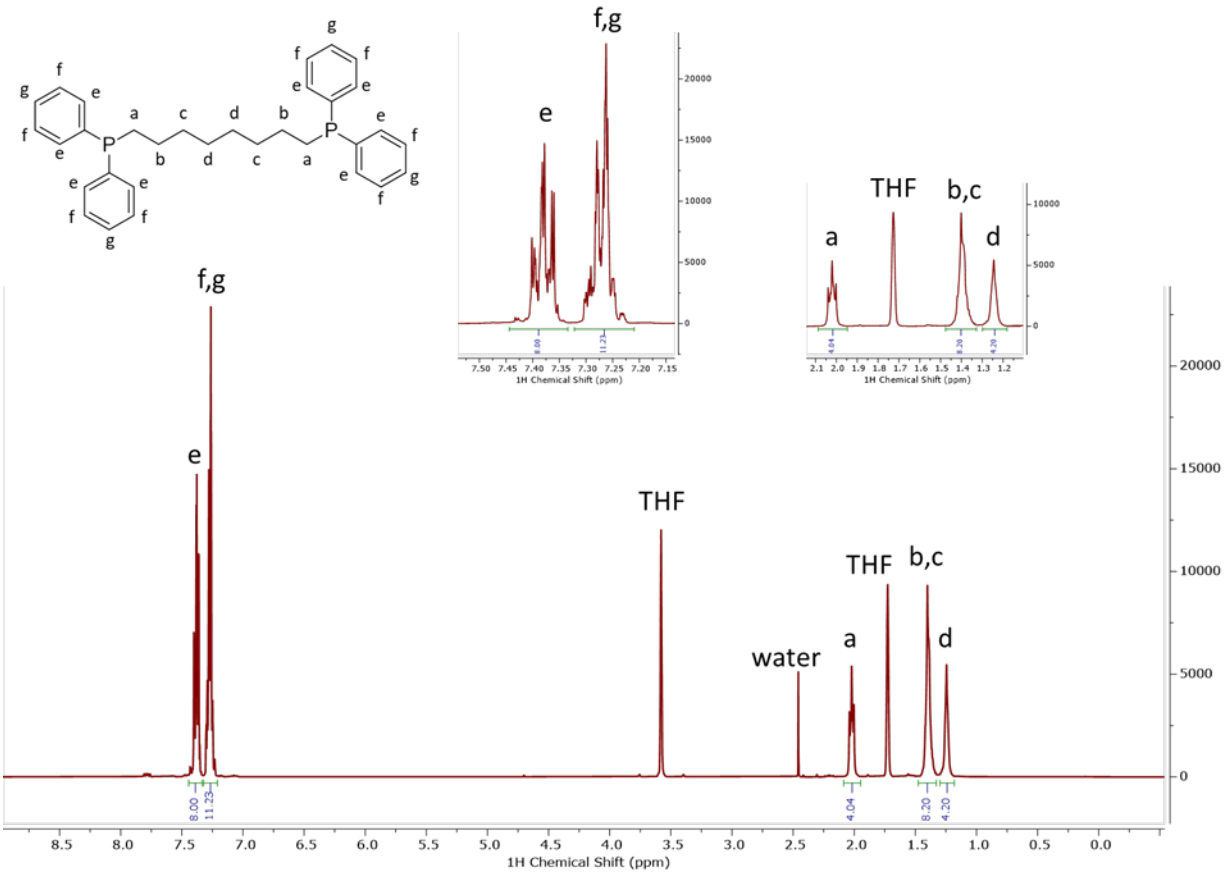

Figure S39: ^{1}H NMR spectrum of the free ligand dppo (400 MHz, THF-d_8).

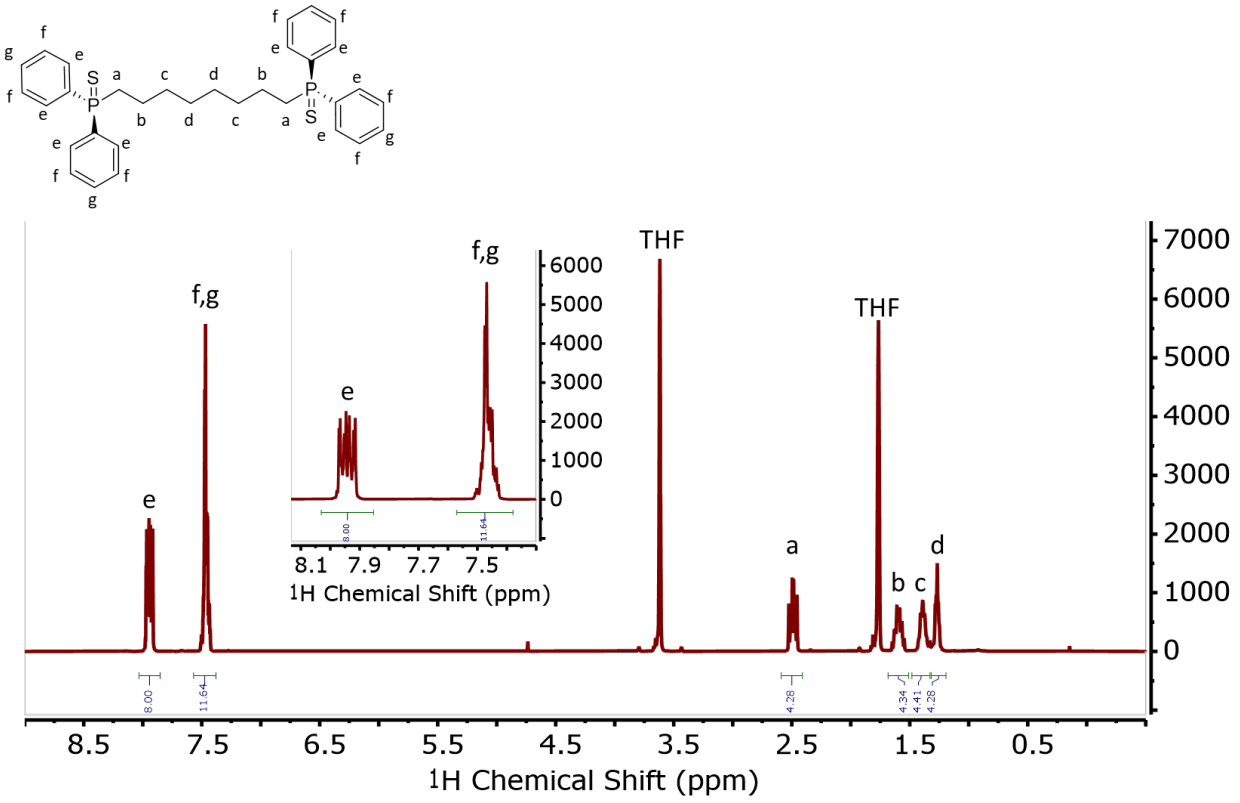

Figure S40: ^{1}H NMR spectrum of independently synthesized dppoS_2 (400 MHz, THF-d_8).

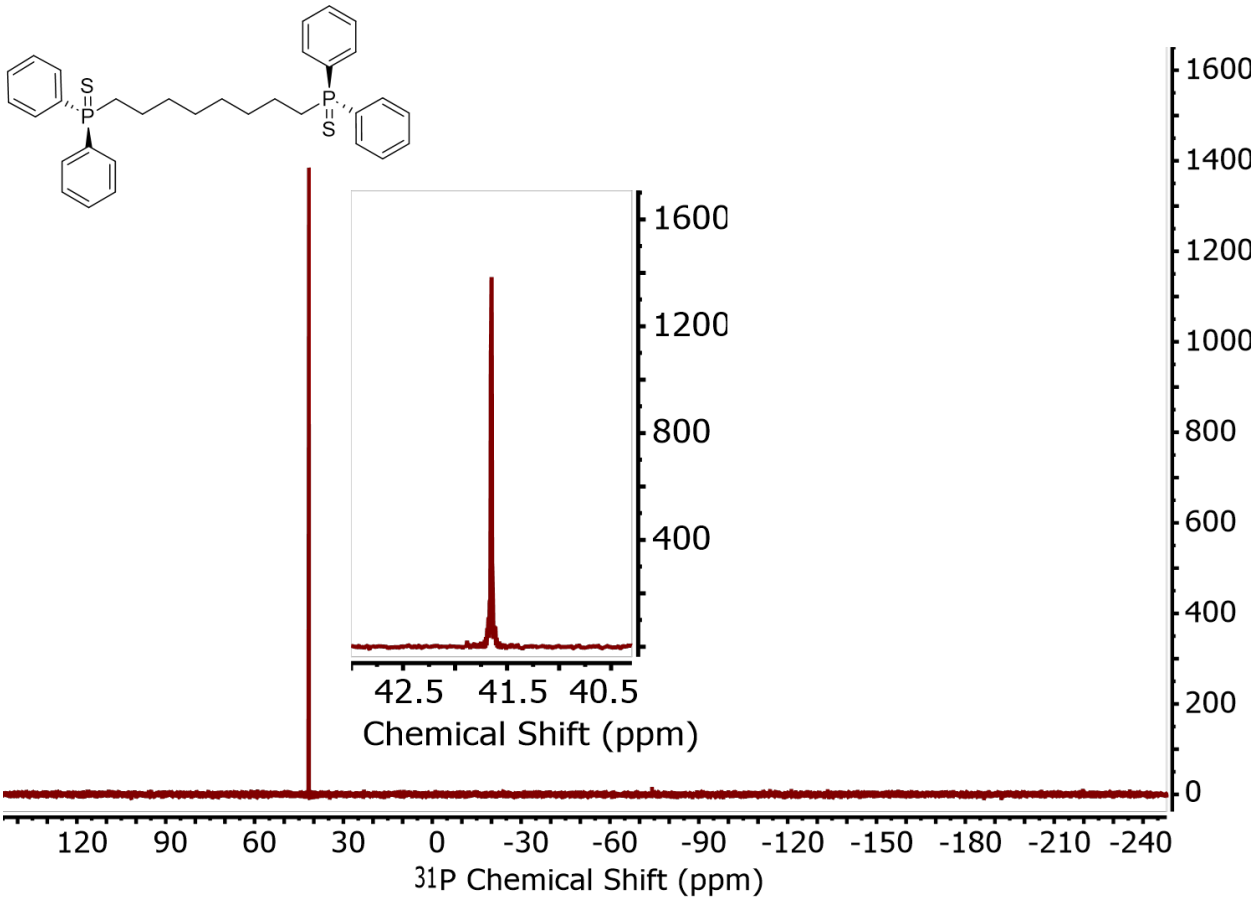

Figure S41: $^{31}P\{^{1}H\}$ NMR spectrum of independently synthesized $dppoS_2$ (162 MHz, THF-d_8).

COMPUTATIONAL DETAILS

All DFT calculations were performed using the Gaussian16 software package. Calculations were performed by unrestricted Kohn-Sham DFT using the BP86 functional and the def2-SVP basis set on all atoms.[12] The D3 model for dispersion correction was used in all calculations.[13,14] Three-dimensional models of optimized structures and orbital maps were created using PyMOL.

These methods are chosen in part for expedience and sake of computational cost when handling large systems containing over 200 atoms. Eichhöfer and coworkers have previously demonstrated the same methods to accurately reproduce predicted electronic transitions and UV-Vis electronic absorption spectra for **1•dppo** and **1•dppt**.[1] In general, we find reasonable agreement between DFT-predicted bond metrics for the truncated model complex **1'•PPh$_2$Et** and crystallographic bond metrics for **1•dppo**, although Cu-Cu bond lengths in the computed structure appear to be systematically underestimated (Figure S42 and Table S5).

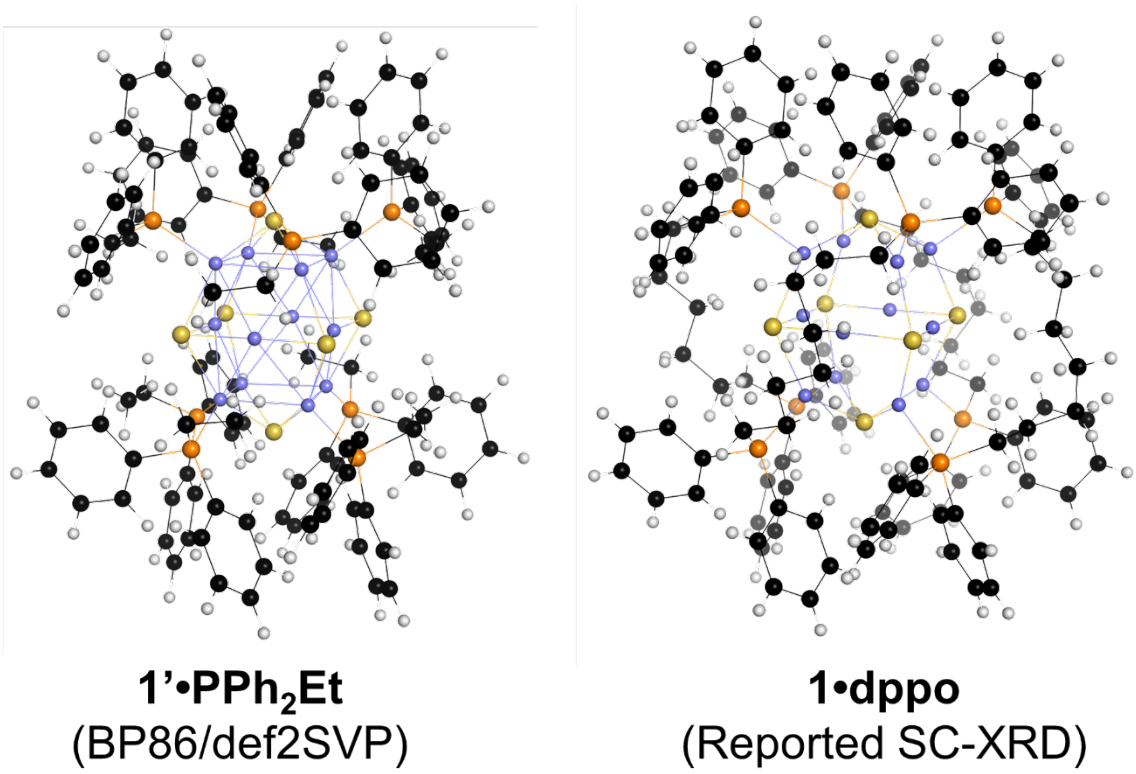

Figure S42: DFT-predicted structure of truncated model complex **1'•PPh$_2$Et** (left) and reported crystallographic structure of **1•dppo** (right).

Table S5: DFT-predicted bond lengths of **1'•PPh_2Et** and crystallographic bond lengths of **1•dppo**

	DFT bond lengths for **1'•PPh_2Et** (Å)	SC-XRD bond lengths for **1•dppo** (Å)
Avg. Cu-Cu (in Cu_4S pyramids)	2.736	2.884
Avg. Cu-S (in Cu_4S pyramids)	2.253	2.262
Avg. Cu-Cu (in Cu_4S_4 equator)	2.445	2.946
Avg. Cu-S (in Cu_4S_4 equator)	2.229	2.175
Avg. Cu-S (bridging Cu_4S and Cu_4S_4 parts)	2.380	2.366

Geometry optimizations were performed on neutral, cationic, and dicationic versions of **1'•PPh_2Et**. In general, more positively charged clusters possess longer Cu-Cu bonds within the central Cu_4S_4 equator substructure and longer Cu-S bonds within apical Cu_4S pyramid substructures while all other bond distances are contracted. Specifically, we note that the average distance between phosphorous atoms and equatorial sulfides is smaller in the charged species **[1'•PPh_2Et]$^+$** and **[1'•PPh_2Et]$^{2+}$** than in the neutral species **[1'•PPh_2Et]**. This change, combined with the accumulation of partial positive charge at phosphorous atoms, may prime phosphines for intramolecular P=S bond formation via the nucleophilic attack of an equatorial sulfide.

Table S6: DFT-predicted bond lengths of **[1'•PPh_2Et]$^{0/+/2+}$**

	1'•PPh_2Et (Å)	**[1'•PPh_2Et]$^+$** (Å)	**[1'•PPh_2Et]$^{2+}$** (Å)
Avg. Cu-Cu (in Cu_4S pyramids)	2.736	2.726	2.720
Avg. Cu-S (in Cu_4S pyramids)	2.250	2.256	2.259
Avg. Cu-Cu (in Cu_4S_4 equator)	2.445	2.737	2.763
Avg. Cu-S (in Cu_4S_4 equator)	2.229	2.225	2.224
Avg. Cu-S (bridging Cu_4S and Cu_4S_4 parts)	2.380	2.379	2.375
Avg. P-apical S	3.742	3.741	3.741
Avg. P-equatorial S	3.502	3.486	3.474

CARTESIAN COORDINATES OF DFT-OPTIMIZED STRUCTURES

Calculated structure: 1'•PPh_2Et

Cu	0.00000000	0.00000000	0.00000000
Cu	0.00085900	-0.15908700	-2.69243000
Cu	0.00039900	2.61115000	-2.85118300
Cu	0.00090200	2.77011900	-0.15738300
Cu	-2.05572000	-0.56219000	-1.42556400
Cu	-2.05587200	1.30575200	-3.39660500
Cu	-2.05519700	3.17069000	-1.42571000
Cu	-2.05641500	1.30498900	0.54633800
Cu	-4.11271200	-0.16011600	-0.15878100
Cu	-4.11180600	-0.00035700	-2.85074600
Cu	-4.11238800	2.77103800	-2.69214000
Cu	-4.11181600	2.61165500	-0.00036400
S	1.15373700	1.30574700	-1.42524600
S	-2.05148900	-0.89605600	0.79165200
S	-2.06024100	-0.89523900	-3.64286500
S	-2.05133200	3.50683300	-3.64277800
S	-2.06029000	3.50612400	0.79159500
S	-5.26510800	1.30558400	-1.42542600
P	1.29867400	-0.66697400	1.74538200
P	1.21459500	-2.04531700	-3.09709600
P	1.29863300	3.27841300	-4.59645400
P	1.21374500	4.65662200	0.24748800
P	-5.32632900	-2.04562700	0.24726200
P	-5.41138700	-0.66747500	-4.59556700
P	-5.32593200	4.65708200	-3.09694600
P	-5.40992400	3.27824600	1.74563200
C	1.36061500	-2.48754500	1.94077300
C	2.42318100	-3.24603000	1.39430900
H	3.29078900	-2.73978900	0.94838300
C	2.36718400	-4.64863300	1.38118500
H	3.20595000	-5.21390500	0.94479300
C	1.24254300	-5.32029700	1.89357500
H	1.19493800	-6.42060800	1.87429800
C	0.17079800	-4.57383000	2.41572900
H	-0.72321500	-5.08756400	2.80411000
C	0.22530000	-3.17065400	2.44118800
H	-0.63739800	-2.60461500	2.82304800
C	3.02278600	-0.04061000	1.90558000
C	4.04731300	-0.69338900	2.62687300
H	3.83558700	-1.63880200	3.15085600
C	5.34160600	-0.14774800	2.66599500
H	6.13665600	-0.66825900	3.22396300
C	5.62430100	1.05841800	1.99611900
H	6.64322000	1.47704600	2.01931500
C	4.60153500	1.72800000	1.30084700
H	4.80831500	2.66898500	0.76717400
C	3.30743400	1.18397800	1.25832900

H	2.50765200	1.69476000	0.69936700
C	0.46951300	-0.01289000	3.28416300
H	-0.56863500	-0.40684300	3.23507000
H	0.96967600	-0.42756800	4.18541900
C	0.43729100	1.51930900	3.27620700
H	1.44924700	1.97136600	3.32270600
H	-0.05503400	1.89094000	2.35038300
H	-0.14811200	1.91178400	4.13202100
H	-3.96327700	0.69792100	4.13049600
C	-4.54942300	1.09103800	3.27548900
H	-5.56165400	0.63972600	3.32299300
H	-4.05836900	0.71922700	2.34905700
C	-4.58050900	2.62327100	3.28384700
H	-3.54210400	3.01648500	3.23427100
H	-5.07991700	3.03808000	4.18546400
C	-5.47123100	5.09873700	1.94148700
C	-4.33564300	5.78138000	2.44192400
H	-3.47322600	5.21497500	2.82387500
C	-4.28054300	7.18453200	2.41636900
H	-3.38631600	7.69792200	2.80471400
C	-5.35195300	7.93141600	1.89413200
H	-5.30384500	9.03170300	1.87475500
C	-6.47690300	7.26021700	1.38180600
H	-7.31542500	7.82583000	0.94538800
C	-6.53350500	5.85764200	1.39500900
H	-7.40132100	5.35172400	0.94913600
C	-7.13421400	2.65235200	1.90573700
C	-8.15851800	3.30543000	2.62705300
H	-7.94642700	4.25070800	3.15115100
C	-9.45305900	2.76034300	2.66599300
H	-10.2479110	3.28109000	3.22402100
C	-9.73620900	1.55444500	1.99585200
H	-10.7553020	1.13623100	2.01885400
C	-8.71365800	0.88457700	1.30050200
H	-8.92086900	-0.05616400	0.76654100
C	-7.41931800	1.42801700	1.25819400
H	-6.61970500	0.91698600	0.69920800
C	1.63165700	-2.19970800	-4.87906800
C	2.95369200	-2.07499000	-5.36062800
H	3.79212500	-2.01432900	-4.65031800
C	3.20419300	-2.02006600	-6.74249700
H	4.23971800	-1.91035900	-7.10225700
C	2.14248000	-2.10290700	-7.66025900
H	2.34117800	-2.05992300	-8.74286500
C	0.82301500	-2.22984700	-7.18648900
H	-0.01689300	-2.28014400	-7.89796700
C	0.56439000	-2.26499900	-5.80835500
H	-0.47620200	-2.29269400	-5.44611900
C	2.80451100	-2.35214000	-2.21273200
C	3.44648100	-3.61155300	-2.21658000
H	2.99489200	-4.45966000	-2.75573000

C 4.66683000 -3.78590900 -1.54297300
H 5.16008400 -4.77130700 -1.55022900
C 5.26207300 -2.70382000 -0.86441200
H 6.21793800 -2.84322900 -0.33474800
C 4.62477300 -1.45138900 -0.84819300
H 5.06358100 -0.60644100 -0.29496100
C 3.39595300 -1.27897400 -1.51095800
H 2.87946000 -0.30516500 -1.46753800
C 0.16257600 -3.53477500 -2.71510200
H -0.77465200 -3.36082200 -3.28694200
H 0.64047600 -4.45704000 -3.10941400
C -0.14254500 -3.61641100 -1.21681400
H 0.76744100 -3.80951500 -0.61641100
H -0.58315500 -2.66387900 -0.85337500
H -0.87424000 -4.42095300 -0.99986400
H -3.23973700 -4.42104800 -1.85244600
C -3.97042100 -3.61585100 -1.63452900
H -4.88079000 -3.80744500 -2.23482600
H -3.52889200 -2.66345100 -1.99718400
C -4.27509900 -3.53527600 -0.13610400
H -3.33762600 -3.36226400 0.43561600
H -4.75333700 -4.45763600 0.25758400
C -5.74186800 -2.19988700 2.02953900
C -7.06332000 -2.07308200 2.51219200
H -7.90224400 -2.01113200 1.80259500
C -7.31260100 -2.01763600 3.89425800
H -8.34766200 -1.90628100 4.25484200
C -6.25025700 -2.10198600 4.81115500
H -6.44798300 -2.05856300 5.89392100
C -4.93138400 -2.23099800 4.33630600
H -4.09097100 -2.28250900 5.04710100
C -4.67394400 -2.26673600 2.95796100
H -3.63369800 -2.29610800 2.59489100
C -6.91704800 -2.35168400 -0.63600100
C -7.56016800 -3.61051100 -0.63069100
H -7.10931300 -4.45843400 -0.09063300
C -8.78075900 -3.78449300 -1.30394500
H -9.27488800 -4.76944500 -1.29556500
C -9.37514200 -2.70258000 -1.98355100
H -10.3312350 -2.84167000 -2.51288900
C -8.73673400 -1.45073500 -2.00115700
H -9.17492700 -0.60592900 -2.55508200
C -7.50762000 -1.27874300 -1.33881100
H -6.99032400 -0.30540800 -1.38325800
C 1.36061700 5.09896500 -4.79174400
C 2.42304500 5.85734000 -4.24482600
H 3.29054300 5.35098700 -3.79883400
C 2.36696300 7.25993000 -4.23129800
H 3.20558100 7.82512800 -3.79453000
C 1.24235800 7.93166100 -4.74369000
H 1.19466800 9.03196300 -4.72407800

C 0.17076000 7.18530000 -5.26627700
H -0.72321200 7.69911300 -5.65464500
C 0.22535200 5.78212800 -5.29217000
H -0.63724800 5.21612000 -5.67429300
C 3.02286700 2.65207200 -4.75621700
C 3.30758200 1.42766100 -4.10867400
H 2.50771700 0.91675200 -3.54994300
C 4.60181000 0.88395300 -4.15069300
H 4.80867400 -0.05690200 -3.61681300
C 5.62465900 1.55365100 -4.84577500
H 6.64368000 1.13525000 -4.86853200
C 5.34189600 2.75961200 -5.51596900
H 6.13697400 3.28021100 -6.07381400
C 4.04744900 3.30495400 -5.47731100
H 3.83565300 4.25020800 -6.00156900
C 0.46959400 2.62419300 -6.13522700
H -0.56859700 3.01800500 -6.08620500
H 0.96977400 3.03888300 -7.03647400
C 0.43769100 1.09199200 -6.12701900
H -0.05418600 0.72039800 -5.20094100
H 1.44974600 0.64019700 -6.17378800
H -0.14795600 0.69918200 -6.98251700
H -3.96352500 1.91077400 -6.98190200
C -4.54939500 1.51837100 -6.12636600
H -4.05735500 1.88991500 -5.20034000
H -5.56125100 1.97058200 -6.17322900
C -4.58194400 -0.01383900 -6.13438000
H -3.54391100 -0.40805400 -6.08519900
H -5.08218000 -0.42837400 -7.03566300
C -5.47421900 -2.48802700 -4.79072300
C -6.53727600 -3.24604100 -4.24452500
H -7.40486300 -2.73941700 -3.79900900
C -6.48174600 -4.64866400 -4.23106700
H -7.32084400 -5.21358000 -3.79485400
C -5.35713600 -5.32080500 -4.74289000
H -5.30989500 -6.42112600 -4.72335100
C -4.28491600 -4.57481400 -5.26474500
H -3.39090800 -5.08894800 -5.65260700
C -4.33890200 -3.17162500 -5.29047900
H -3.47579400 -2.60593100 -5.67193300
C -7.13520700 -0.04025100 -4.75565200
C -8.15993600 -0.69242500 -5.47719500
H -7.94851800 -1.63773300 -6.00150100
C -9.45404000 -0.14631300 -5.51624100
H -10.2492260 -0.66636700 -6.07443900
C -9.73632100 1.05975000 -4.84602900
H -10.7550800 1.47877100 -4.86912800
C -8.71331000 1.72878900 -4.15057000
H -8.91977600 2.66974100 -3.61671500
C -7.41941600 1.18430400 -4.10813400
H -6.61944500 1.69471600 -3.54910900

C	1.62966500	4.81178600	2.02961400
C	0.56192200	4.87738000	2.95832800
H	-0.47845700	4.90518900	2.59547700
C	0.81982700	4.84237900	4.33659200
H	-0.02043400	4.89288700	5.04763900
C	2.13902700	4.71535700	4.81108700
H	2.33709000	4.67249900	5.89381500
C	3.20122100	4.63226700	3.89391400
H	4.23655100	4.52252300	4.25422300
C	2.95145000	4.68696900	2.51189100
H	3.79026500	4.62606200	1.80205600
C	2.80398700	4.96355000	-0.63639500
C	3.39540300	3.89066500	-1.33859300
H	2.87901900	2.91681300	-1.38233400
C	4.62417700	4.06333100	-2.00139300
H	5.06295400	3.21854900	-2.55490100
C	5.26147700	5.31575800	-1.98479200
H	6.21732900	5.45536500	-2.51442500
C	4.66628300	6.39756900	-1.30574000
H	5.15953000	7.38296900	-1.29812600
C	3.44599200	6.22294200	-0.63210600
H	2.99448300	7.07086900	-0.09260200
C	0.16178200	6.14575500	-0.13597200
H	-0.77563700	5.97222800	0.43569200
H	0.63958000	7.06824300	0.25794200
C	-0.14285500	6.22646500	-1.63438800
H	0.76750500	6.41808900	-2.23471300
H	-0.58450000	5.27417400	-1.99714900
H	-0.87348100	7.03175600	-1.85217000
H	-3.23720700	7.03263100	-0.99947400
C	-3.96793100	6.22726600	-1.21662100
H	-3.52581900	5.27501000	-0.85431500
H	-4.87778000	6.41866900	-0.61546000
C	-4.27392300	6.14648700	-2.71478300
H	-3.33701200	5.97308500	-3.28731100
H	-4.75224100	7.06890100	-3.10824300
C	-5.74326700	4.81156600	-4.87885000
C	-7.06551400	4.68846900	-5.36022600
H	-7.90395500	4.62906700	-4.64982800
C	-7.31624300	4.63360000	-6.74206900
H	-8.35195100	4.52514900	-7.10168400
C	-4.93484800	4.84024700	-7.18637300
H	-4.09496400	4.88932000	-7.89796300
C	-6.25453700	4.71489200	-7.65996400
H	-6.45341000	4.67194200	-8.74254100
C	-4.67602300	4.87532000	-5.80828100
H	-3.63535400	4.90170100	-5.44613600
C	-6.91570100	4.96370600	-2.21223800
C	-7.55767900	6.22312700	-2.21580300
H	-7.10623500	7.07129400	-2.75497800
C	-8.77789500	6.39741900	-1.54194900

H -9.27113600 7.38282500 -1.54899500
C -9.37300200 5.31524500 -0.86339900
H -10.3287560 5.45456500 -0.33351400
C -8.73567100 4.06283000 -0.84743000
H -9.17438900 3.21782400 -0.29422600
C -7.50697000 3.89047700 -1.51044100
H -6.99046100 2.91667000 -1.46718800

Calculated structure: [1'•PPh_2Et]$^+$

Cu 0.00000000 0.00000000 0.00000000
Cu 0.02755100 0.14294900 -2.69374000
Cu -0.00003000 -2.60615000 -2.86215900
Cu 0.02749700 -2.74909000 -0.16842800
Cu 2.06596900 0.66197300 -1.43099800
Cu 2.06594100 -1.30301000 -3.33611100
Cu 2.06591100 -3.26810200 -1.43113400
Cu 2.06593100 -1.30317500 0.47397000
Cu 4.10437400 0.14278800 -0.16827700
Cu 4.13192200 0.00009300 -2.86203300
Cu 4.10434300 -2.74902300 -2.69382100
Cu 4.13187500 -2.60632900 -0.00007400
S -1.15819300 -1.30304800 -1.43110200
S 2.04746800 0.88268100 0.79783900
S 2.08449000 0.88287800 -3.65980100
S 2.04739600 -3.48887400 -3.65995200
S 2.08442700 -3.48907000 0.79766300
S 5.29009600 -1.30313300 -1.43104100
P -1.30739300 0.70734100 1.72530800
P -1.12541200 2.08083000 -3.01709300
P -1.30745900 -3.31350500 -4.58744700
P -1.12554600 -4.68689100 0.15497100
P 5.25745000 2.08057400 0.15519400
P 5.43928900 0.70753600 -4.58728800
P 5.25731400 -4.68684200 -3.01736700
P 5.43925000 -3.31381300 1.72519600
C -1.35012200 2.52820800 1.91797600
C -2.41158500 3.29546700 1.38412100
H -3.28372200 2.79823500 0.93729300
C -2.35157800 4.69823400 1.39378400
H -3.19044700 5.27389500 0.97218900
C -1.22501900 5.35799200 1.91641900
H -1.17692500 6.45815300 1.91899200
C -0.15443000 4.60162400 2.42651200
H 0.73764500 5.10803200 2.82804300
C -0.21246400 3.19838900 2.42885100
H 0.64537600 2.62465700 2.81028800
C -3.03454400 0.08959900 1.86488900
C -4.04957800 0.74643100 2.59597100
H -3.82820100 1.68377600 3.13005000
C -5.34892300 0.21304100 2.63349100

H	-6.13646400	0.73515100	3.19974300
C	-5.64619000	-0.98229500	1.95106800
H	-6.66949600	-1.38938600	1.97218400
C	-4.63202700	-1.65650800	1.24771300
H	-4.85154800	-2.59022100	0.70591700
C	-3.33166200	-1.12738500	1.21031700
H	-2.53788100	-1.64658900	0.65181800
C	-0.49274400	0.04088400	3.26589700
H	0.53692400	0.45785500	3.25581600
H	-1.02590900	0.42984300	4.15930600
C	-0.43092600	-1.48979100	3.23364800
H	-1.43537500	-1.96032000	3.23483100
H	0.10186400	-1.83621900	2.32092700
H	0.12838300	-1.88634500	4.10438800
H	4.00325500	-0.72019600	4.10423700
C	4.56257900	-1.11670900	3.23348900
H	5.56697700	-0.64607200	3.23461800
H	4.02970300	-0.77035800	2.32078800
C	4.62454900	-2.64737800	3.26576600
H	3.59491700	-3.06444100	3.25566100
H	5.15771900	-3.03627500	4.15919900
C	5.48193700	-5.13468300	1.91785300
C	4.34427100	-5.80489700	2.42866400
H	3.48639300	-5.23119400	2.81005800
C	4.28629500	-7.20813400	2.42635700
H	3.39420700	-7.71456500	2.82782800
C	5.35696500	-7.96447400	1.91638800
H	5.30892300	-9.06463700	1.91900100
C	6.48355200	-7.30468500	1.39385200
H	7.32249900	-7.88032200	0.97237900
C	6.54349200	-5.90191400	1.38413800
H	7.41566800	-5.40465300	0.93741400
C	7.16638500	-2.69608700	1.86487200
C	8.18142600	-3.35298100	2.59588100
H	7.96010900	-4.29047900	3.12971900
C	9.48072100	-2.81948200	2.63359400
H	10.2682720	-3.34165300	3.19977400
C	9.77791700	-1.62395800	1.95146700
H	10.8011700	-1.21674600	1.97277800
C	8.76373700	-0.94969500	1.24818100
H	8.98319700	-0.01582700	0.70662700
C	7.46343200	-1.47894400	1.21056500
H	6.66965100	-0.95970700	0.65209300
C	-1.53096900	2.17288600	-4.80600000
C	-2.84283700	1.93449000	-5.27185800
H	-3.66801900	1.81765800	-4.55374200
C	-3.09951300	1.84191200	-6.65004400
H	-4.12559100	1.64611200	-6.99877900
C	-2.05455600	1.99850300	-7.57735100
H	-2.25793300	1.92741700	-8.65728200
C	-0.74632500	2.24016500	-7.11857300

H 0.07854600 2.35648800 -7.83938000
C -0.47961200 2.31543700 -5.74307300
H 0.55645800 2.44868400 -5.39463300
C -2.72269600 2.39037900 -2.15736300
C -3.34119300 3.66164500 -2.17018600
H -2.85698000 4.50966100 -2.67971400
C -4.58393900 3.84766100 -1.54304200
H -5.05998400 4.84094800 -1.55739200
C -5.22421100 2.76733000 -0.90415000
H -6.19840500 2.91681100 -0.41268100
C -4.61088500 1.50311500 -0.88182400
H -5.08689300 0.65844600 -0.36008600
C -3.36078300 1.31713600 -1.49901600
H -2.86873900 0.33235600 -1.45532800
C -0.06286200 3.56133200 -2.65276000
H 0.88582500 3.36389300 -3.19674600
H -0.52359900 4.47276600 -3.08914700
C 0.20080400 3.69235200 -1.15048400
H -0.72334100 3.91921300 -0.58523500
H 0.61746000 2.74964200 -0.73616100
H 0.93459200 4.49703300 -0.94344500
H 3.19729400 4.49705100 -1.91795600
C 3.93109500 3.69233800 -1.71108600
H 4.85518300 3.91923500 -2.27641500
H 3.51438500 2.74967400 -2.12546400
C 4.19490700 3.56115600 -0.20884600
H 3.24626400 3.36370700 0.33521200
H 4.65571900 4.47252700 0.22759500
C 5.66323400 2.17240100 1.94407000
C 6.97514300 1.93396100 2.40978200
H 7.80025900 1.81718000 1.69157800
C 7.23194400 1.84127600 3.78794000
H 8.25805000 1.64543300 4.13656700
C 6.18707800 1.99781800 4.71535700
H 6.39056100 1.92665500 5.79526400
C 4.87880500 2.23952700 4.25672200
H 4.05400400 2.35580500 4.97761600
C 4.61196400 2.31488200 2.88125400
H 3.57586200 2.44813500 2.53291000
C 6.85465400 2.39014600 -0.70463600
C 7.47312800 3.66142400 -0.69186200
H 6.98888400 4.50946300 -0.18240400
C 8.71588900 3.84743200 -1.31897600
H 9.19189800 4.84073700 -1.30468800
C 9.35620900 2.76707000 -1.95776900
H 10.3304270 2.91653200 -2.44919600
C 8.74290300 1.50284700 -1.98004600
H 9.21897900 0.65815600 -2.50168100
C 7.49277600 1.31686900 -1.36289300
H 7.00072100 0.33209000 -1.40657600
C -1.35017200 -5.13435900 -4.78015400

C -2.41171900 -5.90156100 -4.24638200
H -3.28388300 -5.40427200 -3.79966300
C -2.35176500 -7.30433200 -4.25599300
H -3.19069700 -7.87994900 -3.83446400
C -1.22517400 -7.96414400 -4.77849500
H -1.17711900 -9.06430600 -4.78103100
C -0.15451600 -7.20782800 -5.28852600
H 0.73757600 -7.71428000 -5.68996400
C -0.21249900 -5.80459200 -5.29092300
H 0.64538700 -5.23090300 -5.67232400
C -3.03460700 -2.69579600 -4.72712100
C -3.33169200 -1.47863000 -4.07288000
H -2.53790800 -0.95931200 -3.51449500
C -4.63203600 -0.94947200 -4.11043400
H -4.85152900 -0.01560500 -3.56888700
C -5.64621400 -1.62383200 -4.81363000
H -6.66949700 -1.21669100 -4.83489400
C -5.34898000 -2.81937000 -5.49571300
H -6.13653100 -3.34162400 -6.06181500
C -4.04965200 -3.35279500 -5.45803000
H -3.82831800 -4.29033700 -5.99178600
C -0.49274900 -2.64700300 -6.12799000
H 0.53684400 -3.06416600 -6.11794500
H -1.02598000 -3.03578500 -7.02143600
C -0.43062700 -1.11634500 -6.09559500
H 0.10230600 -0.77012000 -5.18288000
H -1.43497700 -0.64560900 -6.09666200
H 0.12871500 -0.71982000 -6.96632600
H 4.00342100 -1.88605200 -6.96644400
C 4.56275100 -1.48955400 -6.09569200
H 4.02993900 -1.83600200 -5.18299200
H 5.56718100 -1.96012200 -6.09689600
C 4.62460800 0.04112000 -6.12788200
H 3.59494800 0.45811300 -6.11775800
H 5.15775500 0.43010200 -7.02129300
C 5.48195100 2.52841500 -4.77987900
C 6.54337000 3.29566900 -4.24593000
H 7.41549700 2.79842700 -3.79909300
C 6.48334400 4.69843700 -4.25553800
H 7.32218400 5.27409200 -3.83387800
C 5.35680300 5.35819900 -4.77820600
H 5.30869000 6.45835900 -4.78072700
C 4.28626100 4.60183400 -5.28840500
H 3.39420600 5.10824400 -5.68997700
C 4.34431900 3.19860100 -5.29080700
H 3.48652900 2.62487600 -5.67236300
C 7.16641900 0.08979600 -4.72692600
C 8.18143700 0.74657900 -5.45806800
H 7.96008400 1.68395300 -5.99210600
C 9.48075200 0.21311800 -5.49566400
H 10.2682870 0.73519300 -6.06195500

C 9.77799400 -0.98223800 -4.81326500
H 10.8012670 -1.38940700 -4.83447400
C 8.76384400 -1.65638400 -4.10982400
H 8.98335500 -2.59010300 -3.56803500
C 7.46351300 -1.12719000 -4.07234000
H 6.66975700 -1.64631500 -3.51372600
C -1.53129100 -4.77891200 1.94384400
C -0.47999700 -4.92147400 2.88099000
H 0.55610000 -5.05467300 2.53261100
C -0.74681200 -4.84627100 4.25647200
H 0.07800800 -4.96260300 4.97733600
C -2.05508400 -4.60465000 4.71515800
H -2.25855000 -4.53361400 5.79507700
C -3.09997400 -4.44804000 3.78777900
H -4.12608000 -4.25227900 4.13645000
C -2.84319800 -4.54056900 2.40960600
H -3.66833000 -4.42373800 1.69143100
C -2.72273300 -4.99646400 -0.70489500
C -3.36076100 -3.92324400 -1.36334000
H -2.86870500 -2.93846600 -1.40702900
C -4.61078400 -4.10928500 -1.98068500
H -5.08678400 -3.26464300 -2.50247200
C -5.22408300 -5.37351000 -1.95841000
H -6.19821500 -5.52301800 -2.44999000
C -4.58386400 -6.45381500 -1.31941500
H -5.05986300 -7.44712400 -1.30512900
C -3.34121100 -6.26774100 -0.69210700
H -2.85703300 -7.11573800 -0.18251700
C -0.06295800 -6.16739700 -0.20926000
H 0.88564800 -5.97004900 0.33490100
H -0.52379900 -7.07884800 0.22698600
C 0.20095300 -6.29829800 -1.71150400
H -0.72311300 -6.52501800 -2.27693700
H 0.61775900 -5.35558000 -2.12566200
H 0.93471400 -7.10301800 -1.91849000
H 3.19687500 -7.10312200 -0.94425800
C 3.93068200 -6.29841300 -1.15111800
H 3.51388500 -5.35571700 -0.73690200
H 4.85469900 -6.52522200 -0.58564300
C 4.19469900 -6.16737800 -2.65333000
H 3.24612900 -5.96996600 -3.19753000
H 4.65554600 -7.07879800 -3.08963100
C 5.66309000 -4.77870300 -4.80624600
C 6.97500800 -4.54034600 -5.27197000
H 7.80013600 -4.42361100 -4.55377400
C 7.23180500 -4.44768600 -6.65013100
H 8.25792000 -4.25190800 -6.99876700
C 4.87864200 -4.84581400 -7.11889400
H 4.05382800 -4.96205600 -7.83978000
C 6.18692400 -4.60417800 -7.57754000
H 6.39040400 -4.53303900 -8.65744900

C 4.61180800 -4.92114200 -5.74342300
H 3.57570200 -5.05433600 -5.39507000
C 6.85448600 -4.99645900 -2.15750900
C 7.47298100 -6.26772600 -2.17034100
H 6.98880900 -7.11572100 -2.67993900
C 8.71565600 -6.45378400 -1.54307200
H 9.19168000 -7.44708100 -1.55739900
C 9.35586700 -5.37348400 -0.90406300
H 10.3300160 -5.52298700 -0.41251300
C 8.74254200 -4.10927000 -0.88173800
H 9.21853100 -3.26463200 -0.35993700
C 7.49250200 -3.92323800 -1.49905400
H 7.00042200 -2.93847200 -1.45532500

Calculated structure: [1'•PPh_2Et]$^{2+}$

Cu 0.00000000 0.00000000 0.00000000
Cu -0.04714800 -0.13085600 -2.68907300
Cu -0.00003600 2.61056500 -2.86405100
Cu -0.04709800 2.74140400 -0.17496700
Cu -2.07062500 -0.75498100 -1.43216600
Cu -2.07065200 1.30546000 -3.27248000
Cu -2.07062400 3.36547200 -1.43176500
Cu -2.07060900 1.30509900 0.40850500
Cu -4.09411700 -0.13109200 -0.17515500
Cu -4.14125600 0.00026100 -2.86420000
Cu -4.09415200 2.74164300 -2.68872900
Cu -4.14120500 2.61031100 0.00034200
S 1.16136000 1.30529200 -1.43207100
S -2.04145900 -0.86753100 0.80362900
S -2.09981700 -0.86711800 -3.66800000
S -2.04155200 3.47805800 -3.66757600
S -2.09969900 3.47762700 0.80408800
S -5.30258000 1.30531500 -1.43189900
P 1.31668300 -0.75358700 1.69990400
P 1.06964400 -2.09335500 -2.96839400
P 1.31656000 3.36413300 -4.56401900
P 1.06963000 4.70396500 0.10424900
P -5.21096500 -2.09359200 0.10388600
P -5.45798500 -0.75307500 -4.56418700
P -5.21099600 4.70417900 -2.96772900
P -5.45788300 3.36355200 1.70041000
C 1.34442300 -2.57487000 1.87618300
C 2.41015200 -3.34367800 1.35457700
H 3.28629200 -2.84929100 0.91279300
C 2.35209400 -4.74652800 1.37949900
H 3.19500900 -5.32661400 0.97290900
C 1.22456700 -5.40190500 1.90519600
H 1.18074800 -6.50189500 1.92391800
C 0.14972400 -4.64288900 2.40275200
H -0.73989600 -5.14778300 2.81101400

C	0.20480400	-3.23975100	2.38902900
H	-0.65290300	-2.66399800	2.76788000
C	3.04349300	-0.13945500	1.82859200
C	4.04789800	-0.80132000	2.57031700
H	3.81868000	-1.73614800	3.10524200
C	5.34896600	-0.27317800	2.61947200
H	6.12825300	-0.79754400	3.19444200
C	5.65814500	0.91965800	1.93824200
H	6.68300200	1.32161900	1.96897500
C	4.65353500	1.59872300	1.22571500
H	4.88357700	2.53195600	0.68717700
C	3.35076100	1.07663000	1.17824200
H	2.56417100	1.60364200	0.61790000
C	0.50912500	-0.08684400	3.24356500
H	-0.51046000	-0.52633400	3.26416000
H	1.07098600	-0.45745100	4.12699100
C	0.41850100	1.44179200	3.20115500
H	1.41432500	1.92865100	3.16747400
H	-0.14808600	1.77229400	2.30312100
H	-0.11896900	1.83515600	4.08667000
H	-4.02224700	0.77434600	4.08670600
C	-4.55978100	1.16786600	3.20130000
H	-5.55563900	0.68107400	3.16763200
H	-3.99327900	0.83744100	2.30318000
C	-4.65028400	2.69649500	3.24393000
H	-3.63065900	3.13589800	3.26455000
H	-5.21207600	3.06700900	4.12743500
C	-5.48565100	5.18479300	1.87701300
C	-4.34606100	5.84961200	2.39000400
H	-3.48836900	5.27381300	2.76882200
C	-4.29101300	7.25275000	2.40396000
H	-3.40142600	7.75759900	2.81235300
C	-5.36585900	8.01182300	1.90650200
H	-5.32205700	9.11181100	1.92539300
C	-6.49336100	7.35650700	1.38066600
H	-7.33627800	7.93664300	0.97415100
C	-6.55138100	5.95366400	1.35549900
H	-7.42751000	5.45932900	0.91363400
C	-7.18465700	2.74935400	1.82902100
C	-8.18914300	3.41124700	2.57061300
H	-7.95999500	4.34609800	3.10552000
C	-9.49019600	2.88306100	2.61970400
H	-10.2695450	3.40743900	3.19458000
C	-9.79927000	1.69015200	1.93856000
H	-10.8241130	1.28815100	1.96924900
C	-8.79457900	1.01105400	1.22618700
H	-9.02454000	0.07774700	0.68775300
C	-7.49181800	1.53319700	1.17874700
H	-6.70515100	1.00614900	0.61853400
C	1.46811200	-2.12969100	-4.75975000
C	2.77333700	-1.83022900	-5.20945100

H 3.58628300 -1.68468400 -4.48313000
C 3.03917900 -1.72083700 -6.58426800
H 4.05936000 -1.48198700 -6.92240800
C 2.01025000 -1.91886300 -7.52167200
H 2.22134800 -1.83713200 -8.59917300
C 0.70909000 -2.22023600 -7.07813000
H -0.10024000 -2.37525500 -7.80883200
C 0.43204500 -2.31454300 -5.70577900
H -0.59845200 -2.50796100 -5.37049400
C 2.67038000 -2.40134400 -2.12365200
C 3.27432900 -3.67989800 -2.15419000
H 2.76862600 -4.52533000 -2.64628300
C 4.53510700 -3.87619200 -1.56815600
H 5.00098500 -4.87364200 -1.59750700
C 5.20674500 -2.80091200 -0.95360500
H 6.19578000 -2.95906200 -0.49618400
C 4.60768500 -1.53025900 -0.91514300
H 5.11032300 -0.68899600 -0.41349700
C 3.34086500 -1.33214800 -1.49263200
H 2.86576000 -0.34063300 -1.44131000
C 0.00363500 -3.57254400 -2.62630900
H -0.95093600 -3.36208000 -3.15397100
H 0.45969300 -4.46910900 -3.09655900
C -0.23432900 -3.75175200 -1.12513700
H 0.69900200 -4.00130500 -0.58567900
H -0.63847200 -2.82325100 -0.66761400
H -0.96540900 -4.56224500 -0.93386300
H -3.17570100 -4.56207200 -1.93090500
C -3.90682000 -3.75163600 -1.73953500
H -4.84009200 -4.00108700 -2.27914400
H -3.50265500 -2.82302700 -2.19682400
C -4.14494000 -3.57274100 -0.23835100
H -3.19042100 -3.36242800 0.28946300
H -4.60108800 -4.46938400 0.23166100
C -5.60960300 -2.13025800 1.89521200
C -6.91487600 -1.83097200 2.34488300
H -7.72777900 -1.68530400 1.61853500
C -7.18082300 -1.72189600 3.71970500
H -8.20104300 -1.48318100 4.05782400
C -6.15195500 -1.92007300 4.65714300
H -6.36313800 -1.83859500 5.73464600
C -4.85074300 -2.22126800 4.21362900
H -4.04145600 -2.37639900 4.94435400
C -4.57359500 -2.31524800 2.84127900
H -3.54305600 -2.50850700 2.50602500
C -6.81161000 -2.40142800 -0.74106700
C -7.41563200 -3.67994900 -0.71083700
H -6.91003800 -4.52550100 -0.21883700
C -8.67630800 -3.87608500 -1.29714600
H -9.14224100 -4.87351700 -1.26804500
C -9.34777200 -2.80067800 -1.91166300

H -10.3367390 -2.95870500 -2.36927300
C -8.74862700 -1.53005600 -1.94984300
H -9.25112600 -0.68869700 -2.45146400
C -7.48190400 -1.33210000 -1.37207700
H -7.00668800 -0.34062900 -1.42324900
C 1.34425800 5.18541400 -4.74032200
C 2.40991100 5.95426500 -4.21861400
H 3.28603500 5.45991500 -3.77676500
C 2.35180300 7.35710900 -4.24354600
H 3.19465500 7.93723100 -3.83687600
C 1.22429300 8.01244200 -4.76934200
H 1.18042500 9.11243100 -4.78805100
C 0.14952200 7.25338700 -5.26698800
H -0.74007300 7.75824900 -5.67534700
C 0.20465500 5.85025000 -5.25325800
H -0.65298800 5.27445800 -5.63219800
C 3.04337000 2.75000500 -4.69273300
C 3.35063600 1.53387600 -4.04246300
H 2.56400700 1.00676900 -3.48225800
C 4.65343200 1.01182700 -4.08990600
H 4.88346800 0.07855100 -3.55144400
C 5.65806200 1.69098800 -4.80230700
H 6.68293700 1.28906900 -4.83300400
C 5.34888700 2.88386300 -5.48346800
H 6.12818700 3.40827700 -6.05837700
C 4.04780100 3.41196500 -5.43434800
H 3.81857300 4.34678500 -5.96927400
C 0.50898100 2.69733700 -6.10766800
H -0.51064200 3.13674400 -6.12823500
H 1.07079500 3.06800600 -6.99109600
C 0.41848100 1.16869900 -6.06529000
H -0.14803000 0.83812800 -5.16723000
H 1.41434000 0.68190700 -6.03168000
H -0.11902400 0.77531400 -6.95077500
H -4.02234000 1.83607300 -6.95050900
C -4.55982500 1.44257300 -6.06506500
H -3.99323300 1.77292100 -5.16697500
H -5.55564500 1.92943700 -6.03131100
C -4.65046100 -0.08605600 -6.10773500
H -3.63087500 -0.52554000 -6.12840400
H -5.21231300 -0.45649800 -6.99123600
C -5.48567900 -2.57433200 -4.74071800
C -6.55134900 -3.34325700 -4.21916000
H -7.42747900 -2.84897100 -3.77723800
C -6.49324600 -4.74610300 -4.24429600
H -7.33611700 -5.32627400 -3.83773500
C -5.36573500 -5.40136600 -4.77016500
H -5.32188400 -6.50135200 -4.78906400
C -4.29095000 -4.64223800 -5.26768100
H -3.40134200 -5.14704400 -5.67608000
C -4.34607400 -3.23910600 -5.25374600

H -3.48841400 -2.66327300 -5.63257700
C -7.18479200 -0.13895900 -4.69268800
C -8.18924200 -0.80073000 -5.43442700
H -7.96006400 -1.73550000 -5.96947300
C -9.49031900 -0.27259300 -5.48341700
H -10.2696420 -0.79689800 -6.05839500
C -9.79945400 0.92015400 -4.80201100
H -10.8243100 1.32212500 -4.83262800
C -8.79479600 1.59912100 -4.08945600
H -9.02480400 2.53228500 -3.55078300
C -7.49201800 1.07703000 -4.04213600
H -6.70540600 1.60394800 -3.48173300
C 1.46819500 4.74030200 1.89556600
C 0.43218000 4.92511700 2.84165700
H -0.59833800 5.11852900 2.50643000
C 0.70930500 4.83078000 4.21399100
H -0.09998500 4.98576100 4.94474400
C 2.01049400 4.52941500 4.65745000
H 2.22165400 4.44766000 5.73493700
C 3.03937500 4.33143200 3.71998300
H 4.05957900 4.09258300 4.05805700
C 2.77345400 4.44085600 2.34518500
H 3.58636000 4.29534300 1.61881800
C 2.67031500 5.01188900 -0.74066200
C 3.34072800 3.94268300 -1.37173100
H 2.86567600 2.95113700 -1.42285700
C 4.60741600 4.14079100 -1.94949300
H 5.10993500 3.29951000 -2.45124400
C 5.20643300 5.41147300 -1.91123800
H 6.19535800 5.56963600 -2.36889300
C 4.53489500 6.48676200 -1.29658500
H 5.00074700 7.48422800 -1.26737900
C 3.27423100 6.29046700 -0.71030800
H 2.76860400 7.13590400 -0.21813900
C 0.00359600 6.18312600 -0.23781200
H -0.95094600 5.97263000 0.28989100
H 0.45963500 7.07972300 0.23239900
C -0.23445900 6.36232000 -1.73897500
H 0.69880900 6.61203800 -2.27846000
H -0.63846700 5.43376500 -2.19649800
H -0.96568400 7.17269800 -1.93019500
H -3.17546900 7.17240200 -0.93288900
C -3.90668800 6.36205300 -1.12424200
H -3.50257800 5.43337700 -0.66704500
H -4.83988500 6.61157400 -0.58454900
C -4.14495300 6.18328100 -2.62542600
H -3.19047800 5.97295100 -3.15331400
H -4.60107000 7.08000200 -3.09532800
C -5.60958100 4.74085000 -4.75904300
C -6.91487000 4.44166700 -5.20873300
H -7.72780500 4.29610800 -4.48240300

C -7.18079000 4.33255000 -6.58355700
H -8.20102300 4.09390500 -6.92168700
C -4.85064900 4.83168500 -7.07744400
H -4.04132900 4.98670200 -7.80815600
C -6.15187700 4.53058600 -7.52097700
H -6.36304000 4.44908000 -8.59848200
C -4.57352900 4.92570600 -5.70508900
H -3.54298400 5.11888600 -5.36980600
C -6.81167200 5.01197900 -2.12275500
C -7.41558600 6.29056400 -2.15290800
H -6.90997900 7.13606500 -2.64498700
C -8.67624200 6.48677800 -1.56658600
H -9.14209000 7.48425100 -1.59563800
C -9.34776800 5.41140700 -0.95206400
H -10.3366740 5.56951600 -0.49434900
C -8.74875400 4.14072000 -0.91400000
H -9.25126900 3.29937200 -0.41235700
C -7.48207900 3.94268500 -1.49182300
H -7.00702800 2.95113400 -1.44082100

References

(1) Yang, X.-X.; Issac, I.; Lebedkin, S.; Kühn, M.; Weigend, F.; Fenske, D.; Fuhr, O.; Eichhöfer, A. Red-Luminescent Biphosphine Stabilized '$Cu_{12}S_6$' Cluster Molecules. *Chem. Commun.* **2014**, *50* (75), 11043–11045. https://doi.org/10.1039/C4CC04702H.

(2) Eichhöfer, A.; Buth, G.; Lebedkin, S.; Kühn, M.; Weigend, F. Luminescence in Phosphine-Stabilized Copper Chalcogenide Cluster Molecules—A Comparative Study. *Inorg. Chem.* **2015**, *54* (19), 9413–9422. https://doi.org/10.1021/acs.inorgchem.5b01146.

(3) Fulmer, G. R.; Miller, A. J. M.; Sherden, N. H.; Gottlieb, H. E.; Nudelman, A.; Stoltz, B. M.; Bercaw, J. E.; Goldberg, K. I. NMR Chemical Shifts of Trace Impurities: Common Laboratory Solvents, Organics, and Gases in Deuterated Solvents Relevant to the Organometallic Chemist. *Organometallics* **2010**, *29* (9), 2176–2179. https://doi.org/10.1021/om100106e.

(4) Breuer, R.; Schmittel, M. 1,1′-Biferrocenylenes—The More Redox Stable Ferrocenes! New Derivatives, Corrected NMR Assignments, Redox Behavior, and Spectroelectrochemistry. *Organometallics* **2012**, *31* (5), 1870–1878. https://doi.org/10.1021/om201215w.

(5) Metz, D. J.; Glines, A. Density, Viscosity, and Dielectric Constant of Tetrahydrofuran between -78 and 30.Degree. *J. Phys. Chem.* **1967**, *71* (4), 1158–1158. https://doi.org/10.1021/j100863a067.

(6) Macchioni, A.; Ciancaleoni, G.; Zuccaccia, C.; Zuccaccia, D. Determining Accurate Molecular Sizes in Solution through NMR Diffusion Spectroscopy. *Chem. Soc. Rev.* **2008**, *37* (3), 479–489. https://doi.org/10.1039/B615067P.

(7) Gavezzotti, A. The Calculation of Molecular Volumes and the Use of Volume Analysis in the Investigation of Structured Media and of Solid-State Organic Reactivity. *J. Am. Chem. Soc.* **1983**, *105* (16), 5220–5225. https://doi.org/10.1021/ja00354a007.

(8) Dehnen, S.; Schäfer, A.; Fenske, D.; Ahlrichs, R. New Sulfur- and Selenium-Bridged Copper Clusters; Ab Initio Calculations on $[Cu_{2n}Se_n(PH_3)_m]$ Clusters. *Angew. Chem. Int. Ed. Engl.* **1994**, *33* (7), 746–749. https://doi.org/10.1002/anie.199407461.

(9) Liaw, B.-J.; Lobana, T. S.; Lin, Y.-W.; Wang, J.-C.; Liu, C. W. Versatility of Dithiophosphates in the Syntheses of Copper(I) Complexes with Bis(Diphenylphosphino)Alkanes: Abstraction of Chloride from Dichloromethane. *Inorg. Chem.* **2005**, *44* (26), 9921–9929. https://doi.org/10.1021/ic051166+.

(10) Yu, Y.-Z.; Bai, J.; Peng, J.-M.; Yao, J.-S.; Zhuo, C.-X. Modular Access to Meta-Substituted Benzenes via Mo-Catalyzed Intermolecular Deoxygenative Benzene Formation. *J. Am. Chem. Soc.* **2023**, *145* (16), 8781–8787. https://doi.org/10.1021/jacs.3c01330.

(11) Fargher, H. A.; Sherbow, T. J.; Haley, M. M.; Johnson, D. W.; Pluth, M. D. C–H···S Hydrogen Bonding Interactions. *Chem. Soc. Rev.* **2022**, *51* (4), 1454–1469. https://doi.org/10.1039/D1CS00838B.

(12) Weigend, F.; Ahlrichs, R. Balanced Basis Sets of Split Valence, Triple Zeta Valence and Quadruple Zeta Valence Quality for H to Rn: Design and Assessment of Accuracy. *Phys. Chem. Chem. Phys.* **2005**, *7* (18), 3297–3305. https://doi.org/10.1039/B508541A.

(13) Grimme, S.; Antony, J.; Ehrlich, S.; Krieg, H. A Consistent and Accurate Ab Initio Parametrization of Density Functional Dispersion Correction (DFT-D) for the 94 Elements H-Pu. *J. Chem. Phys.* **2010**, *132* (15), 154104. https://doi.org/10.1063/1.3382344.

(14) Grimme, S.; Ehrlich, S.; Goerigk, L. Effect of the Damping Function in Dispersion Corrected Density Functional Theory. *J. Comput. Chem.* **2011**, *32* (7), 1456–1465. https://doi.org/10.1002/jcc.21759.